

SISSA

Scuola
Internazionale
Superiore di
Studi Avanzati

Neuroscience Area – PhD course in
<Molecular Biology>

**SERPINA3/SerpinA3n: a novel
promising therapeutic target in prion
diseases**

Candidate:

Arianna Colini Baldeschi

Advisor:

Professor Giuseppe Legname

Academic Year 2019-20



INDEX

1. INTRODUCTION

1.1 PRION DISEASES

1.1.1 Prion protein

1.1.2 Prion protein structure

1.1.3 Proteolytic processing of PrP^C and implication in health and disease

1.1.4 Prion protein expression and functions

1.1.5 PrP^C to PrP^{Sc} conversion

1.1.6 Prion strains and species barriers

1.2 ANIMAL PRION DISEASES

1.3 HUMAN PRION DISEASES

1.3.1 Idiopathic prion diseases

1.3.2 Genetic prion diseases

1.3.3 Acquired prion diseases

1.4 DIAGNOSIS

1.5 THERAPY

1.5.1 Small molecule approach

1.5.2 Gene therapy and monoclonal antibodies

1.5.3 Knock-out and knock-down strategies

1.5.4 RNA interference technique

1.5.5 Antisense oligonucleotides

1.6 *IN VITRO* AND *IN VIVO* MODELS FOR PRION DISEASES

1.7 SERPIN SUPERFAMILY

1.7.1 Mechanism of inhibition

1.7.2 SERPINA3/SerpinA3n gene and structure

1.7.3 Pathophysiological roles of SERPINA3/SerpinA3n

1.7.4 SERPINA3/SerpinA3n role in prion diseases

1.8 NEUROINFLAMMATION AND PRION DISEASES

1.8.1 Neuroinflammation, SERPINA3/SerpinA3n and prion diseases

1.9 THE JAK-STAT PATHWAY

2. AIM OF THE STUDY

3. MATERIALS AND METHODS

3.1 Immortalized cell lines

3.2 Mouse models

3.3 Dissociated neurons protocol

3.4 *De novo* infection protocol of immortalized cell line and primary cell cultures

3.5 Compounds

3.6 Structure-based Virtual Screening (SBVS) and similarity search

3.7 Assessment of cell viability and MTT assay

3.8 Acute and chronic treatment

3.9 Collection of conditioned media (CM), cell lysis, PNGase F and Proteinase K (PK)

Digestion

3.10 Western blot

3.11 Recombinant full-length mouse PrP production and purification

3.12 RT-QuIC procedure

3.13 shRNAs production

3.14 SerpinA3n shRNA transfection

3.15 Stable transfection with plasmid to generate SerpinA3n KO ScN2a cell line

3.16 RNA extraction and Reverse transcription quantitative polymerase chain reaction (RT-qPCR)

3.17 Pharmacokinetic

3.18 Bioinformatic research on SerpinA3n promoter

3.19 Fractionation protocol for cellular lysates: Rapid Efficient And Practical (REAP) protocol

3.20 Immunofluorescence of fixed cells

3.21 Statistical analysis

4. RESULTS

4.1 SerpinA3n expression in uninfected and prion-infected cell lines

4.2 Structure based virtual screening

4.3 MTT analysis and acute cell treatment of first library (A-U)

4.4 Identification of the second library of compounds

4.5 MTT analysis and acute cell treatment of second library (1-8)

4.6 Chronic treatment of ScGT1 and ScN2a cell lines with compound 5

4.7 *De novo* infection of GT1 cell line and treatment with compound 5

4.8 Investigation of *in vitro* effect of compound 5 on prion fibril formation

4.9 Investigation of PrP localization after compound 5 treatment

4.10 Binding specificity of compound 5 for SerpinA3n

4.11 SerpinA3n genetic inhibition

4.12 Pharmacokinetic of compound 5

4.13 Analysis of SerpinA3n and Jak/Stat3 pathway relationship in prion diseases development

4.13.1 Immortalized prion-infected cell lines evaluation

-Bioinformatic research of Stat3 binding sites on SerpinA3n promoter

-RT-qPCR reference genes selection

-RT-qPCR results

-Western blot analysis

-Immunofluorescence

4.13.2 FVB primary mixed culture evaluation

-RT-qPCR results

-Western blot analysis

-Immunofluorescence

4.13.3 Mouse brains evaluation

-RT-qPCR results

-Western blot analysis

5. DISCUSSION

5.1 SerpinA3n inhibitors

5.2 The JAK/STAT3 pathway

6. CONCLUSIONS

7. APPENDIX

8. BIBLIOGRAPHY

SUMMARY

Prion diseases, also known as transmissible spongiform encephalopathies (TSEs), belong to a class of fatal neurodegenerative disorders characterized by vacuolation and neuronal loss in the brain paralleled by cognitive and motor impairments.

The main pathological event at the basis of these disorders is the conformational conversion of the physiological cellular prion protein (PrP^C) into the misfolded and pathological isoform, called PrP^{Sc}, which acts as a corruptive seed, initiating a chain-reaction of PrP^C-misfolding and aggregation.

So far, several studies have focused on the ability of small molecules to interfere with the conversion mechanism, by either binding and stabilizing PrP^C or blocking PrP^{Sc} aggregation and accumulation.

However, we are still quite far from finding a cure, thus new therapeutic strategies and targets are required.

Mounting evidence suggests that in addition to gene coding for the PrP (*PRNP*) other genes may contribute to the genetic susceptibility of TSEs.

Indeed, recently, several studies reported that *SERPINA3* (also known as alpha-1-antichymotrypsin), and its orthologue in mouse *Serpina3n*, is strongly up-regulated in different model of prion diseases, both at mRNA and protein level.

Moreover, increased overexpression of this serpin it is found in prion-infected human specimen, suggesting its possible involvement in the pathogenesis and progression of these disorders.

Since serpins are serine protease inhibitors, we hypothesized that *SERPINA3/Serpina3n* are involved in prion progression *via* inhibition of the protease, or the proteases, involved in prions clearance.

Thus, given that all of the PrP- targeted therapeutic strategies developed until now have not been successful in the clinical practice, one of the aims of the thesis is to propose a novel drug strategy to clear prions interfering neither with PrP^C nor with PrP^{Sc}.

Therefore, we decided to test, in models of prion diseases, the activity of anti-SERPINA3 small molecules to evaluate possible changes in prion accumulation.

Moreover, we have investigated how this serine protease inhibitor is upregulated during prion infection, focusing on the signaling cascade involved in this process.

In the second part of the PhD project, we tried to identify pathways correlating prion accumulation and *SERPINA3/Serpina3n* upregulation, with a special focus on the role of the JAK/STAT3 pathway.

1. INTRODUCTION

Neurodegenerative diseases are devastating disorders affecting million people worldwide. The incidence of these diseases is high, and approximately 35 million of people worldwide are affected. Nowadays, neurodegeneration represents one of the main threats to public health and one of the major causes of death.

Indeed, the World Health Organization (WHO) reported that this number is predicted to further increase, reaching more than 100 million people affected by 2050 (WHO) (**Figure1**).

This group of diseases include prion diseases, Parkinson's disease (PD), Alzheimer's disease (AD), Huntington's disease (HD) and Amyotrophic Lateral Sclerosis (ALS) among others (Benetti, Gustinich, & Legname, 2012).

These disorders affect the nervous system determining the progressive loss of function and death of nerve cells, causing severe motor symptoms (such as ataxia, tremors and balance impairment) and a deleterious and fatal cognitive decline (such as insomnia, memory loss and apathy).

Among them neuro-infections constitute the sixth cause of neurological consultation in primary care services worldwide and, even with the advent of effective antibiotics and vaccines, remain a major challenge in many parts of the world (WHO neurological disorders report web).

Among these maladies, prion diseases represent fatal neurodegenerative disorders with a still uncertain mechanism of action.

Prion diseases affect both humans and animals and during the '90s were the cause of the BSE pandemic and, from that moment on, the entire scientific community focused its attention into finding a possible cure.

Even though the spreading of these maladies is limited, many efforts are trying to explain the mechanism at their basis.

Indeed, prion diseases have the unique feature of being transmissible even though the infectious material lacks a genetic component.

In fact, according to the prion paradigm the main event that leads the development of prion pathology is the conformational conversion of the physiological cellular prion protein (PrP^C) into the pathological misfolded isoform (PrP^{Sc}, where Sc stands for scrapie).

Noteworthy, in the last decade, several studies highlighted a relationship between prion disease pathogenesis and the mechanisms at the basis of other neurodegenerative disorders like AD, PD making the research in prion diseases still appealing.

Neurodegenerative disorders share the presence of pathological protein aggregates as the hallmark of the disease, which are responsible for the typical pathological lesions: amyloid- β

(A β) deposits and tau inclusions as neurofibrillary tangles (NFTs) in AD (Goedert, Spillantini, & Crowther, 1991; Hardy & Higgins, 1992), α -synuclein (α -syn) inclusions in Lewy bodies in PD (Spillantini et al., 1997), huntingtin aggregates in HD (Vonsattel & DiFiglia, 1998), Cu/Zn superoxide dismutase (SOD1) and TAR DNA-binding protein 43 (TDP-43) in ALS (Neumann et al., 2006; Rosen, 1993) and prions in human and animal transmissible spongiform encephalopathies (Prusiner, Scott, DeArmond, & Cohen, 1998) (**Table1**).

These proteins are characterized by the alteration of their folding: basically, what happens is a conformational change in the secondary or tertiary structure of the protein, which leads it to be toxic and/or to a loss of its biological activity.

The main feature of misfolded proteins is the enrichment in β -sheet structures instead of α -helix ones, determining the stabilization of oligomers and making the aggregates insoluble and infectious. This conformational change can be induced by mutations, chemical modifications, and environmental changes, but in the majority of cases unknown causes determine this changing, like in sporadic prion diseases.

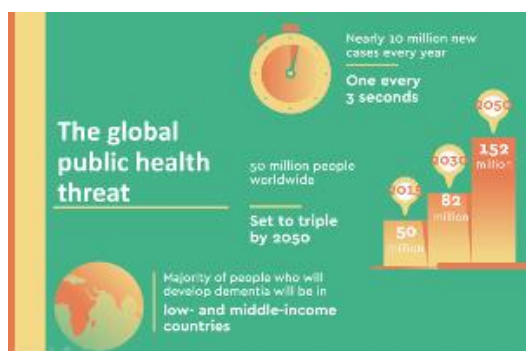


Figure 1. Dementia World Health Organization report

NEUROLOGICAL DISEASES	PROTEIN AGGREGATES
ALZHEIMER'S DISEASE	Aβ and tau
PARKINSON'S DISEASE	A-synuclein
HUNGTINTON'S DISEASE	Hungtintin
AMYOTRPHIC LATERAL SCLEROSIS	SOD-1 and TDP-43
PRION DISEASES	Prions

Table 1. Schematic illustration of typical misfolded proteins for different neurological diseases.

1.1 PRION DISEASES

Prion diseases, also known as transmissible spongiform encephalopathies (TSEs) are a group of fatal neurodegenerative disorders that affect both animals and humans.

Among animals can be found bovine spongiform encephalopathies (BSE), also known as ‘mad cow disease’, chronic wasting disease (CWD) in moose and deer, feline spongiform encephalopathies (FSE) in cats and Scrapie in sheep and goat among others.

In humans they include Creutzfeldt-Jacob disease (CJD), Kuru, Gerstmann-Sträussler-Scheinker disease (GSS) and fatal familial insomnia (FFI) among others.

Human prion diseases can be classified into three different classes, based on their aetiology: sporadic, inherited and acquired.

The prevalence of these diseases in human population is rather low (~1 to 2 cases per million population per year, mostly among aged population) and the incubation period may be quite long from as little as 5 years to up to 40 years in Kuru. Once first symptoms arise the disease progression is very rapid.

From a histological point of view, they are all characterized by similar features, as the presence of spongiform vacuolation, astrogliosis and amyloid plaques deposition even though the clinical profiles can differ among the distinct prion diseases (Budka, 2003).

They have been discovered as infectious maladies around 1930, when two researchers of the Toulouse national veterinary school study J. Cuillé and P. L. Chelle in 1938 demonstrated the transmissibility of scrapie to sheep.

Moreover, thirty years later D. C. Gajdusek demonstrated prion diseases infectivity through chimpanzee inoculation with Kuru and Creutzfeldt-Jacob disease brains (Gajdusek, Gibbs, & Alpers, 1966; Gibbs et al., 1968). Despite this convincing evidence, the cause of the infectivity of these diseases remained unexplained for sometime.

Only into 1982, Stanley B. Prusiner defined the prion diseases-causing agent, calling it ‘PRIONS’, standing for "PRoteinaceous Infectious ONLY particles", lacking nucleic acids (Bolton, McKinley, & Prusiner, 1982; Prusiner, 1982) (**Figure 2**).

Additional studies were carried out to find the molecular and biochemical structures of these particles, to explain the mechanism of infection which is based on the conformational conversion of the cellular prion protein (PrP^C) into the so-called prion, or scrapie prion protein (PrP^{Sc}).

During these attempts, it was discovered that a 27-30 kDa protein was the major protein present in the brain homogenate extract from scrapie-infected hamsters after partial digestion with protease; however the same protein has been also identified in the brains of infected animals

prior to the appearance of clinical signs, excluding it from the possibility to be the pathological isoform, even if it was identified as a part of it (Bolton, McKinley, & Prusiner, 1984).

Hereafter, the isolation of the infective particle proceeded to identify the specific pathological particle. By the mean of immunoblots, a 33-35kDa PrP was found in brain homogenates of scrapie-infected hamsters (33-35 PrP^{Sc}) and a similar protein was also found into healthy brains (33-35 PrP^C). Only thanks to the action of Proteinase K-digestion it has been possible to discriminate the two of them, shedding light on the properties of the infectious particle.

Indeed, after the enzymatic digestion it has been shown that 33-35 PrP^{Sc} was degraded to PrP 27-30, while 33-35 PrP^C was totally degraded (Meyer et al., 1986).

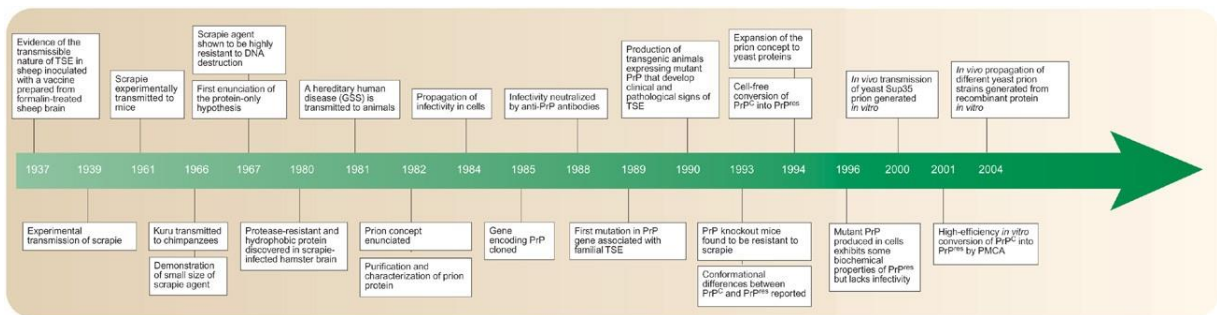


Figure 2. Timeline of the events related to the discover of TSEs (Soto & Castilla, 2004).

1.1.1 Prion protein

The prion protein can exist in two different forms, the cellular prion protein (PrP^C) and the scrapie prion protein (PrP^{Sc}). As mentioned above, the first one represents the normal cellular form of the causative agent of PrP^{Sc}.

PrP^C is the host-encoded isoform. It is a cell-membrane glycoprotein encoded by the *PRNP* gene, located on the short arm of the chromosome 20 in humans and the *Prnp* gene located on the chromosome 2 in mice.

PRNP gene is highly conserved among different species, and depending on the species, it can contain either 2 or 3 exons, with the entire coding region limited to the last exon, thus excluding possible alternative splicing (Colby & Prusiner, 2011), and it can transcribe an mRNA of 2.1-2.5 kb in length (Prusiner, 1991; Wulf, Senatore, & Aguzzi, 2017).

Mutations in the *PRNP* gene are associated with the development of different clinical phenotypes of prion diseases, including CJD, GSS and FFI. More than 40 mutations are known and they can be classified as: point mutations (i.e., single nucleotide substitutions), which can cause an amino change (missense mutation), or be silent (do not cause alteration in the amino acid sequence), or less commonly can cause the coding to prematurely terminate (stop or nonsense mutation); and mutations of insertions and deletions, which have been associated with prion diseases (Acevedo-Morantes & Wille, 2014; Lloyd, Mead, & Collinge, 2013).

PrP^{Sc} has the peculiarity of being infectious itself, which make it different from all the other proteins.

In particular, it possesses the unique feature of being infectious even if devoid of informational nucleic acid, inducing the normal PrP^C into a likeness of itself (Prusiner, 1982).

Importantly, numerous experiments provide evidence for PrP^C to be a key player in prion replication induced-neurodegeneration: it was demonstrated that mice lacking the prion gene are resistant to the disease and that PrP^{Sc} alone is not enough to cause the disease (G. Mallucci et al., 2003).

1.1.2 PrP^C structure

PrP^C is a sialoglycoprotein linked to the outer leaflet of the cell membrane *via* a C-terminal glycosylphosphatidylinositol (GPI)-anchor.

It is synthesised as a precursor protein of 253 amino acids (aa) with a molecular weight of 35-36 kDa (**Figure 3**). The N-terminal domain functions as a signal peptide needed for its translocation to the endoplasmic reticulum (ER).

However, not all the precursors can be transferred to the ER, probably due to a fail into the translation of the code from the signal peptide, remaining into the cytoplasm (Castle & Gill, 2017).

Generally, the majority of the PrP^C precursor molecules translocate properly into the ER, where they undergo to the cleavage of a C-terminal signal peptide and the addition of a glycosylphosphatidylinositol (GPI) anchor, giving rise to the mature form of the protein of about 208 aa (from the aa 23 to the 230) (Benetti & Legname, 2015; Castle & Gill, 2017).

The tridimensional structure (**Figure 4**) is well conserved among the mammals and it consists of two main domains: the C-terminal domain, which is the most structured part of the protein, and the N-terminal domain, which is mostly unstructured, even if it has been shown to possess some stable regions that can allow the protein to interact with other components (Taubner, Bienkiewicz, Copie, & Caughey, 2010).

In fact, the unstructured N-terminal domain consists of unusual glycine-rich repeats which are known as the octa-repeat regions (OR). This segment seems to be fundamental for the binding to different cations, like copper, zinc, and iron among others (Benetti & Legname, 2015), even if the role of those binding is still not completely understood.

Conversely, the C-terminal domain presents a globular structure consisting of 3 alpha-helices, 2 short anti-parallel beta-strands and loops (Benetti & Legname, 2015; Castle & Gill, 2017).

Moreover, a disulfide link is present between the alpha-helix 2 (H2) and the alpha-helix 3 (H3), where two N-linked glycosylation sites are also present (**Figure 3**) (Acevedo-Morantes & Wille, 2014; Wulf et al., 2017).

When the PrP^C moves from the ER to the Golgi, the N-glycans can be attached to the protein and, at that moment, the protein is ready to be targeted to the cell membrane where it can be exposed on the extracellular space through the GPI-anchor bond (Castle & Gill, 2017).

However, some PrP^C molecules can be found retained into the inner part of the cell, meaning that PrP^C trafficking consists of different recycling processes (Ballmer et al., 2017; Magalhaes et al., 2002; Sunyach et al., 2003).

Following these recycling pathways, PrP^C can be found into different intracellular compartments which become other sites of prion conversion, as well as the plasma membrane (**Figure 5**) (Beranger, Mange, Goud, & Lehmann, 2002; Goold et al., 2011; Marijanovic, Caputo, Campana, & Zurzolo, 2009).

Unravelling the structure of a protein is a fundamental step to understand its function. Concerning prion protein, discovering the structure of PrP^C is particularly needed since its destabilization causes the conversion into the pathological isoform, PrP^{Sc}.

In fact, in the physiological condition, PrP^C is prevalently folded in alpha-helices, while in pathological conditions it acquires a beta-sheet folding (**Figure 6**).

In this scenario, different studies put the attention to find the structural determinants involved in the folding and stability of this protein. Particularly, it has been shown that the N-terminal domain of the PrP^C is necessary to maintain the folding of the globular domain, through its stabilization, and also it seems that the OR region is involved in this process (Benetti & Legname, 2015), probably due to the presence of the metal binding sites on it (Benetti et al., 2014).

Moreover, even if the structure of PrP^{Sc} is known (Glynn et al., 2020) and different prions share the same conformation and biochemical features (like protease-resistance core, insolubility in non-denaturing detergents, high enrichment in beta-sheets structure etc), different forms of resistant prion protein (PrP^{Sc}) possess different infectivity and give rise to different strains (Tanaka, Chien, Naber, Cooke, & Weissman, 2004; Telling et al., 1996).

Thus, a deep investigation of the PrP^{Sc} structure can allow to shed light also to better understand the existence of different prion strains and prion disorders.

Recently, the generation of synthetic prions gave the opportunity to go into details of prion transmission and structure (Bistaffa et al., 2019; Legname & Moda, 2017; Moda et al., 2015). Since *in vitro*-generated prions can offer higher control over fibril polymorph distributions, they may give more rapidly structural insights into prion assemblies (Terry et al., 2019).

In this scenario, the discovering of the atomic structures of both recombinant and tissue-isolated prion assemblies would lead to a better understand also of strain specific features (Glynn et al., 2020).

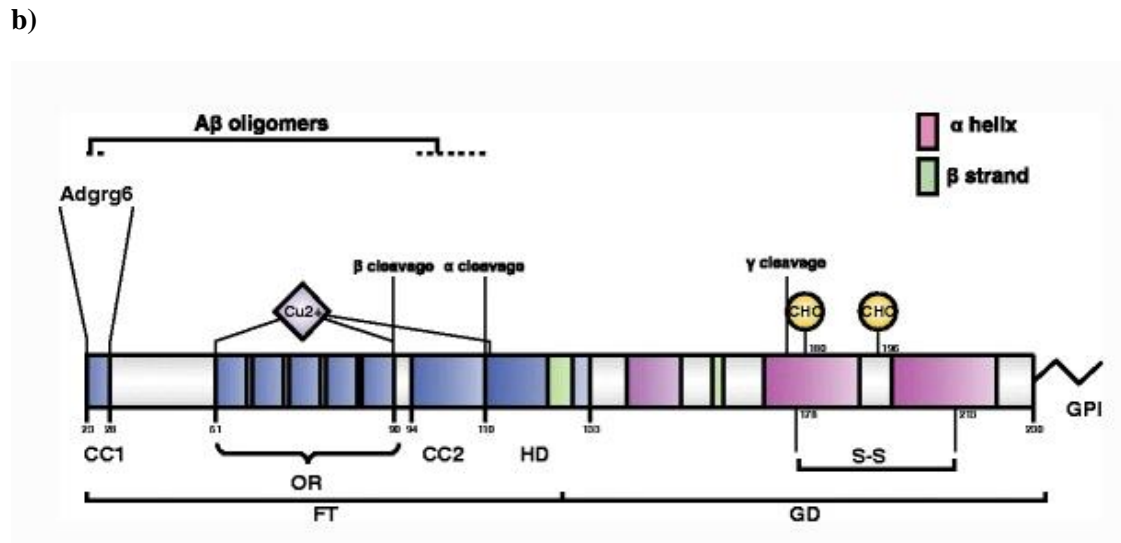
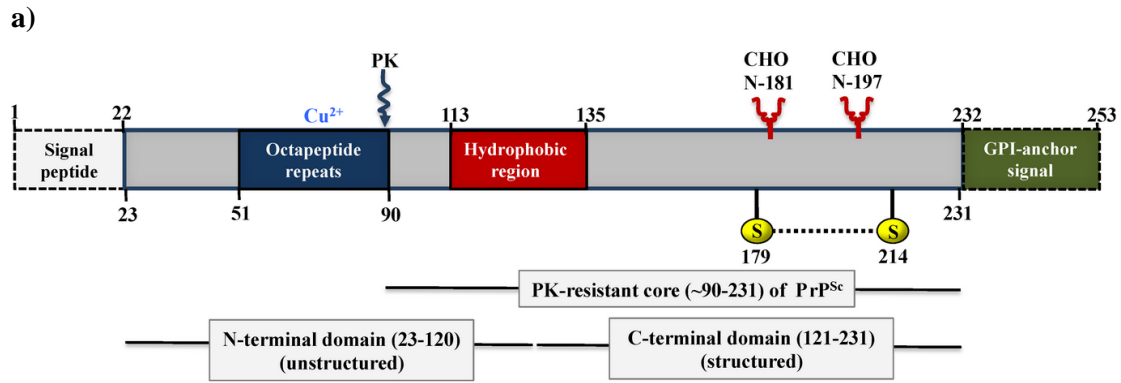


Figure 3. Schematic representations of the primary sequence of PrP^C in humans and mice.

a) Schematic illustration of the primary sequence of the human PrP^C (Acevedo-Morantes & Wille, 2014) and the mouse PrP^C b), showing protein domains, sites of post-translational modification, and binding sites for divalent cations and protein interactors of functional relevance (Wulf et al., 2017).

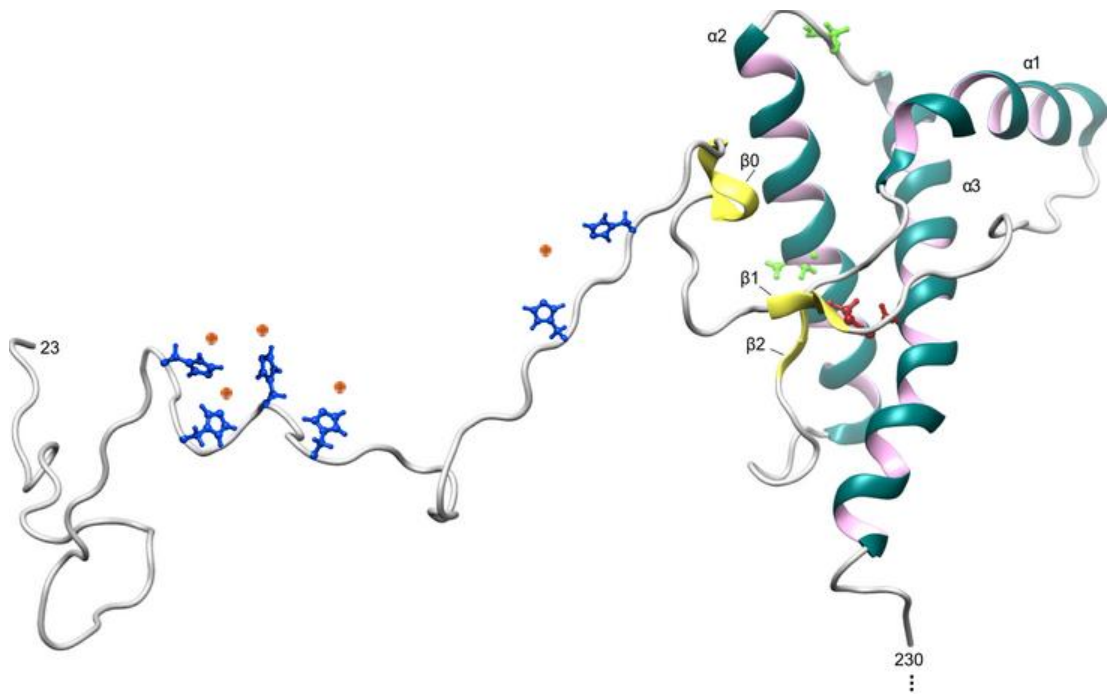


Figure 4. Schematic representation of the three-dimensional (3D) structure of PrP^C (Legname, 2017).

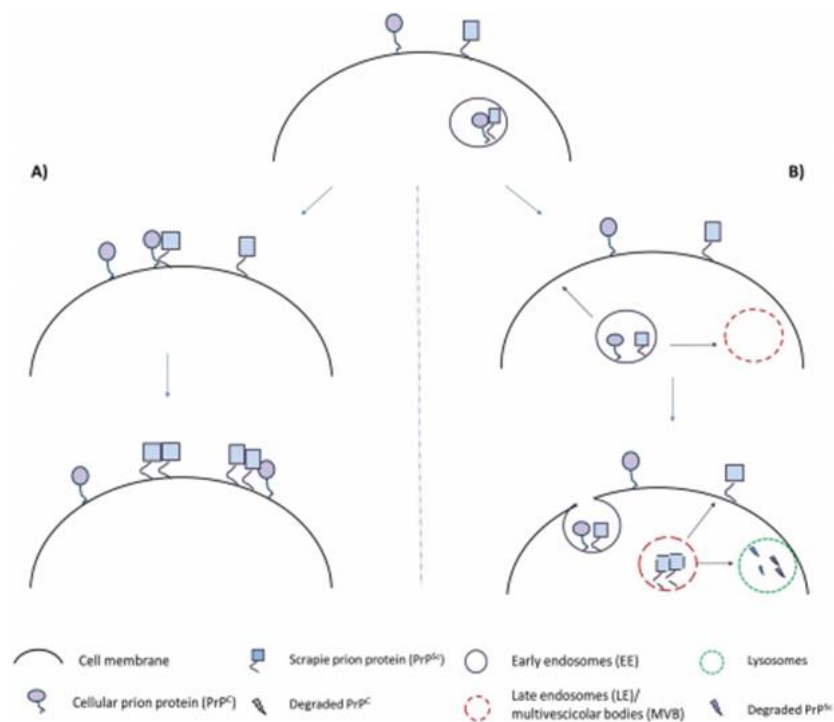


Figure 5. Misfolding of the cellular prion protein (PrP^C) into the scrapie isoform (PrP^{Sc}). Schematic representation of the mechanisms and sites of prion conversion (Colini Baldeschi, Vanni, Zattoni, & Legname, 2020).

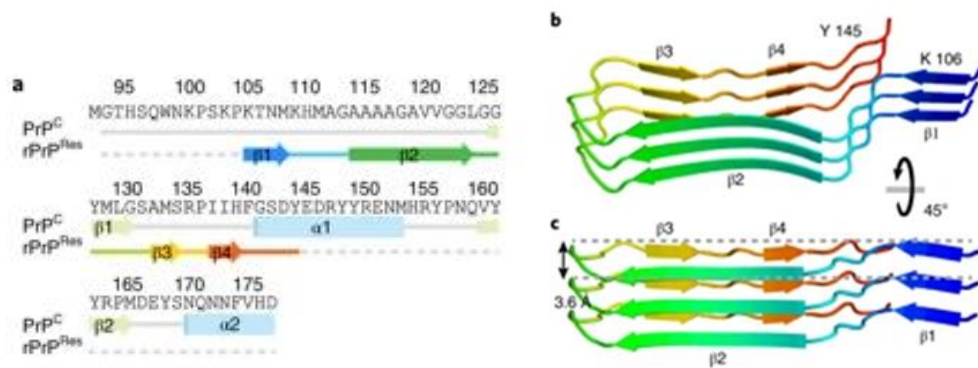


Figure 6. Representation of the difference in the structure of PrP^C and PrP^{Res} a) Differences in the structure of PrP^C and PrP^{Res}; b,c) two different view of the three beta-sheets present in the structure of PrP^{Res} (Glynn et al., 2020).

1.1.3 Proteolytic processing of PrP^C and implication in health and disease

PrP^C can undergo to different post-translational modifications, among which proteolytic processing. This modification differs from the others for its character of irreversibility.

When a protein is subjected to this process it can be cleaved in different fragments, which can have also different functions, thus, this mechanism could be the explanation for the absence of a specific function for several proteins, as well as PrP^C (Linsenmeier et al., 2018).

As showed in **Figure 3 (b)**, PrP^C presents three different sites of cleavage, called α , β and γ , which give rise to different fragments of the protein.

The α -cleavage can occur between 110-111 aa and it seems to be caused by the action of members of the disintegrin and metalloproteinase domain-containing protein (ADAM) family. There are many reports about the members of the ADAM family involved in the α -cleavage, and up to now not all the members have been linked to this process.

Among those involved in this process, it has been shown a role for the ADAM 8, 9, 10 and 17 (Altmeppen et al., 2012; Liang & Kong, 2012; Linsenmeier et al., 2017).

The α -cleavage can happen in acidic endosomal compartments or in the Golgi (Castle & Gill, 2017) and leads to the formation of two different fragments, called the N-terminal fragment (N1) and the C-terminal fragment (C1) (**Figure 7**).

The N1 fragment is released from the plasma membrane, while the C1 fragment is retained on the plasma membrane by the presence of the GPI anchor.

It has been reported that this event has a physiological relevance; in fact, the N-terminal part of the protein is involved in a lot of functions, since it determine the stabilization of the globular

domain and also it contains the region where the interaction with copper and other cations takes part (Altmeppen et al., 2012; Benetti et al., 2014).

Moreover, both isoforms produced, N1 and C1, seem to have different functions.

It has been shown that the N1 fragment has a neuroprotective role. Particularly, it has been reported that this fragment can reduce cell death by reducing p53-dependent cell death (Guillot-Sestier, Sunyach, Druon, Scarzello, & Checler, 2009) and probably stimulating the activity and interaction of microglial cells with the other cell types in the brain (Carroll et al., 2020); moreover, it has been shown that transgenic mice expressing a PrP^C lacking of the N-terminal displayed more evident signs of neurodegeneration if compared with mice expressing a normal PrP^C (A. Li et al., 2007). N1 is also able to counteract the toxicity of the A β -oligomers, by the inhibition of its assembly into fibrils or reducing the derived cell death (Guillot-Sestier et al., 2012; Nieznanski, Choi, Chen, Surewicz, & Surewicz, 2012).

Concerning the C1 fragment, its role is a matter of debate, and controversial data are available. It has been shown from one group that it exerts toxic effect *in vitro*, by enhancing the cell-death (Sunyach, Cisse, da Costa, Vincent, & Checler, 2007) while another group highlighted its neuroprotective function against prion infection (Westergard, Turnbaugh, & Harris, 2011) and a role into myelin maintenance in the peripheral nervous system (Bremer et al., 2010).

The other proteolytic processes that can happen are the β and γ -cleavage: the first one starts at the end of the octarepeat region and give rise to the N2 and C2 fragments, while the correct site of the second one needs to be defined.

The β -cleavage is made by the action of calpains, lysosomal proteases and by the direct action of Reactive Oxygen Species (ROS) and it has been mainly linked to a pathophysiological condition. In particular, C2 fragment has been found both in prion-infected cells and in brains from CJD patients, and it also shares different features with the resistant core of the PrP^{Sc} (PrP27-30), like the insolubility in non-denaturing detergents and a peculiar pattern of electrophoretic mobility (Liang & Kong, 2012; Linsenmeier et al., 2017).

Recently, the γ -cleavage has been proposed. In 2016, Lewis and collaborators found another fragment of PrP^C, smaller than 10kDa, called C3, to which they referred as the product of another proteolytic process that they named as γ -cleavage.

The prevalence of this proteolytic event is not so high, even if it has been found in CJD brains, leaving the possibility of a pathological role of this event (V. Lewis et al., 2016).

The precise site of cleavage is not yet known but it seems to happen at the C-terminal of the protein, possibly through the action of several matrix metalloproteases (MMPs) and during the

endocytic recycling and/or retrograde transport of PrP^C to the Golgi/Trans-Golgi-Network (TGN) (V. Lewis et al., 2016).

Lastly, PrP^C can be subjected to another cleavage, which give rise to the so-called shed-PrP^C (Stahl, Borchelt, & Prusiner, 1990; Tagliavini et al., 1992). It resembles a full-length PrP, lacking only few aminoacid together with the GPI-anchor and it derives from the action of the ADAMs, especially the ADAM10 (Taylor et al., 2009). The function of this cleavage is not yet clear, but it has been proposed to be implicated in the regulation of the PrP membrane levels and functions (Linsenmeier et al., 2017). However, it has been recently shown that the soluble form of the PrP can influence the neurite outgrowth by interacting with the membrane anchored PrP, as demonstrated by Amin and colleagues in 2016 (Amin et al., 2016). Moreover, it has also been correlated with the establishment of prion pathology. Indeed, there are different studies that claim shed-PrP as a neuro-protector against PrP^{Sc} accumulation (Altmepfen et al., 2015; Chesebro et al., 2010; McNally, Ward, & Priola, 2009) while other studies claim that the presence of a GPI-anchorless PrP would allow the spreading of the pathology (P. A. Lewis et al., 2006).

Since PrP is subjected to several proteolytic processes, it is plausible that these events are involved in the various PrP functions and roles, both in health and in disease.

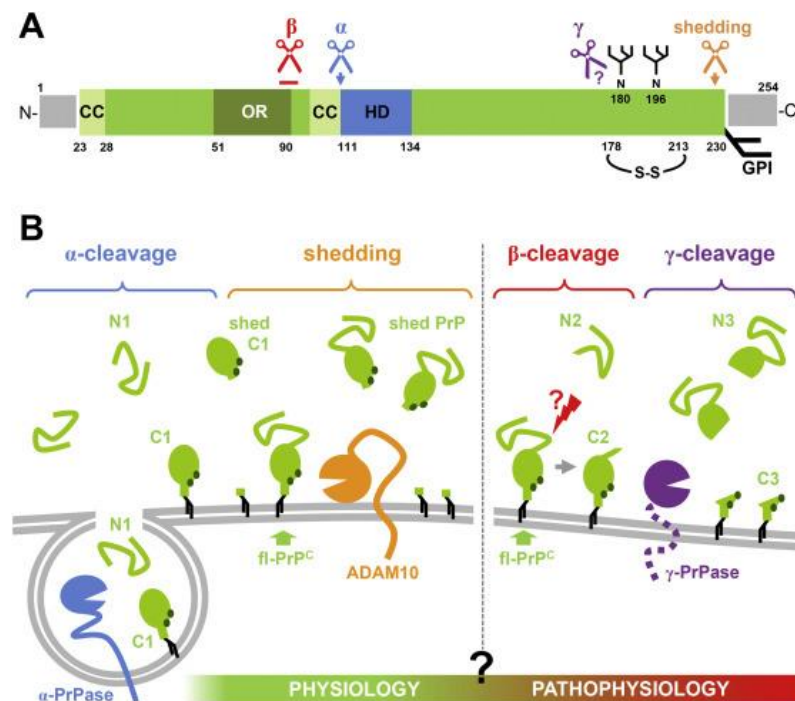


Figure 7. Representation of the PrP^C proteolytic cleavage. A) Representation of the cleavage sites on the PrP^C sequence. B) Representation of the different PrP fragments derived from the different cleavage processes (Linsenmeier et al., 2017).

1.1.4 PrP^C expression and functions

PrP^C is expressed throughout the entire life of an organism, starting from the embryogenesis, and during the adulthood it reaches very high expression levels.

It is an endogenous, cell-surface glycoprotein with a wide expression in the organism; it is present in different organs and tissues, but mainly in peripheral and central nervous systems (PNS and CNS).

However, its physiological role is not yet well understood and a lot of studies, both *in vivo* and *in vitro*, reported several discrepancies (Wulf et al., 2017).

In the CNS, PrP^C is present both in neurons and in glia cells. In neurons is prevalently localized at the synaptic level (Mironov et al., 2003) where it seems to be targeted by the presence of the sialic acid on the GPI-anchor (Bate, Nolan, McHale-Owen, & Williams, 2016).

Due to this localization, it has been correlated with the regulation of synaptic activity. In fact, it has been shown that mice devoid of PrP^C show a reduced long-term potentiation (LTP) in the hippocampus and a weaker inhibitory GABAergic synaptic transmission (Collinge et al., 1994). LTP is engaged in synaptic plasticity and in learning and memory capacity and it has been shown that *Prnp* KO mice present deficiencies in spatial learning and memory, due to the reduced LTP activity (Coitinho et al., 2007).

Moreover, PrP^C can be also involved in sleep homeostasis. In fact, some prion disorders, such as fatal familial insomnia (Lugaresi et al., 1986), present the disruption of the sleep-wake cycle as the principal symptom (Khan & Bollu, 2020). Indeed, it has been shown that mice devoid of *Prnp* gene presented an alteration of the circadian rhythm with sleep interruption (Tobler et al., 1996).

These roles can be explained by the fact that PrP^C can interact with different players at the cell membrane, activating different molecular responses into the cell.

Particularly, it has been shown that PrP^C can interact with N-methyl-D-aspartate receptors (NMDAR), inducing its post-translational modification, like the S-nitrosylation (Gasperini, Meneghetti, Pastore, Benetti, & Legname, 2015).

As mentioned before, the N-terminal region of PrP^C seems to be involved in the interaction with different cations, like copper, which seems to be a key player in the modulation of the NMDA receptor through S-nitrosylation (Benetti & Legname, 2015; Khosravani et al., 2008)

The alteration of the NMDAR regulation causes excitotoxicity and neuronal cell death following a massive calcium influx, which determines the production and release of nitric oxide (NO) and copper (Cu) into synaptic slot.

The S-nitrosylation can impact on the NMDA receptor, inhibiting it by the modification of two residues on the subunit GluN1 and three residues on the subunit GluN2A and it seems that PrP^C has a role in this process through the copper binding.

Since PrP^C has a high affinity to copper ions and it shows a high expression levels in hippocampal synapses, it is likely to bind copper when it is released in the synaptic slot.

When PrP^C binds to Cu (II), it can determine oxidization of NO to NO⁺ through a reduction of Cu (II) in Cu(I). At this point NO⁺ is able to bind to the subunits GluN2A and GluN1, inducing the S-nitrosylation of NMDAR, fundamental to reduce the calcium influx and the subsequent neurotoxic effects (Gasperini et al., 2015).

Thus, copper, PrP^C and NO seem to act synergistically to regulate NMDAR, activating a process of neuroprotection, which seems to be lost in prion diseases. This neuroprotective role seems to be lost also in AD, since it has been shown that A β can alter the availability of the copper for the NMDAR, disrupting its function of neuroprotection (You et al., 2012).

PrP^C has also been associated with the regulation of cell stress. Indeed, it has been proposed to directly interact with the stress-inducible protein 1 (STI1), inducing the activation of the pro-survival proteinase kinase A (PKA) pathway (Lopes et al., 2005).

Moreover, it has been related with the regulation of ROS and lipid peroxidation; it has been shown that cells transfected with PrP^C present lower ROS levels compared to the not transfected controls (Rachidi et al., 2003).

It seems also that PrP^C is able to protect against the exposure to oxidative toxins, maybe acting on the antioxidant enzymes, like SOD1, that convert ROS into less toxic species (D. R. Brown, Schulz-Schaeffer, Schmidt, & Kretzschmar, 1997; Paterson, Curtis, & Macleod, 2008); however, not all the evidence agree with this hypothesis (Steinacker et al., 2010).

Moreover, it has been proposed that PrP^C can impact on the Endoplasmic Reticulum (ER) stress induced by the accumulation of misfolded or unfolded protein within the ER itself. In that case, it has been observed that *PRNP* gene expression can be induced by the ER-stress; in fact, it has been demonstrated that PrP levels are increased in cells treated with compounds able to induce this kind of stress (Dery et al., 2013).

Since PrP^C is a GPI-anchored protein present on the plasma membrane, it can interact with a variety of proteins and it can be involved in the transmembrane signalling pathway (Mouillet-Richard et al., 2000).

Indeed, it has been reported that the 37/67-kDa laminin receptor (LR), involved in cell migration, extracellular matrix remodelling and invasion (Khumalo et al., 2013), can interact also with PrP^C (Rieger, Edenhofer, Lasmezas, & Weiss, 1997) acting as a cell surface receptor

(Gauczynski et al., 2001). In favour of this hypothesis, it has been shown that this interaction can be interrupted by using a 37/67-kDa LR inhibitor, that acts stabilizing PrP^C on the cell membrane and inducing the recycling into the cytoplasm of the 37/67 kDa LR itself (Sarnataro et al., 2016).

Interestingly, PrP^C has been shown to interact not only with the receptor but also with laminin, determining the induction of neuritogenesis (Graner et al., 2000).

Moreover, PrP^C can promote the neurite outgrowth also through the interaction with neuronal cell adhesion molecule (NCAM); in fact, through crosslinking experiments, it has been demonstrated that PrP^C forms complexes with NCAM, even though the exact function of these complexes has not been elucidated (Schmitt-Ulms et al., 2001).

In 2005, it has been proposed that PrP^C and NCAM co-localize at the neuronal cell surface and that their interaction leads to the re-localization of the latter into lipid rafts, determining the activation of the Fyn tyrosine kinase, which mediates neurite outgrowth (Santuccione, Sytnyk, Leshchyn'ska, & Schachner, 2005). Recently, structural studies revealed the surface-interacting epitopes at the basis of this interaction. Indeed, it has been shown that the N-terminal part of the prion protein takes part into the binding of the extracellular domain of NCAM, specifically with the fibronectin type-3(FNIII1, 2) domain (Slapsak et al., 2016).

Moreover, in 2016 our group studied the involvement of PrP in the neurite outgrowth *via* the focal neurite stimulation; indeed, in this study they demonstrated that recPrP can induce neurite outgrowth also interacting with membrane anchored PrP^C (Amin et al., 2016).

The N-terminal region of the cellular prion protein has also been related to interact with G-protein coupled receptor 126 (GPR126) on the surface of Schwann cells, suggesting a PrP^C involvement of in the myelin maintenance of the peripheral nervous system (PNS) (Bremer et al., 2010; Kuffer et al., 2016).

Lastly, even if PrP^C is prevalently expressed into the CNS and PNS, it has been found also in immune cells, like natural killers, T-lymphocytes, mast cells and macrophages (Haddon et al., 2009; R. Li et al., 2001; Mattei et al., 2004). It seems that PrP^C can take part in the inflammatory response, since it has been shown that cultured and activated mast cells, among the release of many inflammatory mediators, showed an increased PrP^C shedding (Haddon et al., 2009). Moreover, it has been shown that knocking-down PrP^C can increase the development of pro-inflammatory phenotype by the T-cells (Hu et al., 2010). Recently, it has also been proposed that PrP^C contributes to immunological quiescence, modulating the inflammatory response of immune cells and protecting parenchymal cells from inflammation insults (Bakkebo et al., 2015).

1.1.5 PrP^C to PrP^{Sc} conversion

After the discovery of the TSEs transmissibility in 1937, countless works were carried out to find the responsible agent of prion diseases infectivity.

Due to the long incubation time of these disorders, it was thought that the causative agent of the infection should be a “slow” virus, but it has been shown that the etiological agent was totally different from a virus (Cho, 1976).

Moreover, due to its small dimension and the resistance to UV and radiation, it has proposed to be a virino, encapsulated into a very tight protein coat which would be able to protect it from degradation (Kimberlin, 1982).

However, no one was able to find any nucleic acids responsible for the TSEs transmission, so the scientific community started to believe that the factor responsible for disease transmission might be a protein with the ability to replicate in the body, as suggested in 1967 by J.S. Griffith. To understand the real nature of this agent it was necessary to isolate the protease-resistant prion-protein (called PrPres) from the infectious material (Bolton et al., 1982; Prusiner, 1982). Thanks to these analyses, it has been shown that PrP mRNA derived from a single host gene, highlighting that PrP can exist in two different isoforms, called normal cellular prion protein (or PrP^C) and scrapie prion protein (PrP^{Sc} o PrPres).

These two isoforms have the same chemical profile, and the conversion seems to involve only conformational changes, as the shifting from alpha helices to beta-sheets structures.

This event gives rise to the different biochemical features between the two isoforms, as well as the protease resistance, solubility alteration and aggregates formation.

The confirmation of PrP infectivity has been proved in 1993 from Bueler H. et al. when they demonstrated that mice devoid of *Prnp* gene were unable to develop prion diseases and to be infected (Bueler et al., 1993).

This evidence was also supported by other studies which again demonstrated that prion protein was the only agent necessary to induce infectivity (Kocisko et al., 1994; Saborio, Permanne, & Soto, 2001).

Thus, according to the “protein-only hypothesis”, PrP^{Sc} is the infectious particle responsible for prion propagation and it can replicate by inducing the autocatalytic conversion of PrP^C into its scrapie isoform (Prusiner et al., 1998).

The molecular details at the basis of this conversion are not well understood. Up to now there are two models that try to explain this intricate process: the “seeding/nucleation process” (**Figure 8b**) and the “template-assisted model or refolding model” (**Figure 8a**).

The first one supposes that monomeric PrP^{Sc} exists in equilibrium with PrP^C and it is stabilized only when it aggregates in oligomers, which can act on other monomeric PrP^{Sc} to be part of the polymer. The second one states that PrP^{Sc} itself contains the information of the refolding and only when in contact with PrP^C can determine its conversion, passing through the presence of an intermediate structure. This last model attests that PrP^{Sc} monomers are needed for prion replication instead of larger aggregates. However, Caughey and colleagues in 2005 demonstrated that small oligomers, made of less than six subunits, were not infectious in Syrian hamsters (Silveira et al., 2005).

Growing evidence supports the hypothesis that small aggregates of PrP^{Sc} rather than monomers or large fibrillar structures can catalyse the conversion of PrP^C.

Recently, another model has been proposed: the “nucleated-assisted model” (**Figure 8c**). This model postulates that PrP^{Sc} never exists as monomer but it requires two different intermediates and cofactors to be converted into PrP^{Sc} oligomers (Abid & Soto, 2006).

PrP^{Sc} is the major component of the infectious agent, but in the last years one of the most interesting and debated issue in prion biology regards the possible involvement of additional factors during the conversion of PrP^C into PrP^{Sc}. And the discovery of these possible factors can amplify the understanding of this intricate mechanism of conversion.

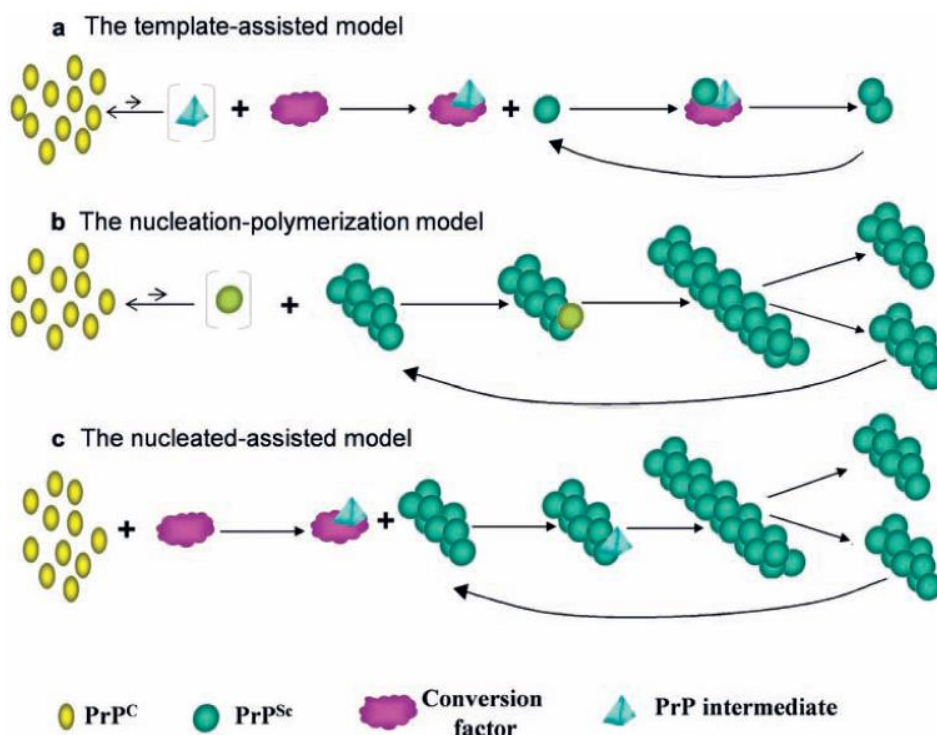


Figure 8. Schematic representation of the different models proposed for the PrP^C-PrP^{Sc} conformational conversion (Abid & Soto, 2006).

1.1.6 Prion strains and species barriers

Prion diseases are characterized by a multitude of clinical presentations, different neuropathological profile and also diverse molecular subtypes. All of these differences can be explained by the existence of many prion strains, despite the absence of a nucleic acid as a part of the infectious prions (Soto & Castilla, 2004).

The first demonstration of prion strains existence goes back to the 1961, when Pattison and Millson described the appearance of different symptoms in goats injected with sheep brain homogenates. Indeed, they observed that some goats developed the drowsy syndrome while others were affected by scratching syndrome (Pattison & Millson, 1961).

Later, in 1973, Dickinson and colleagues infected mice with five different strains of scrapie, observing different lesion profiles (H. Fraser & Dickinson, 1973).

It has been shown that when prions are isolated from one species and inoculated in another one, they become less efficient into the transmission of the pathology, increasing the incubation time and also inducing different neuropathological profiles (M. E. Bruce & Fraser, 1991). The difference in the infectivity of these strains when passed from one species to another one introduced the concept of 'species-barriers' (M. Bruce et al., 1994).

Numerous studies have been made regarding the barrier existing between hamster and mice; indeed, it has been shown that hamster scrapie strain Sc237 is not pathogenic to mice. However, when injected into mice overexpressing the hamster PrP it becomes infectious and mice subjected to pathology (Scott et al., 1989). Thus, it seems that the species-barrier is caused by the differences in the PrP primary sequence of the host and the inoculum.

Prion strains are characterized by different biochemical features of PrP^{Sc} as a different banding pattern by western blot analysis and different rate of glycosylation (**Figure 9**) (Collinge, Sidle, Meads, Ironside, & Hill, 1996; Parchi et al., 1996; Safar et al., 1998). They can determine different phenotypes, as the formation of different PrP^{Sc} isoforms, PK sensitive and resistant, for examples as observed when BSE prions are injected into mice (Lasmézas et al., 1997).

The existence of different PrP^{Sc} conformations is in contrast with the idea that the primary sequence of a protein enciphers for one specific folding.

In this scenario, the sequence homology between host PrP and the inoculum is only one of the causes for the existence of the species barrier, since also the presence of different conformations seems to take part in this process.

Regarding the interspecies transmissibility, one relevant case has been represented by the transmission of BSE prions to humans (Hill et al., 1997) but also in other animals (Bons et al.,

1999; Kirkwood, Cunningham, Austin, Wells, & Sainsbury, 1994; G. A. H. Wells et al., 2003), since it can induce the generation of new prion strains potentially dangerous for human health. In light of this scenario, major attention is now put on Chronic Wasting Disease (CWD), a recently discovered prion disorder affecting cervids (Williams, 2005), since a lot of hunters are used to consume cervid meat and scavenging animals have been found to be in contact with cervids prions, possibly inducing the production of new prion strains.

If the prion-only hypothesis is put in doubt by the definition of scrapie as derivative of different PrP^{Sc} conformations, the existence of different polymorphisms supported this hypothesis (Westaway et al., 1987). Different animals present several polymorphisms and they are connected with different responses to prion strains: for example in sheep the polymorphism at residues V136, R154 and Q171 (VRQ) has been related to an higher susceptibility to scrapie compared with others polymorphisms (Baylis & Goldmann, 2004). Similarly, the polymorphism at codon 129 in humans has been described to be involved in different susceptibility to PrP^C-PrP^{Sc} conversion, since the presence of Methionine, rather than Valine, at this position has been shown to facilitate the conversion process (Palmer, Dryden, Hughes, & Collinge, 1991; Tahiri-Alaoui, Gill, Disterer, & James, 2004).

Prion strains possess very peculiar features, in particular it has been shown that when they are adapted into the host and become more stable they can manifest and maintain their characteristics (Bartz, Bessen, McKenzie, Marsh, & Aiken, 2000).

Moreover, it has been shown that different prion strains can co-exist into the host, as reported for subjects heterozygous at the codon 129 (Schoch et al., 2006). Lastly, it has also been demonstrated that some prions can increase their incubation time when injected with another strain, phenomenon known as “competition of prion strains” (Bartz, Aiken, & Bessen, 2004).

Even if, initially the existence of prions strains creates some debates in light of the ‘prion-only hypothesis’ is now clear that this event is the only one able to clarify the different clinical features of prion diseases.

Moreover, since prion strains can represent a potential risk for public health, the awareness and understanding of their existence can help to prevent from possible new pandemics.

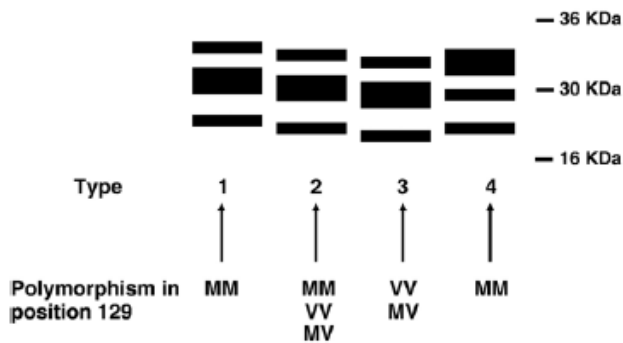


Figure 9. Different PrP^{Sc} western blot profiles after a PK digestion in different strains of human prions (Morales, Abid, & Soto, 2007).

1.2 ANIMAL PRION DISEASES

Scrapie	Sheep	Infection in susceptible sheep
BSE	Cattle	Infection from contaminated food
Transmissible mink encephalopathy (TME)	Mink	Infection from sheep or cattle in food
Chronic wasting disease (CWD)	Mule, deer, elk	Fecal/oral/aerosol routes of infection from other affected cervids; arose spontaneously or possibly from a scrapie source
Feline spongiform encephalopathy	Cats	Infection from BSE-contaminated food
Exotic ungulate encephalopathy	Nyala, oryx, kudu	Infection from BSE-contaminated food

Table 2. Classification of animal prion diseases (modified from T. Wisniewski and F. Goñi 2016).

Animal prion diseases include scrapie in sheep and goats, transmissible mink encephalopathy (TME) in mink, BSE in cattle, CWD in cervids, FSE in cats and exotic ungulate encephalopathy in antelopes (Houston & Andreoletti, 2018) (**Table 2**).

The first one to be described was Scrapie, which is known from 1732 (Imran & Mahmood, 2011) even if the transmission is not yet well understood and remains unclear.

Clinical signs include behavioral modifications, ataxia, aggressiveness among others, but the most peculiar ones is the appearance of an intense pruritus (Pattison & Millson, 1961).

BSE or ‘mad cow disease’ was first described in 1986 (G. A. Wells et al., 1987) in cattle and it was initially attributed to the transmission of sheep scrapie to cattle via contaminated feed.

It has been shown to be naturally transmitted to other animals (Sigurdson & Miller, 2003), but also to humans in the form of variant CJD (vCJD) by the consumption of beef products derived from classical BSE-infected cattle (Ironside et al., 1996).

TME was firstly discovered in 1947 in Minnesota and then described also in other countries. Its origin is still unknown but it is mostly attributed to the consumption of infected feed (Imran & Mahmood, 2011).

CWD was first discovered in Colorado in 1967 (Williams & Young, 1980) affecting wild and captive cervids in 25 US states and two Canadian provinces, as well as in South Korea (Y. H. Lee et al., 2013); more recently, it was identified in wild reindeer and moose in Norway and Finland too (Sigurdson, Bartz, & Glatzel, 2019). The origin is still unknown but the possibility of a zoonotic transmission of CWD prions via diet is of particular concern in North America where hunting of cervids is a popular sport. However, even if up to date, no evidence of human transmission has been reported (Sandberg et al., 2010), recent studies reported the potential infectivity of CWD also to humans, making CWD a new potential BSE epidemic species (Barria et al., 2014).

FSE is a TSE affecting wild and captive cats; it appeared at the same time of the BSE pandemic leading to believe that the consumption of BSE-contaminated feed was the causative agent. In fact, the biochemical analysis of FSE-infected brain revealed a similar pattern with the BSE (Eiden et al., 2010).

Lastly, exotic ungulate encephalopathy (EUE) affects the exotic zoo ruminants of the family Bovidae. As for FSE first cases were reported during BSE period indicating contaminated food as the causative agent of this type of TSE (Sigurdson & Miller, 2003).

1.3 HUMAN PRION DISEASES

Etiology	Disease
1. Idiopathic (sporadic)	Sporadic Creutzfeldt–Jakob disease (CJD)
	Sporadic fatal insomnia
	Variably protease-sensitive prionopathy
2. Genetic (inherited)	Genetic CJD
	Gerstmann–Sträussler–Scheinker disease
	Prion protein cerebral amyloid angiopathy
	Fatal familial insomnia
3. Acquired (infectious)	Kuru
	Iatrogenic CJD
	Variant CJD

Table 3. Classification of human prion diseases according to the etiology (Diane L. Ritchie, James W. Ironside 2017)

Human prion diseases have been discovered in early 90’s. The first one to be described was CJD, by the name of Creutzfeldt and Jakob, who firstly referred to this peculiar kind of fatal neurodegenerative disease.

Later, in 1936 Gerstmann, Sträussler and Scheinker described another disorder denominated as GSS, which has been characterized by the presence of amyloid plaques in the cerebellum.

In 1957 a new fatal neurodegenerative disorder has been identified in Papua New Guinea. It has been called “kuru” and it has been associated with the common practice of cannibalism among the local tribes, since when this practice has ceased number of cases decreased drastically (Gajdusek & Zigas, 1957).

These disorders are devastating and invariable diseases that occur worldwide but, fortunately, they are very rare with an incidence of 1-2 cases per million of population (Imran & Mahmood, 2011). They can be divided into three different categories, based on the etiology: idiopathic, genetic and acquired.

The idiopathic group, also known as sporadic, accounts for 80-85% of the cases among all human prion disorders and includes sporadic CJD (sCJD), sporadic fatal insomnia and variably protease-sensitive prionopathy. The inherited or genetic group accounts for 10-15% of all the cases including genetic CJD (gCJD), GSS, prion protein cerebral amyloid angiopathy and FFI.

The last group accounts for only the 5% of all cases and comprises kuru, iatrogenic CJD and variant CJD (**Table 3**).

These diseases have a long pre-clinical incubation period, which can extend from months to several years, after which the affected individuals usually complain with vague sensory feelings, such as depression, followed by progressive motor paralysis, dementia and often cerebellar ataxia. Other atypical characteristics of prion diseases are the apparent lack of obvious inflammation and of disease-specific immune response (Igel-Egalon, Beringue, Rezaei, & Sibille, 2018).

Common histopathological features are spongiform degeneration of the CNS, formation of amyloid plaques, reactive gliosis and neuronal loss.

For many decades the diagnosis has been made by postmortem histopathological examination, searching for the typical spongiform change occurring widely in the CNS (Budka et al., 1995). Other typical features of this group of maladies are neuronal loss, gliosis, hyperplasia and the presence and accumulation of PrP^{Sc} plaques in the brain (Budka, 2003).

1.3.1 Idiopathic prion diseases

Sporadic prion diseases include sporadic CJD (sCJD), sporadic fatal insomnia and the recently identified variably protease-sensitive prionopathy (VPSPr).

sCJD is the commonest among all human prion disorders and accounts for 1-2 cases per million of population per annum (Collinge, 2001), while VPSPr is very rare with an onset age usually in the late sixties to seventies (Puoti et al., 2012).

All of them are mainly characterized by a rapid cognitive decline leading to dementia, ataxia and often by myoclonus too (Belay, 1999).

Up to date, the cause of sCJD and VPSPr are still unknown. It has been proposed that sCJD can arise spontaneously, possibly for a somatic mutation in the *PRNP* gene or for a spontaneous misfolding of the PrP^C into the scrapie isoform while VPSPr has not been associated with possible *PRNP* mutations. However, none of these has been proven yet (Aguzzi, Baumann, & Bremer, 2008).

1.3.2 Genetic prion diseases

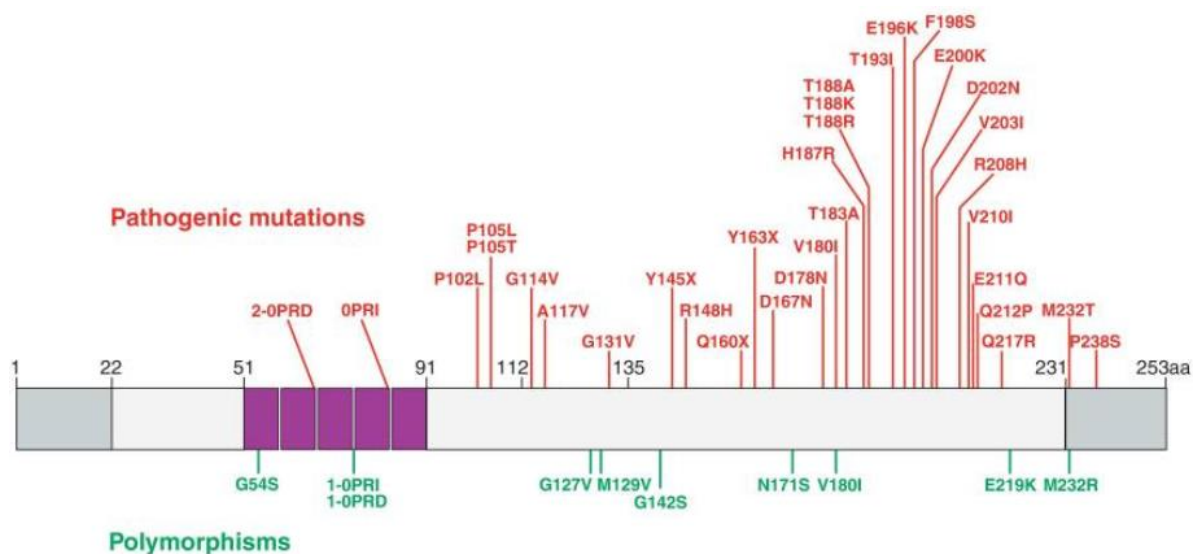


Figure 10. *PRNP* gene polymorphisms and mutations (Lloyd et al., 2013).

Genetic prion diseases are inherited disorders with high penetrance, accounting for the 10-15% of all prion diseases, and attributable to the presence of an autosomal dominant mutation of the *PRNP* gene. More than 40 pathogenic mutations have been identified: most of them are caused by missense mutations, but also insertion, deletion, and amber mutations have been described (Lloyd et al., 2013) (**Figure 10**).

It has been proposed that mutations can render PrP^C more susceptible to transformation into PrP^{Sc} and they can influence the wide variety of clinic-pathological phenotypes reported for this class of diseases (K. Brown & Mastrianni, 2010).

Genetic CJD is the most common one and more than 50% of cases have been reported without a positive family history of the disease. In these cases, *PRNP* sequencing can be useful to unravel possible mutations linked to genetic CJD, as for E200K mutation (Ritchie & Ironside, 2017). It typically begins with rapidly progressive dementia, ataxia and different motor impairments (Geschwind, 2015).

GSS has an incidence of 1 in 100 million of population per year and usually begins as a slowly progressive ataxic or motoric disorder with a later dementia onset (Arata et al., 2006; Kovacs et al., 2002). P102L mutation is the first one associated with this disease but a lot of others point mutations have been linked to GSS (Head et al., 2015) 2015). FFI is a very rare form of genetic prion diseases, caused by a single mutation in the *PRNP* gene termed D178N (Medori et al., 1992). It typically affects the thalamus and, therefore, the main

clinical features are progressive insomnia, endocrine abnormalities and tachycardia, later followed by motor and cognitive impairments (Collins, McLean, & Masters, 2001). Importantly, more than the 60% of patients with genetic prion diseases had no family history of prion diseases, but, more often, neurologic or psychiatric diseases were observed that likely had been misattributed to other etiologies (Kovacs et al., 2005).

1.3.3 Acquired prion diseases

Acquired prion diseases count for less than 1% of all prion maladies and are attributed to the transmission of the infectious agent from an affected individual to a healthy one.

They include Kuru, iatrogenic CJD (iCJD) and vCJD.

This group of diseases is commonly known because of the BSE or ‘mad cow disease’ epidemic in the UK and in other European countries, between 1980s and 90s, which was demonstrated to be transmissible to humans, causing a new form of prion disease termed vCJD, leading to enormous public and scientific concerns (K. Brown & Mastrianni, 2010; Maheshwari et al., 2015). In particular, vCJD was transmitted to humans via meat consumption of cattle infected with prions (Aguzzi, 1996; Aguzzi & Weissmann, 1996; M. E. Bruce et al., 1997).

Kuru was the first discovered form of acquired prion diseases in the Fore people of Papua New Guinea, mainly in women and young children of both sexes; the cause was attributed to rituals of cannibalism, in particular to the consumption of prion infected material, such as brain and viscera (Liberski, 2013). Although the incidence of Kuru has been strongly reduced through cessation of endocannibalism practices, some rare cases still occur occasionally since the incubation period can be longer than 50 years (Collinge et al., 2006; Whitfield, Pako, Collinge, & Alpers, 2017).

iCJD was first described in 1974 in a patient who developed CJD 18 months after transplantation of a cadaveric corneal graft from a donor who had been later confirmed to have CJD (Duffy et al., 1974). Since then, several cases of human prion diseases have been associated with CJD iatrogenic transmission, mainly caused by the use of contaminated neurosurgical instruments, depth electrodes, dura mater grafts and human pituitary hormones treatments (Will, 2003).

1.4 DIAGNOSIS

Prion diseases are maladies that affect the CNS and, as for other neurodegenerative pathologies, the diagnosis is mainly based on the clinical examination, evaluating if patients' symptoms fit the standard guidelines (Budka et al., 1995).

However, the diagnosis of TSEs is quite difficult. First of all, clinical symptoms appear after a long period of incubation and when they become visible the pathology is already in an advanced stage. Moreover, classical clinical symptoms are dementia and loss of movement coordination, which are similar to those of other neurodegenerative disorders, like AD and PD, leading to often mistake them.

Differently from the other neurodegenerative disorders, prion diseases are characterized by the presence and the accumulation of misfolded prion protein, which is peculiar for this illness. However, since PrP^{Sc} lacks nucleic acid component and it is uneven distributed in body tissues, is difficult to be detected with standard methodology, like PCR or serology (Kubler, Oesch, & Raeber, 2003).

Thus, since the neuropathological examination reveals the presence of spongiform vacuolation, gliosis and PrP^{Sc} deposits in the brains, currently the definite diagnosis seems to be possible only post-mortem by histological analysis or biopsy of brain tissue (Budka, 2003).

However, brain biopsy is invasive and expensive so recently less invasive biopsy methods have been evaluated, using for example olfactory mucosa, skeletal muscle, or skin (Glatzel, Abela, Maissen, & Aguzzi, 2003; Mammana et al., 2020). After the biopsy, the protocol provides the use of Proteinase K (PK) treatment and the following Western blot analysis to evaluate the presence of the PrP^{Sc}.

Other methods used to diagnose prion disorders are the electroencephalography (EEG) and the magnetic resonance imaging (MRI). The first one was used since 1954 and seems to be useful to diagnose sCJD cases thanks to periodic sharp wave complexes found in these patients. However, this technique has a low sensitivity leading to high levels of false positive, and differences in sCJD subtypes complicate even more the diagnosis (Hansen, Zschocke, Sturenburg, & Kunze, 1998; Wieser, Schindler, & Zumsteg, 2006). On the other hand, the MRI is used mainly to exclude other causes of pathology and it is useful to discriminate from vCJD and sCJD. However, it strongly depends on the interpretation and the expertise of clinicians (Collins et al., 2000; Will et al., 2000).

Unfortunately, all these tests are not sufficient to diagnose TSEs by themselves; thus, in order to perform a correct diagnosis, clinicians need to combine them with the observation of clinical signs.

As mentioned above, generally the definite diagnosis of TSEs happens post-mortem and the development of a pre-symptomatic test is needed.

Recently, two techniques have been developed to detect even very low amounts of PrP^{Sc} in different samples (urine, blood, olfactory mucosa) amplifying them: the protein misfolding cyclic amplification (PMCA) and the Real-Time Quaking-Induced Conversion (RT-QuIC) (**Figure 11 a,b**).

The first one, developed in 2001, consists in the incubation of a large excess of PrP^C from a healthy brain homogenate with a very low amount of PrP^{Sc} coming from infected samples to promote its aggregation. Then, the sample is sonicated to break PrP^{Sc} aggregates and to increase the number of so called “seed” (Saborio et al., 2001). So, increasing the number of cycles of PMCA it has been possible to increase exponentially the number of seeds, giving the possibility to amplify a single molecule of PrP^{Sc} (Barria, Gonzalez-Romero, & Soto, 2012). The presence of newly generated PrP^{Sc} can be confirmed by biochemical assay, such as the resistance to PK digestion or insolubility in non-ionic detergents.

The second one, appears in 2008 and it differs from PMCA since the tested samples can either contain or not the pathological form of prion protein. Basically, the samples are added to a large excess of recombinant prion protein and if the tested sample contains prions it can induce the aggregation of the recombinant protein. In this case, the presence of newly generated PrP^{Sc} is followed by using in the mixture a Thiofavin-T dye (ThT) able to bind only to the β -sheets of aggregated proteins. Thus, an increase in ThT fluorescence resembles an increase in PrP^{Sc} aggregates formation, meaning that the tested sample contains prions (Atarashi et al., 2008). The efficiency of this method is so high that even 10-40 particles of PrP^{Sc} can be detected. Moreover, since it has been shown to detect prions from CSF and olfactory mucosa (Atarashi et al., 2011; Zanusso et al., 2003), it has been suggested as a possible ante-mortem for TSEs.

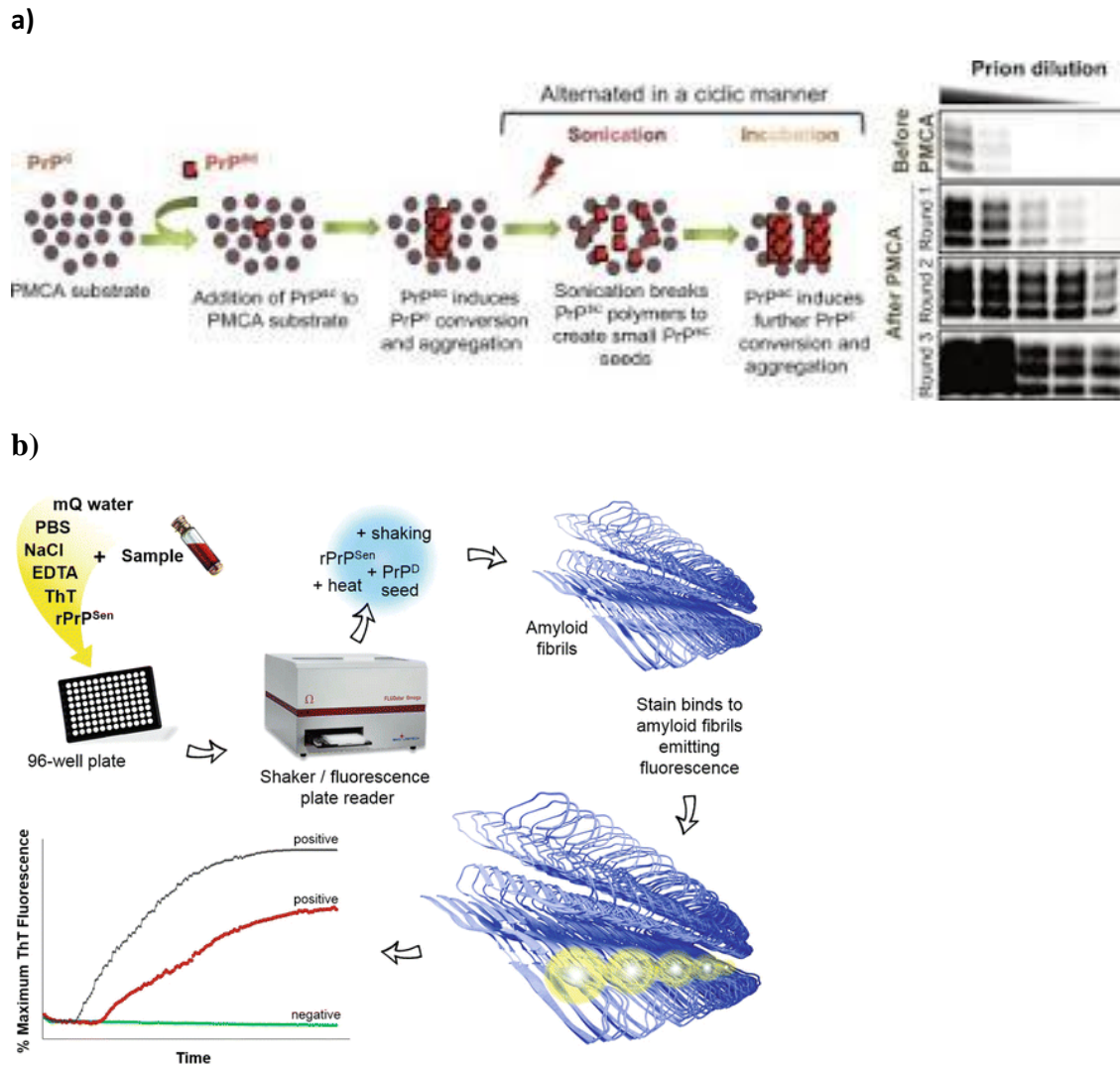


Figure 11. Representative scheme of the protein misfolding cyclic amplification (PMCA) and the Real-Time Quaking-Induced Conversion (RT-QuIC). a) Schematic representation of PMCA assay (Moda, 2017); b) schematic representation of RT-QuIC assay (Caughey et al., 2017).

1.5 THERAPY

To date, no effective therapies have been developed for these fatal neurodegenerative disorders, however a lot of efforts have been spent to find a possible cure.

As already mentioned, the only requirement to develop these diseases is the co-existence of the two forms of prion protein: PrP^C and PrP^{Sc}. For this reason, blocking the conversion is the main goal under a therapeutic point of view, and throughout years several approaches have been made to hamper this interaction (Aguzzi, Glatzel, Montrasio, Prinz, & Heppner, 2001).

At the beginning, the majority of the efforts have been spent to create molecules able to block specifically PrP^{Sc}, since it represents the pathological isoform responsible for the misfolding of PrP^C. However, since not always the appearance of PrP^{Sc} aggregates follows the development or the severity of the pathology, recently, different approaches focused their action on the inhibition of the cellular prion protein with the idea of removing the only substrate needed for the conversion (Barreca, Iraci, Biggi, Cecchetti, & Biasini, 2018).

To do that, a lot of approaches have been tested, as knocking-out or knocking-down of *PRNP* gene, antisense oligonucleotides, and RNA interference techniques (G. Mallucci et al., 2003; Raymond et al., 2019; White & Mallucci, 2009).

Unfortunately, even if different molecules have been tested so far also in clinical trials and a lot of other strategies have been developed to inhibit prion conversion, no cure is still available.

1.5.1 Small molecule approach

In the last thirty years a lot of molecules have been designed to block PrP^{Sc} or PrP^C to try to inhibit the conversion mechanism (**Figure 12**).

At the beginning, the majority of them have been directed toward PrP^{Sc} inhibition and, in this scenario, we can mention beta-sheet breakers (Soto et al., 2000).

Beta-sheet breakers are short peptides which interact with PrP through sequence homology and designed to unwind the beta sheet structures. This mechanism was proved *in vitro*, and then tested in mice where it has been shown to lower the appearance of clinical symptoms.

Similarly, branched polyamines are designed to act on PrP^{Sc}, making it more susceptible to the PK treatment (Supattapone et al., 2001).

However, as mentioned above, not always PrP^{Sc} presence follows the development of the disease and the existence of prion strains can create different actions of these molecules. Thus, a lot of molecules have been designed not to specifically bind PrP^{Sc}.

Particularly, different molecules have been generated to stabilize the cellular isoform of prion protein, to prevent its misfolding. In this group of molecules, we can find: Chlorpromazine, GN8, Fe (III)-TMPyP, Methylene Blue and Quinacrine. Even if, they have been tested both *in vitro* and *in vivo*, except for Chlorpromazine, and the majority of them were able to decrease prion load, only Quinacrine has been used in clinical trials due to its capacity to easily overcome the Blood-Brain Barrier (BBB) (Cavaliere et al., 2013; Collinge et al., 2009; Kocisko et al., 2006; Kuwata et al., 2007; Stincardini et al., 2017).

However, it has been shown to be not particularly beneficial to patients and also extremely hepatotoxic.

Other compounds used in clinical trials are: Doxycycline, Penotosan polysulfate (PPS) and Amphotericin B. Among them only Doxycycline passes in phase II trial, but even the encouraging results other trials are needed (Adjou et al., 2000; Haik et al., 2014; Terada et al., 2010).

Thus, despite all the efforts spent to design or found molecules/drugs able to reduce prion load and slow down the pathology, up to now none of them has been demonstrated to be effective.

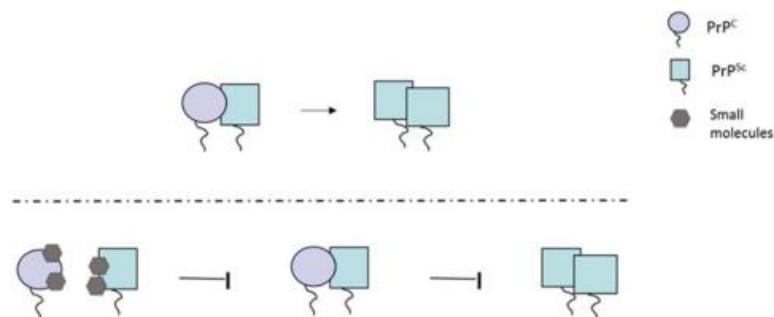


Figure 12. General scheme of the PrP^C-PrP^{Sc} interaction inhibition using small molecules (Colini Baldeschi et al., 2020).

1.5.2 Gene therapy and monoclonal antibodies

Using monoclonal antibodies to block PrP^C-PrP^{Sc} interaction has been demonstrated a lot of years ago (**Figure 13**). However, despite an initial period of emphasis, this strategy has been abandoned due to the difficulty to solve the problem of immunotolerance. Indeed, being PrP a physiological protein, using antibodies against prion protein revealed a lot of issues, even though the generation of PrP KO mice allows to overcome the problem (Polymenidou et al., 2004; Prusiner et al., 1993).

Respect to small molecules, antibodies possess a higher binding affinity due to the larger contact surface and specific epitope recognition.

A lot of studies have been performed using anti-PrP antibodies, showing their ability to decrease prion load; however, one of the main limitations in using antibodies is that the majority of the *in vivo* studies used full-length PrP antibodies, which were difficult to manipulate.

Later, the issue has been exceeded when single-chain fragment (ScFv) has been created. Another problem concerning the antibodies' strategy consists in their high susceptibility to be degraded, limiting their bioavailability. In this case, using viruses as carrier of antibodies or the so called 'intrabodies' their availability was increased. Moreover, using AAVs it has been shown an increased diffusion of ScFv in the brain (Donofrio, Heppner, Polymenidou, Musahl, & Aguzzi, 2005; Moda et al., 2012).

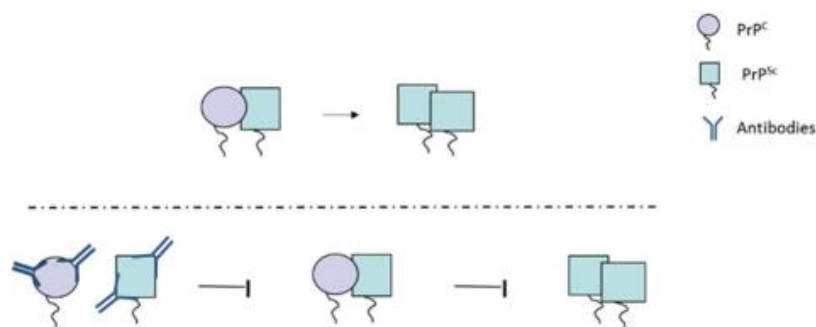


Figure 13. General scheme of the PrP^C-PrP^{Sc} interaction inhibition using antibodies (Colini Baldeschi et al., 2020).

1.5.3 Knock-out and knock-down strategies

As already mentioned, PrP^C is the only substrate needed for PrP^{Sc} accumulation, thus its inhibition or deletion can be a useful strategy to block prion conversion.

Following this direction, several attempts have been carried out to lower PrP expression in order to block prion conversion, since it has also been shown that the ablation of PrP^C is not detrimental (Bueler et al., 1992; G. R. Mallucci et al., 2002).

In light of this, it has been shown that mice lacking *Prnp* gene were effectively resistant to develop prion disorders (Bueler et al., 1993). Later, also the knock-down strategy has been followed to decrease PrP^C trying to prevent prion accumulation and even in that case, lowering PrP^C has been demonstrated to efficiently decrease prion load (White et al., 2008). Even if these data point out that lowering PrP^C can prevent prions accumulation and it seems to be sufficient to block prion replication, other studies reported slightly different results (Pulford et al., 2010). Moreover, all these results have been observed in neuronal population and since astrocytes seem to be fundamental in sustaining prion replication, it would be necessary to lower PrP^C in both populations to obtain better results (Raeber et al., 1997).

1.5.4 RNA interference technique

In the context of PrP^C knock-down strategy, RNA interference (RNAi) represents the gold standard.

Basically, RNAi is a physiological mechanism that is able to reduce the expression of a target gene using an exogenous double-stranded RNA (dsRNA) able to bind to the corresponding target mRNA (**Figure 14**) (Fire et al., 1998).

To do that, two different constructs are used: small interfering RNAs (siRNAs) and short-hairpin RNAs (shRNAs); siRNAs are dsRNAs with 2 nucleotides at 3' end which lead to the degradation of the target mRNA in a sequence-specific manner, while shRNAs act forming a stem-loop structure on the target mRNA (Brummelkamp, Bernards, & Agami, 2002).

One of the limitations of this strategy is that PrP is mainly express into the brain, and to block prion replication both siRNAs and shRNAs need to pass the BBB.

In this scenario different strategies have been carried out to increase their diffusion in the brain such as, lentiviral vectors for the shRNAs delivery and liposome-siRNA-peptide complexes (LSPCs) strategy for siRNAs. However, all of these strategies have been used in animals and are not efficient or safe enough to be used in humans (Bender et al., 2019; Kumar et al., 2007).

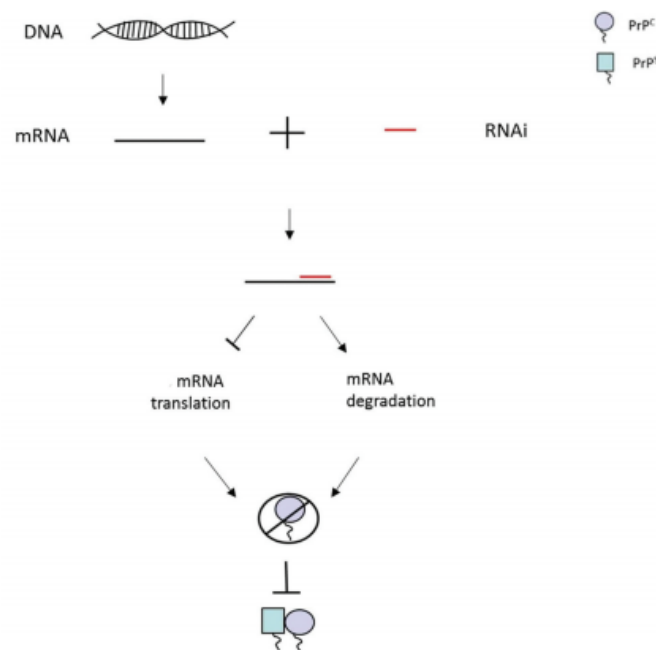


Figure 14. General scheme of the PrP^C-PrP^{Sc} interaction inhibition using RNAi technique (Colini Baldeschi et al., 2020).

1.5.5 Antisense oligonucleotides

In the same context of lowering PrP^C levels, Antisense Oligonucleotides (ASOs) appear as the most promising strategy.

Basically, ASOs are synthetic oligonucleotides made of 15-25nts that can bind to the target mRNA, forming a heteroduplex, leading it to the degradation by the action of the RNase H.

Moreover, ASOs can be modified to inhibit the RNA translation inhibiting the protein synthesis. In this scenario, they appear as an appealing strategy for all of those neurodegenerative diseases caused by the abnormal accumulation of misfolded proteins.

In fact, ASOs have been designed and used to lower toxic proteins responsible for pathologies like HD, where ASOs have been designed to target mRNA for HTT and have been demonstrated to be effective in diseased mouse models (Kordasiewicz et al., 2012).

Moreover, ASOs can be used also to target specific region of mRNA, modulating its splicing and reducing protein expression, as it has been shown for spinal muscular atrophy (SMA). Indeed, it has been demonstrated that ASOs designed to promote the inclusion of exon 7 in SMN2 gene were able to compensate the loss of the mutated SMN1, modulating the mRNA splicing. This is also the first FDA-approved treatment for SMA (Chiriboga et al., 2016; Wurster & Ludolph, 2018).

Due to their wide use, they were used also for prion diseases and a recent study revealed that an ASO designed against PrP^C was able to increase prion-infected mice survival time, acting in a sequence-specific manner (Raymond et al., 2019).

However, despite all these encouraging results, to be effective ASOs need to overcome the problem of the intrinsic instability of the phosphodiester linkage to nucleases. To do so, ASOs have been subjected to two sequential modifications: first of all, they have been modified using a phosphorothioate (PS) instead of one non-bridging phosphate oxygen atom, to make the backbone more stable to the degradation (C. A. Stein, Subasinghe, Shinozuka, & Cohen, 1988), and then they have been modified at the 2' position of the sugar moiety, introducing 2-O-methylnucleosides to increase their tolerability and the possibility to be used in humans (Goel et al., 2006).

Despite all these modifications, their applicability for neurodegenerative disorders is still limited by the presence of BBB and the problems derived from the delivery system.

Thus, further modifications and implementations are needed in order to be used in humans.

1.6 *IN VITRO* AND *IN VIVO* MODELS FOR PRION DISEASES

Cell lines and cell-based *in vitro* models for prion disorders are widely used to study these pathologies.

Cell-lines represent a good model to study prion disorders; first of all, they are low costs, then they represent a simple model to be reproduced and standardized and they are also easily to manipulate. However, as a very simplified and *in vitro* model not always corresponds to what happens in human body.

Moreover, it has been shown that very few cell lines are permissible to prion infection and it has also been demonstrated that the infection susceptibility is exclusively limited to the mouse-adapted prion strains, with the only exception of RK13 cells, in which the expression of the ovine PrP^C render them permissible to sheep scrapie agent infection (Vilette, 2008).

The first cell line able to reproduce a stable prion infection was the Scrapie Brain Model (SBM) (Clarke & Haig, 1970) derived from brain tissue of mice inoculated with the Chandler strain of mouse-adapted scrapie prions (Chandler, 1961).

However, SBM lack of a control since it derives from infected tissue; thus, later on the goal was to infect immortalized cell lines with prions.

After that moment different cell lines, both neuronal and not neuronal, have been successfully infected exposing them to brain homogenates from infected animals (**Table 4**).

Until now, any murine glia-based cell culture models have been generated to propagate mouse-adapted prions, leaving a gap on the understanding of prion diseases, given the important role played by brain non-neuronal cells in disease pathophysiology.

However, recently a new study revealed for the first time the stable prion infection in immortalized mouse astrocytes (C8D) (Tahir et al., 2020).

Moreover, another recent study highlighted the possibility to stably infect an immortalized human cell line (SH-SY5Y) with prions, overcoming the risk of infection to humans. Basically, in the study the authors deleted the *PRNP* gene and then they substituted it with the ovine one, which is innocuous for humans (Avar et al., 2020).

Cell line	Cell type	Animal of origin	Prion strain	References
Neuron-like				
SMB-PS	Mesoderm-derived brain cells	Mouse	RML, 139A, 22F, 79A	Birkett et al., (2001) and Clarke and Haig, (1970)
N2a (PK1, R33)	Neuroblastoma	Mouse	RML, 22L, 139A, Fukuoka-1	Butler et al., (1988); Klohn et al., (2003) and Mahal et al., (2007)
GT1	Hypothalamus	Mouse	RML, 22L, 139A, Fukuoka-1	Nishida et al., (2000); Nishida, Katamine, and Manuelidis, (2005) and Schätzl et al., (1997)
CAD5	Catecholaminergic	Mouse	RML, ME7, 22L, 301C, 139A, 79A, RML[IND24]	Berry et al., (2013); Mahal et al., (2007) and Oelschlegel et al., (2012)
SN56	Septum	Mouse	RML, 22L, ME7	Baron, Magalhaes, Prado, and Caughey, (2006)
PC12	Pheochromocytoma	Rat	139A, ME7	Rubenstein et al., (1984), Rubenstein et al., (1992)
CRBL	Cerebellar (p53 ^{-/-})	Mouse	RML	Mays et al., (2008)
1C11	Neuronal stem cell	Mouse	RML, 22L, Fukuoka-1	Mouillet-Richard et al., (2008)
Non-neuronal				
L929 (LD9)	Fibroblast	Mouse	RML, ME7	Mahal et al., (2007); Vorberg, Raines, Story, et al. (2004b)
NIH-3T3	Fibroblast	Mouse	RML, 22L, ME7	Vorberg, Raines, Story, et al. (2004b)
C2C12	Myoblast	Mouse	RML, 22L, ME7	Dlakic et al., (2007) and Herbst et al., (2013)
MSC 80	Schwann cell	Mouse	RML	Follet et al., (2002)
MG20	Microglia	PrP-over-expressing mouse	RML, ME7	Iwamaru et al., (2007)
Genetically engineered cells				
N2a#58	N2a cells over-expressing MoPrP	Mouse	RML, 22L, 139A	Nishida et al., (2000)
HpL3-4	Hippocampal cells stably expressing MoPrP	Mouse (PrP ^{-/-})	22L	Maas et al., (2007)
CF10	Neural stem cells stably expressing MoPrP	Mouse (PrP ^{-/-})	22L	McNally, Ward, and Priola, (2009)
NpL2	Hippocampal cells stably expressing MoPrP	Mouse (PrP ^{-/-})	RML, 22L	Marshall et al., (2017)
RK13	Kidney epithelial cells stably expressing MoPrP	Rabbit	RML, 22L, Fukuoka-1, M1000	Courageot et al., (2008) and Lawson et al., (2008)

Abbreviations: PK, proteinase K; RML, Rocky Mountain Laboratory.

Table 4. Summary of the cell lines used as *in vitro* models for prion disorders (Krance et al., 2020).

As already mentioned, immortalized cell-lines are a very simplified model to study prion disorders, especially for the absence of the diverse cell populations present in the CNS.

Thus, primary cells, organotypic slices and neurospheres have been extensively used to complete the puzzle, since they are also less expensive and easier to be manipulated respect to *in vivo* mouse models (Cronier, Laude, & Peyrin, 2004; Falsig et al., 2008; Giri et al., 2006; Victoria, Arkhipenko, Zhu, Syan, & Zurzolo, 2016).

However, some limitations occur: first of all, the non-dividing nature of neuronal cells and the non-proliferating nature of organotypic slices impact on their lifespan in culture, limiting also

the time for prion replication. Indeed, it is not always easy to discriminate the newly generated PrP^{Sc} from the possible residual inoculum.

To overcome the problem of proliferation, neurospheres represent a good model, but they are extremely difficult to generate, manipulate, and reproduce.

In this scenario animal models remain the best tool to study prion diseases, as only they permit a complete and extensive overview of clinical phenotypes, neuropathological characteristics, transmission barriers, and the role of pathogenic mutations (Brandner & Jaunmuktane, 2017).

At the beginning, the experiments have been conducted on wild-type and inbred mice. Among these mice the most widely used are: C57Bl/6L, C57Bl/6N, C57BL/10, FVB, and 129/Ola, while RIII, VM, NZW, and CD1 are less widely used. They were used to transmit sheep scrapie and adapt it to be propagated (Brandner & Jaunmuktane, 2017).

However, with the advent of transgenic mouse models the research of prion disorders has been drastically changed.

Indeed, immediately after the generation of *Prnp* null mice (Bueler et al., 1993), they were used to generate transgenic mouse models, crossing them with ones expressing human PrP carrying the desired mutation to study and giving a deep understanding of human prion disorders (Asante, Gowland, Linehan, Mahal, & Collinge, 2002).

However, different mouse lines express different PrP levels and different reads-out on incubation time and prion replication, thus chimeric mouse models (MHu2M) have been developed to overcome these issues, even if they poorly recapitulate other aspects of human prion disease (Telling et al., 1994).

To conclude, the appearance of the Cre-lox recombination system allowed the generation of conditional knock-out/knock-in mouse models to modify PrP expression, and the investigation of the mechanism at the basis of prion conversion (G. Mallucci et al., 2003).

1.7 SERPIN SUPERFAMILY

Serpins are the largest and most widely distributed superfamily of protease inhibitors (Law et al., 2006). They have been discovered in 1980 by Hunt and Dayhoff, when they found similarities between ovalbumin and two human proteins, antithrombin and α 1-antitrypsin (Hunt & Dayhoff, 1980).

The name of this superfamily is an acronym standing for **SER**in **P**rotease **INH**ibitors, derived from their main function; however, not all the members of this family act in the same way.

In fact, this family is composed by a multitude of proteins which are all similar from a structural point of view, but they exert different functions (Irving, Pike, Lesk, & Whisstock, 2000).

Indeed, a lot of serpins do not act as inhibitors but rather as chaperones, hormone transporters or tumour suppressors (Nagata, 1996; Pemberton, Stein, Pepys, Potter, & Carrell, 1988; Zou et al., 1994) and they are involved in a lot of physiological functions, like blood coagulation, immunity and inflammation (Heit et al., 2013).

Serpins have been found in all the five kingdoms of life and around 1500 sequences have been identified (Silverman et al., 2001).

Serpin genes are found in cluster in the same chromosomes, reflecting gene duplications and a potential common precursor. Interestingly, despite their chromosomal proximity, they are functionally divergent (Heit et al., 2013).

In Eukaryotes, according to their structural similarity, they are divided into the so-called clades, from A to P. Human serpins are grouped in the first nine clades (A-I) and thirty out of thirty-seven act as inhibitors (Gettins & Olson, 2016).

The two largest clades are extracellular clade A (13 members in chromosome 1, 14, X) and intracellular clade B (13 members on chromosome 18 and 6) (Silverman et al., 2001).

Mouse serpins account for 60 functional genes, many of which are orthologous of the human SERPIN gene and some have been expanded into multiple paralogous genes (Heit et al., 2013).

Serpins are widely distributed throughout the body, even if liver represents the major site of their expression and production.

The structure is well conserved among the members of serpins family; they consist of 350-400aa with a molecular weight variable from 40kDa to 100kDa, depending on the number of glycosylations (Heit et al., 2013; Sanrattana, Maas, & de Maat, 2019).

From a structural point of view, they are made of 8-9 α -helices (from hA to hI) and 3 β -sheets (A,B,C), but the most important part is the Reactive Center Loop (RCL), which represents the active site where the inhibition process takes place (Law et al., 2006).

In fact, in the native state of serpins the RCL is exposed to function as a “bait” for the target proteases, inhibiting their activity by the binding of their active site and the formation of a stable complex (**Figure 15**) (Gettins & Olson, 2016; Law et al., 2006; Silverman et al., 2001).

As inhibitors they are considered promiscuous proteins since they present more than a target enzyme, even though it seems that all the target enzymes belong to the same cascade (Sanrattana et al., 2019).

1.7.1 Mechanism of inhibition

Serpins use the so called ‘Stressed-to-Relaxed (S-to-R) transition’ to inhibit their target proteases. In fact, the native serpins are trapped into an intermediate, metastable state, which results in a dramatic increase in thermal stability (Law et al., 2006).

In the native state, serpins’ RCL is exposed and available to bind to their target proteases.

However, a more stable conformation, called the latent state, exists. In this conformation the RCL is inserted into the centre of β -sheet A, expanding it to a six stranded antiparallel-sheet as the fourth strand, with the concomitant extraction of β -strand C1 to permit the insertion of s4A (Gettins & Olson, 2016).

However, the latent conformation does not possess inhibitory activity, so it has been suggested that this transition to latency might be used as an important control mechanism in regulating homeostasis in certain serpin (Law et al., 2006).

Concerning the inhibition mechanism, the initial step expects the formation of a non-covalent complex between protease and serpin. Once the protease has been bound to serpin, the subsequent cleavage allows the energetically favourable RCL insertion into β -sheet A.

At this point, two different pathways can occur: on one hand, thanks to the S-to-R transition, the protease active site can be disrupted by the formation of a final covalent complex with serpin and the energy required for this translocation it is thought to come from the greater stability of the cleaved conformation of serpin (Gettins & Olson, 2016); on the other hand, serpins can escape from the formation of the metastable state, remaining inactive with the RCL inserted into the β -sheet A, and the target protease free to be active (**Figure 15**) (Law et al., 2006).

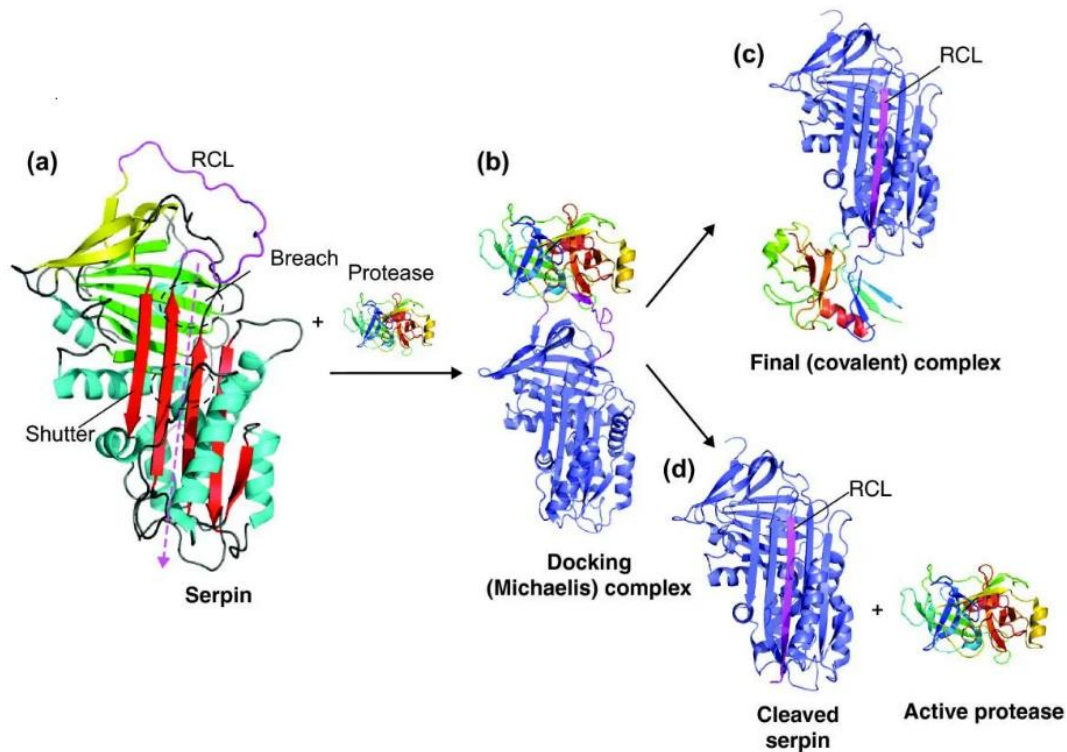


Figure 15. Serpins mechanism of inhibition. (a) Representation of native serpin structure with sheet A (red), sheet B (green), sheet C (yellow), helices (hA-hI) (light blue) and the reactive center loop (RCL) (magenta). (b) Formation of the Michaelis-like complex between the serpin and the target protease (multicolors) docked onto the RCL. Upon docking, two possible pathways can occur: the serpin can undergo the S to R transition, and the protease hangs distorted at the base of the molecule, resulting in the final serpin-enzyme complex (c) or the serpin can escape the conformational trap structure, forming an inactive and cleaved serpin (with the RCL inserted into the structure as a fourth β -sheet A) and an active protease (modified from (Law et al., 2006)).

1.7.2 SERPINA3/SerpinA3n gene and structure

Human SERPINA3 (also known as ACT which stands for 1-antichymotrypsin) is a 66kDa glycoprotein belonging to the serine protease inhibitor family of acute phase proteins; it belongs to the clade A and among the serpins of this group it is one of the extracellular proteins (C. Baker, Belbin, Kalsheker, & Morgan, 2007; Ianni et al., 2010).

It is encoded by a single gene present on chromosome 14q32.1, and it has been shown that it undergoes a considerable expansion in mouse, as well as SERPINA1, as results of multiple gene duplication events. In fact, mouse clade A3 serpin is represented by a cluster of 14 genes (named Serpina3a-n) located on chromosome 12F1 (Forsyth, Horvath, & Coughlin, 2003).

During this expansion process there is a high degree of overall sequence similarity in the elements surrounding the divergent RCL, and this leads to a variable specificity to different target protease (Forsyth et al., 2003).

It has been shown to inhibit several proteases like chymotrypsin, cathepsin G, mast cell chymases, kallikrein 2 and 3 among others (C. Baker et al., 2007; Kalsheker, 1996; Law et al., 2006).

This serpin is normally found in blood, liver, kidney, and lung (C. Baker et al., 2007) but it has been shown to be present also in the brain, where the astrocytes represent the main source of production (Gopalan, Wilczynska, Konik, Bryan, & Kordula, 2006).

Among the 14 different members present in mouse clade A3 gene cluster, SerpinA3n has been hypothesized to be the functional orthologue of human anti-chymotrypsin and the two genes share around 61% of homology (Horvath et al., 2005).

As SERPINA3, SerpinA3n is widely distributed throughout the body with a high expression in thymus, spleen, lung, testis but also in the brain, where as well as its orthologue in human, astrocytes are the main site of production (Horvath, Forsyth, & Coughlin, 2004; Pasternack, Abraham, Van Dyke, Potter, & Younkin, 1989).

Regardless the sequence homology, SerpinA3n presents a difference in the structure at the level of the protease specificity determining region (RCL), where a Methionine is substituted by a Lysine (Horvath et al., 2005).

It inhibits a lot of proteases, like chymotrypsin, trypsin, Cathepsin G, and human leukocyte elastase, taking part in the leukocyte inflammatory response, and Granzyme β in Sertoli cells inhibiting Granzyme β -mediated apoptosis (Horvath et al., 2005; Sipione et al., 2006).

1.7.3 Pathophysiological roles of SERPINA3/SerpinA3n

Both SerpinA3n/SERPINA3 are involved in the same physiological processes as complement cascade, apoptosis, wound healing, inflammation, and extracellular matrix remodeling. Furthermore, together with their biological role, they also share other similarities as the overexpression in some pathologies (Aslam & Yuan, 2019).

In humans, serpin polymerization can cause different conformational diseases called serpinopathies, including angioedema, thrombosis, emphysema, cirrhosis, and familial dementia (Heit et al., 2013). Nonetheless, other serpin-related diseases are caused by null mutation or point mutations that alter the inhibitory function or specificity of serpins (P. E. Stein & Carrell, 1995).

SERPINA3 has been shown to be dysregulated in different pathologies like chronic obstructive pulmonary disease, Alzheimer's disease, stroke, Parkinson's disease, cystic fibrosis and more (C. Baker et al., 2007).

Its overexpression has also been related to the progression and severity of multiple types of cancer, as melanoma, endometrial cancer, colon cancer, breast cancer, gliomas (Kulesza et al., 2019; Luo et al., 2017; G. D. Yang et al., 2014; Zhou, Cheng, Tang, Martinka, & Kalia, 2017); in fact, it has been demonstrated that the silencing of SERPINA3 leads to the inhibition of the migration and invasion of metastasis in liver and colon cancer (Cao et al., 2018).

Moreover, in prostate cancer complex of SERPINA3 with Prostate-Specific Antigen (PSA) is used as clinical marker (Stephan et al., 2002).

Conversely, in hepatocellular carcinoma (HCC) tissues and cells, it has been shown that SERPINA3 is downregulated and its overexpression leads to hepatocellular proliferation inhibition (Santamaria et al., 2013; Zhu et al., 2017).

Moreover, being acute phase proteins, SERPINA3/SerpinA3n can take part in several inflammatory diseases; in fact, recent studies highlighted their involvement in retinal and hypothalamic neuroinflammation, allergic airway inflammation, atherosclerosis and myocarditis (Sergi et al., 2018; Wagsater et al., 2012).

An extensive part of research has also been focused on the role of SERPINA3 in AD; in particular, it has been shown that this serine protease inhibitor is upregulated in the brain of AD patients by the action of different inflammatory mediators, as by IL-1, TNF, OSM, IL-6/ soluble IL-6 complexes (C. Baker et al., 2007; Das & Potter, 1995; Kordula et al., 1998).

Moreover, other studies reported a strong association between SERPINA3 and A β (Abraham, Selkoe, & Potter, 1988), as further investigated with *in vitro* experiments where SERPINA3-A β complexes formation has been assessed (P. E. Fraser, Nguyen, McLachlan, Abraham, & Kirschner, 1993; Janciauskiene, Rubin, Lukacs, & Wright, 1998).

Also, *in vivo* experiments showed that a great upregulation of this serpin leads to A β peptide deposition and cognitive impairments (Nilsson et al., 2004; Nilsson et al., 2001).

Dysregulated levels of SERPINA3 have also been found in motor cortex of sALS patients and frontal cortex of MSA brains (Mills, Ward, Kim, Halliday, & Janitz, 2016; Sanfilippo et al., 2017).

Moreover, it has been reported that also individuals affected by schizophrenia or bipolar disorders presented dysregulated levels of this serpin, as a downstream activation of the immune system inflammatory response (Fillman, Sinclair, Fung, Webster, & Shannon Weickert, 2014).

As already mentioned, SerpinA3n is capable to inhibit Granzyme β in Sertoli cells (Sipione et al., 2006) and this function has been related with its ability to decrease the rate of aortic rupture and death in mouse model of abdominal aortic aneurysm, via inhibition of the granzyme - mediated decorin degradation and enhancing collagen remodeling (Ang et al., 2011).

Moreover, since Granzyme β can induce T-cell mediated neurotoxicity and it has been also found to be upregulated in Multiple Sclerosis lesions, it has been demonstrated that using SerpinA3n it is possible to block Granzyme β -mediated neurotoxicity, inducing neuroprotection for neurons (Haile et al., 2015; Haile et al., 2011). Indeed, SerpinA3n treatment reduce axonal and neuronal injury in an Experimental Autoimmune Encephalomyelitis model and maintain myelin integrity, reducing the severity of the disease (Haile et al., 2015).

1.7.4 SERPINA3/SerpinA3n role in prion diseases

Concerning prion diseases, several studies revealed that SERPINA3/SerpinA3n are upregulated in different models of prion diseases.

Indeed, SerpinA3n mRNA levels have been reported to be highly expressed in different mouse models of prion disorders (Campbell, Eddleston, Kemper, Oldstone, & Hobbs, 1994; Dandoy-Dron et al., 2000; Riemer et al., 2004; Xiang et al., 2004). Moreover, it has been shown that this serine protease inhibitor seems to follow the progression of the pathology, increasing during the course of the disease (Vanni et al., 2017).

The same upregulation has also been reported for the human form of this serpin, SERPINA3. Indeed, it has been shown that this serpin was highly upregulated also in other models of prion-disorders, like BSE-infected cynomolgus macaques and rodents (Barbisin et al., 2014; Chen et al., 2017).

Note of worthy, the overexpression of SERPINA3 has also been reported in humans, indeed it has been shown that SERPINA3 was upregulated both at the transcript and the protein levels in prefrontal cortex of post-mortem brains derived from different prion disorders (Vanni et al., 2017). Moreover, analysis from CNS of sCJD patients revealed elevated levels of SERPINA3 RNA together with upregulated levels of the protein in the Cerebrospinal fluid (CSF) and urine of the same patients (Miele et al., 2008).

1.8 NEUROINFLAMMATION AND PRION DISEASES

Neuroinflammation has not immediately been associated with prion disorders. In fact, an immune activation has been always related to neurodegenerative disorders like AD, PD, ALS, multiple sclerosis and HD, but also in schizophrenia, bipolar disorders and brain injury (Fillman et al., 2014; Y. Lee et al., 2014; Ransohoff, 2016; Wofford, Loane, & Cullen, 2019) .

This was due to the fact that the CNS is an immune-privileged site, and as such the immune response acts to limit bacterial and viral infections (Amor et al., 2014).

However, one of the main hallmarks of prion diseases is the activation of glial cells upon prion infection with the consequent production of many inflammatory mediators, as cytokines and chemokines (C. A. Baker, Lu, Zaitsev, & Manuelidis, 1999; Campbell et al., 1994; Tribouillard-Tanvier, Striebel, Peterson, & Chesebro, 2009; Van Everbroeck et al., 2002).

The exact role for glial cells in prion diseases is still not completely understood, but it seems that they take part in the degeneration of these disorders (C. A. Baker et al., 1999; C. A. Baker, Martin, & Manuelidis, 2002; Campbell et al., 1993). In fact, several studies demonstrated that when exposed to aggregated PrP peptide p106-126 both astrocytes and microglia become neurotoxic (D. R. Brown, Schmidt, & Kretzschmar, 1996; Song et al., 2012; Veerhuis et al., 2002).

Moreover, glial cells are known to be involved in many other disorders affecting the CNS (like ischemia, degenerative processes, infections among others) and it has also been shown that activated glia is able to produce both neurotrophic and neurotoxic factors, which could lead to its role in these diseases (Rock et al., 2004).

To activate glial cells, prions should interact with astrocytes or microglia. Several studies reported a possible involvement of different receptors, as pattern-recognition receptors or G protein-coupled receptor formyl peptide receptor-like 1 (FPRL1), in this process since they were observed to take part in the cytokines induction after PrP peptide p106-126 and Amyloid-beta exposure (Fassbender et al., 2004; Le et al., 2001).

Thus, it seems reasonable to believe that upon prion infection several inflammatory responses are activated via the activation of glial cells.

1.8.1 Neuroinflammation, SERPINA3/SerpinA3n and prion diseases

Glial cells play a key role in the establishment of neuroinflammatory responses in several disease, like neurodegenerative disorders, ischemia, brain injury among others.

Indeed, during the course of these disorders both microglia and astrocytes are activated and consequently they produce different proinflammatory mediators, as chemokines and cytokines, which take part in neuroinflammation.

In fact, it has been shown that proinflammatory mediators produced by reactive astrocytes take part in hippocampal neuroinflammation, contributing to CNS diseases (Burda & Sofroniew, 2014).

Importantly, SERPINA3/SerpinA3n are mainly produced by reactive astrocytes in the brain and it has been shown that many cytokines, particularly IL-1 and IL-6, induce a significant increase in SERPINA3 expression (C. Baker et al., 2007; Campbell et al., 2014).

Moreover, SERPINA3/SerpinA3n are acute phase genes and, as such, they are involved in inflammatory responses (Zamanian et al., 2012).

Thus, since SERPINA3/SerpinA3n have been found greatly upregulated during prion infection and thus prion accumulation is associated with the activation of glial cells, there is a close correlation between all these elements, suggesting a possible implication of these serine protease inhibitors in prion pathogenesis.

1.9 THE JAK-STAT PATHWAY

The Janus kinase/signal transducers and activators of transcription (JAK/STAT) pathway is one of the many pathways in animals used to transduce signal from membrane into the cells.

It represents the principal target for cytokines and growth factors (Leaman, Leung, Li, & Stark, 1996) as, CNTF, LIF, IL6, IL1 β and others (Kisseleva, Bhattacharya, Braunstein, & Schindler, 2002; Nicolas et al., 2013; Rajan, Symes, & Fink, 1996).

The pathway is activated when JAKs are bound by the ligands, which induce the trans-phosphorylation of two JAK members located in proximity one to each other. Then, the phosphorylated JAK can phosphorylate STAT proteins that can shift from the cytoplasm to the nucleus, determining the transcription of several target genes (Rawlings, Rosler, & Harrison, 2004).

In mammals there are four members of JAKs and seven members for STATs (Darnell, 1997).

Among the different signalling activated by this cascade, it has been reported that the canonical JAK/STAT3 signalling pathway is the one involved in a variety of processes of inflammatory and anti-inflammatory signalling (Jung et al., 2015; Nabavi et al., 2019; Nicolas et al., 2013; Porro, Cianciulli, Trotta, Lofrumento, & Panaro, 2019; X. Yang et al., 2010).

Moreover, it is known to be implicated in other processes, like astrogliosis (O'Callaghan, Kelly, VanGilder, Sofroniew, & Miller, 2014); in particular, it has been shown that activated STAT3 is present in reactive astrocytes in acute injury (Ceyzeriat, Abjean, Carrillo-de Sauvage, Ben Haim, & Escartin, 2016) but also in neurodegenerative disorders like AD, HD (Ben Haim et al., 2015) and prion disorders (Na et al., 2007)

Many inflammatory mediators produced during prion infection are also activators of the JAK-STAT pathway and it has been shown that in scrapie-infected mice there was the upregulation of some players of JAK-STAT pathway at the protein and transcript levels, in particular phosphorylated Stat1 (pStat1) and pStat3 (Carroll, Striebel, Race, Phillips, & Chesebro, 2015; Na et al., 2007). Interestingly, functional STATs binding sites were found in the regulatory regions of SERPINA3 gene (C. Baker et al., 2007) and it has been shown to regulate its expression (Kulesza et al., 2019).

Several studies by Campbell and colleagues, highlighted the role of the IL6 in the activation of the JAK-STAT pathway in the pathogenic brain (Campbell, 1998; Campbell et al., 1993; Campbell, Hofer, & Pagenstecher, 2010).

IL6 can activate this pathway *via* two different signaling: the classic and the trans-signaling (Scheller, Chalaris, Schmidt-Arras, & Rose-John, 2011), which differ only for the receptor.

In the first one, IL6 binds to IL6-receptor alpha (IL6R α), while in the second one it binds to the soluble form of the receptor (s)IL6R (Rose-John, Scheller, Elson, & Jones, 2006)

However, in both cases the binding induces the oligomerization of the gp130, which gives rise to the pathway activation (Heinrich et al., 2003).

In 2014, Campbell and collaborators generated bigenic mice (termed *GFAP-IL6/sgp130* mice) characterized by an astrocytes-limited production of IL6 and the inhibitor of IL6 trans-signalling. They observed that mice expressing IL6 trans-signalling inhibitor, showed decreased levels of pSTAT3 and SerpinA3n transcripts and decreased levels of gliosis (Campbell et al., 2014).

Thus, since prion disorders are characterized by a strong gliosis and, recently, a great upregulation of SERPINA3/SerpinA3n has been found, we can hypothesis the IL6 signalling *via* the JAK/STAT3 pathway as the missing link in the SERPINA3/SerpinA3n overexpression upon prion infection.

2. AIM OF THE STUDY

Prion diseases are rare and fatal neurodegenerative disorders caused by the conformational conversion of the cellular prion protein (PrP^C) into the pathological isoform (PrP^{Sc}), which has the unique feature to be infectious.

Throughout the years, numerous attempts have been tried to find a cure, without success.

Until now, all the therapeutic strategies developed have been targeted to the inhibition of the PrP^C-to-PrP^{Sc} conversion but none of them was successful in clinical practice.

Moreover, mounting evidence highlighted the involvement of other genes in the development of prion disorders, and several studies reported the overexpression of SERPINA3/SerpinA3n levels in different models of prion diseases. Thus, we tried to elucidate the involvement of these serine protease inhibitors in prion pathogenesis.

Indeed, we hypothesized that SERPINA3/SerpinA3n can determine the inhibition of the protease, or proteases, generally involved in prion clearance.

So, we decided to test our hypothesis using anti-SERPINA3 small molecules to inhibit the action of this serine protease inhibitor, observing what happen to prion accumulation.

Here we want to propose a novel therapeutic strategy to treat prion disorders, without interfering with PrP^C and/or PrP^{Sc}.

Moreover, since little is known about the molecular mechanism at the basis of this upregulation, we decided to investigate how SERPINA3/SerpinA3n are upregulated upon prion infection.

In recent years, accumulating evidence reported the involvement of SERPINA3/SerpinA3n in different neuroinflammatory diseases, including prion diseases, but the mechanism controlling their expression have not been elucidated yet.

Thus, we decided to study the pathway involved in the upregulation of these serine protease inhibitors upon PrP^{Sc} deposition, focusing on the JAK/STAT3 pathway.

3. MATERIALS AND METHODS

3.1 Immortalized cell lines

Mouse neuroblastoma cell line, either not-infected (N2a) and chronically infected with Rocky Mountain Laboratory (ScN2a RML) or with 22L prion strain (ScN2a 22L), were grown in Minimal Essential Medium (MEM)-1% L-glutamax complemented with 10% fetal bovine serum (FBS), 1% non-essential amino acids (NEAA), and 1% penicillin-streptomycin.

Immortalized mouse hypothalamic neurons (GT1) and chronically infected GT1 cells, with both RML and 22L prion strains (ScGT1 RML and ScGT1 22L), were grown in Dulbecco's modified Eagle's medium (DMEM)-1% GlutaMAX supplemented with 10% FBS and 1% penicillin-streptomycin. All cell lines were cultivated in 10 and/or 6 cm² Petri dishes at 37 °C under 5% CO₂.

3.2 Mouse models

Age- and sex-matched CD1 mice (CrI:CD1(ICR) strain code 022, Charles River) were used for RT-qPCR, WB analysis and as source of prions to infect de novo primary mixed cell cultures from FVB mice. Rocky Mountain Laboratory (RML) prion infected brain homogenate was prepared at a 10% w/v in phosphate-buffered saline (PBS). 2.5µL of 10% brain homogenate was stereo-tactically injected in the hippocampus of 2-months old outbred CD1 mice (n = 8). Not inoculated age- and sex-matched CD1 mice were used as controls (n = 8). Pre-symptomatic animals (n = 4) were sacrificed 3 months post inoculation (3mpi), while terminal stage animals (n = 4) were monitored daily for clinical signs of prion disease and sacrificed at the end stage (5mpi). Adult animals were sacrificed with CO₂, brains were extracted, immediately frozen in liquid nitrogen and stored at -80 °C. Brains of prion-infected and age-matched controls were either homogenized for WB analysis or subjected to RNA extraction.

For the pharmacokinetic study male C57BL/6 mice, weighing 22-24 g, were used (Charles River). All procedures were performed in accordance with the Ethical Guidelines of European Communities Council (Directive 2010/63/EU of 22 September 2010) and accepted by the Italian Ministry of Health. All efforts were made to minimize animal suffering and to use the minimal number of animals required to produce reliable results, according to the "3Rs concept". Animals were group-housed in ventilated cages and had free access to food and water. They were

maintained under a 12-hour light/dark cycle (lights on at 8:00 am) at controlled temperature ($21^{\circ}\text{C} \pm 1^{\circ}\text{C}$) and relative humidity ($55\% \pm 10\%$).

3.3 Dissociated neurons protocol

Primary cell cultures were prepared from hippocampal neurons of FVB mice. All procedures were approved by the local veterinary authorities and performed in accordance with the Italian law (decree 26/2014) and the EU guidelines (2007/526/CE and 2010/63/UE).

Hippocampi were dissected from 0–2-day-old postnatal animals. The isolated tissue was quickly sliced and digested in a digestion solution containing Trypsin (Sigma-Aldrich) and DNase (Sigma-Aldrich). The reaction was stopped with Trypsin inhibitor (Sigma-Aldrich) and cells were mechanically dissociated in a dissection medium containing DNase. After centrifugation, the cell pellet was resuspended in the culture medium and distributed in 6 well Multiwell (Falcon), or on coverslips (12 mm diameter), previously coated with polyornithine (50 mg/mL, Sigma-Aldrich). Plating was carried out at a density of 150.000 cells per well (in this case the cells were concentrated in the central region of the well) or coverslip.

Hippocampal neurons were cultured in culture medium consisting of MEM (Gibco), supplemented with 35 mM glucose (CarloErba Reagents), 1 mM Apo-Transferrin, 15 mM HEPES, 48 mM Insulin, 3 mM Biotin, 1 mM Vitamin B12 (Sigma-Aldrich) and 500 nM Gentamicin (Gibco) and 5-10% dialyzed FBS (Gibco). Two days after plating, 2 μM cytosine- β -d-arabinofuranoside (Sigma-Aldrich) was added to the culture medium, to reduce the growth of glial cells. The cells were maintained at 37°C , in a humidified atmosphere with 5% CO_2 .

3.4 *De novo* infection protocol of immortalized cell lines and primary cell cultures

ScGT1 RML cells were grown at confluence and lysed using 130watt ultrasonic processor with thumb-actuated pulser for small volume applications (Sonic Material). The resulted lysates (coming from three 10 cm^2 Petri dishes) were added to the medium of GT1 cells, grown at 10-20% of confluence. Medium was refreshed three days after infection and, after seven days of growing, cells were split for four times and at each passage they were lysed in order to be tested for PrP^{Sc} presence. For primary cultures infection, brain homogenates of CD1 mice infected with RML prions were used to infect primary mixed cultures, following the protocol published in 2016 by Victoria et al. (Victoria et al., 2016).

3.5 Compounds

All the compounds were dissolved in 100% ethanol (library A-U) and dimethyl sulfoxide (DMSO) (library 1-8), to a 200 mM stock solution. From these stock solutions, intermediate dilutions were prepared as needed. For cell treatment, stock solutions were further diluted in PBS 1X to a final concentration of 10mM. Each compound was then diluted in cell culture medium to reach a final concentration of 20 or 40 μ M. In the cell medium, the final concentration of DMSO was never above 0.1%. Detailed treatment conditions are provided in following methods. Mock controls were treated with vehicle only, under the same conditions.

3.6 Structure-based Virtual Screening (SBVS) and similarity search

The X-ray structure of SERPINA3 (pdb: 1AS4) (Lukacs, Rubin, & Christianson, 1998) was used as receptor for our SBVS campaign. The protein was prepared using the protein preparation wizard protocol (Sastry, Adzhigirey, Day, Annabhimoju, & Sherman, 2013) implemented in Maestro. Hydrogens were added and charges and protonation states were assigned titrating the protein at pH 7. Short minimization steps were performed to relieve the steric clashes. The grid, used for subsequent docking calculations, was centered on a pocket at the interface of β -sheets B and C and α -helix H. Such pocket, called sB/sC pocket, has been identified for plasminogen activator inhibitor 1 (pdb: 4G8O) and it is deemed to be conserved also for other serpins (S. H. Li et al., 2013). An in-house collection of ~15,000 nonredundant and diverse drug-like molecules was employed as virtual library. The ligands were prepared using the LigPrep tool, implemented in Maestro. Hydrogens were added and ionization states were generated at pH 7.4 \pm 0.5. The library was filtered to retain only the molecules that obey Lipinsky's rules (Lipinski, 2004) and that do not bear reactive functional groups. The SBVS was performed through Glide software (Friesner et al., 2004), using Single Precision and retaining one pose for each ligand. After a visual inspection of the best scored poses, a first set of compounds (i.e., A-U) was selected for biological assay. Finally, based on the common structural features of the most active compounds (i.e. G and H), a similarity search was performed on the virtual library using Canvas (Duan, Dixon, Lowrie, & Sherman, 2010). A second set of compounds (i.e., 1-8), bearing the 5-aminopyrazole scaffold, was selected for biological assays. Schrödinger suite version 2015-4 was used for our calculations.

3.7 Assessment of cell viability and MTT assay

Both un-infected and chronically infected, with RML or 22L prion strain, N2a and GT1 cells, were maintained in culture and grown to 80% confluence. The medium was changed, and the cells were detached. Cell density was determined by cell counting using Scepter™ 2.0 Cell Counter (Millipore) and adjusted to 1×10^4 cell/mL with MEM (N2a, ScN2a RML and ScN2a 22L) or 2×10^4 with DMEM (GT1, ScGT1 RML and ScGT1 22L). Cell suspension was added to each well of a 96-well, tissue culture-treated, clear bottom, plate (Costar) and cells were allowed to settle for 1 day at 37 °C under 5% CO₂ prior to the treatment with compounds. Each compound was diluted in the cell medium to a final concentration of 20 and 40 μM. After 24 h, cell culture medium was removed and replaced by compound-containing medium. The plate was incubated at 37 °C under 5% CO₂ for 5 days. The Thiazolyl Blue Tetrazolium Bromide (MTT, SIGMA) was diluted in PBS 1X to a working dilution of 5 mg/mL. Cells were incubated with 20μL of MTT solution for 3 h at 37 °C. After incubation, 100μL of 1:1 DMSO/2-Propanol solution was added to each well and the plate was kept at room temperature (RT) for 5 min before reading. The emission intensity was quantified using the EnSpire Multimode Plate Reader (Perkin Elmer). 70% of viability was set as threshold of toxicity.

3.8 Acute and chronic treatment

All the treatments were performed following the dilutions and concentrations described in the compound section (see **paragraph 3.5**). After compounds preparation, cells were treated for four days in acute treatment with only one dosage (at 20 or 40μM) or for one month in chronic treatment with a dosage (at 20 μM) every week and then lysed to perform the experiments. Mock controls were treated with vehicle only (DMSO and ETOH), under the same conditions.

3.9 Collection of conditioned media (CM), cell lysis, PNGase F and Proteinase K (PK) Digestion

For extracellular SerpinA3n detection, conditioned media of un-infected and prion infected N2a and GT1 cell lines were collected, cleared, and concentrated following Gueugneau et al., 2018 protocol. After 24 h incubation in serum-free medium, the CM was cleared by centrifugation (10 min at 300 g followed by 20 min at 2000 g) to discard cell debris. Cleared CM were subsequently concentrated using an Amicon Ultra-4 30 kDa cut-off spin Column (Millipore,

Watford, UK). For intracellular protein detection, after removing the medium, cells were washed with PBS and lysed on ice in lysis buffer (10 mM Tris–HCl pH 8.0, 150 mM NaCl, 0.5% nonidet P-40, 0.5% deoxycholic acid sodium salt). Nuclei and large debris were removed with a centrifugation at 13000 rpm for 3 min at 4 °C in a bench microfuge (Eppendorf, Hamburg, Germany). Protein concentration of cleared cell lysate and conditioned media was determined using the bicinchoninic acid (BCA) protein quantification kit (Thermo Fisher Scientific, Waltham, Massachusetts, USA). For intracellular or extracellular SerpinA3n detection, 100 µg of cell lysate or 50 µg of conditioned medium, respectively, were added into 5X SDS- PAGE loading buffer in a 1:5 ratio. 6 h PNGaseF (New England Biolabs) treatment of conditioned medium was performed starting from 50 µg of protein, following manufacturer's instruction in denaturing reaction condition. For PrP detection, cell lysates were split into two parts. One part was treated with 5 µg of PK (Roche Diagnostics Corp., Mannheim, Germany) at 37 °C for 1 h. The reaction was arrested with 2 mM of phenylmethylsulphonyl fluoride (PMSF, Sigma-Aldrich). The PK-digested samples were precipitated by centrifugation at 55,000 rpm for 75 min at 4 °C in an ultracentrifuge (Beckman Coulter, Brea, California, USA) and the pellet was resuspended in 1X SDS- PAGE loading buffer. The non-PK-digested samples were added into 2X SDS-PAGE loading buffer in a 1:1 ratio. All samples were boiled for 10 min at 100 °C. All samples were stored at -20 °C until further processing or analysis.

3.10 Western blot

Samples were loaded onto 8%, 10% or 12% Bis/Tris Acrylamide gels (NuPAGE, Invitrogen), separated by SDS-Page and transferred to PVDF membrane. The membranes were blocked with 5% non-fat milk in TBST (Tris 200 mM, NaCl 1.5 mM, 1% Tween-20, Sigma-Aldrich). For extracellular SerpinA3n Ponceau S staining of the membrane, before milk blocking, was performed to verify the accuracy of sample loading. For SerpinA3n detection, membrane was incubated with polyclonal SerpinA3n antibody (1:500 R&D Systems) followed by a rabbit anti-goat HRP secondary antibody (1:1000). For PrP detection, anti-PrP Fab W226 (1:5000, recognizing residues 144–152) antibody was used, followed by a goat anti-mouse HRP secondary antibody (1:1000). For Gfap detection, anti-Gfap monoclonal antibody (Sigma-Aldrich 1:1000) and goat anti-mouse HRP secondary antibody (1:1000) were used. pStat3 and total Stat3 were detected with monoclonal anti-pStat3 (Tyr705) antibody (Cell Signaling 1:1000) and polyclonal anti-Stat3 (Sigma-Aldrich 1:1000), followed by goat anti-mouse and goat anti-rabbit HRP secondary antibody (1:1000), respectively. Nuclear fractions were detected

using monoclonal mouse monoclonal anti-Nup62 antibody (Sigma-Aldrich 1:1000) and cytosolic fraction was detected using polyclonal anti- β -Tubulin3 (1:3000, Thermo Fisher), followed by goat anti-mouse and goat anti-rabbit HRP secondary antibody (1:1000), respectively. Monoclonal anti- β -actin-peroxidase antibody (1:10,000 Sigma-Aldrich) and monoclonal anti-Vinculin antibody (Sigma-Aldrich 1:10000) were used to normalize results. The membrane was visualized by chemiluminescence using Amersham ECL Prime (GE Healthcare Life Sciences). Densitometric analysis was carried out using UVIBand software. Data are expressed as mean \pm SD, and the values of the controls are adjusted to 100%. Each experiment was performed in technical duplicates or triples.

3.11 Recombinant full-length mouse PrP production and purification

The mouse construct was expressed in competent BL21 Rosetta2 (DE3) cells Escherichia coli (Stratagene). Freshly transformed overnight culture was inoculated into Luria Bertani (LB) medium and 100 μ g/mL ampicillin and 30 μ g/mL chloramphenicol. At 0.8 OD₆₀₀ expression was induced with isopropyl b-D galactopyranoside (IPTG) to a final concentration of 1 mM. Cells were grown in a BioStat-B plus fermentor (Sartorius). The cells were lysed by a homogenizer (PandaPLUS 2000) and the inclusion bodies were suspended in buffer containing 25 mM Tris-HCl, 5 mM EDTA, 0.8% TritonX100, pH 8, and then in bi-distilled water several times. Inclusion bodies containing MoPrP (23-231) were dissolved in 5 volumes of 8 M guanidine hydrochloride (GdnHCl), loaded onto pre-equilibrated HiLoad 26/60 Superdex 200-pg column, and eluted in 25 mM Tris-HCl (pH 8.0), 5 mM ethylenediaminetetraacetic acid, and 5 M GdnHCl at a flow/rate of 1.5 mL/min. Protein refolding was performed by dialysis against refolding buffer [20 mM sodium acetate and 0.005% NaN₃ (pH 5.5)] using a Spectrapor membrane (molecular weight, 10000 Da). Purified protein was analyzed by SDS-polyacrylamide gel electrophoresis under reducing conditions and Western blot.

3.12 RT-QuIC procedure

After purification, aliquots of the recombinant PrP (Full length MoPrP) (23-231) were stored at -80 °C in 10 mM phosphate buffer (pH 5.8). Before each test, the protein solution was thaw at room temperature and filtered using Millex-GV filter 0.22 μ m (Millipore).

The final reaction volume was 100 μ L loaded into the plate (ViewPlate-96 F TC/50x1B, Perkin Elmer) and the reagents (Sigma) were concentrated as follow: 150 mM NaCl, 0.002% SDS, 1X PBS, 1 mM EDTA, 10 μ M ThT and FLMoPrP 0.2 mg/mL.

The seed consists of sonicated ScN2a-RML cells. Before the sonication, the cells were collected in 100 μ l of PBS 1X, after the sonication the sample was quantified using the BCA assay, in order to use it as a seed (1 μ g of the protein).

After the addition of 10 μ L of seed, the plate was sealed with a sealing film (Perkin Elmer) and inserted into a FLUOstar OPTIMA microplate reader (BMG Labtech). The plate was shaken for 1 minute at 600 rpm (double orbital) and incubated for 1 minute at 45 °C.

Fluorescence readings (480 nm) were taken every 30 minutes (30 flashes per well at 450 nm). A sample was considered positive if at least two out of three wells start the aggregation at the same time of the positive control (moPrP+seed), around 12h of reaction.

3.13 shRNAs production

The shRNA design and production were carried out thanks to the collaboration of Doctor Thanh Hoa Tran. He used the backbone of pHIV-Luc_ZsGreen plasmid to generate the shRNAs used for our experiment of silencing. The shCTRL was created using a short hairpin against Luciferase in the structure, while the shSerpina3n was created using a short hairpin against Serpina3n. The sequencing of both shRNAs was performed using LKO1 or U6 as primers and after the midi prep (Qiagen) the shRNAs were quantified in order to be used for the further experiment.

3.14 Serpina3n shRNA transfection

For the shRNA transfection we plated ScN2a RML cells into 6cm² Petri dishes and we transfected them when the cells reached 50% of confluence, using the Effectene Transfection Reagent (QIAGEN).

We prepared the mix by adding 150 μ L of BUFFER EC and 3 μ g of plasmids into 1.5mL Eppendorf and we mixed them gently. Then, we added to the mixture 8X ENANCHER (24 μ L/mix), we mixed it 10 seconds by vortexing, and we waited 5 minutes.

Then, we added 300 μ L of Effectene and we mixed it gently by pipetting 5 times. We waited 10 minutes and then we added 500 μ L of medium (Optimem), mixing gently by pipetting 2 times.

Then, we added the mix to each plate, drop by drop, and we left it in culture for 24h before changing the medium. After 3 days cells were collected and analysed.

3.15 Stable transfection with plasmid to generate SerpinA3n KO ScN2a cell line

In order to further investigate the role of SerpinA3n we generated KO cell lines, thanks to the collaboration of our post-docs Silvia Vanni and Thanh Hoa Tran. Lipofectamine 2000 was used for all plasmid transfection experiments according to the manufacturer's protocol. Briefly, cells were plated in 96-wells plates for each experiment at a density of 1000 cells/well. Lipofectamine and Optimem medium were mixed and incubated for 5 min, then added to (plasmid + Optimem medium) and kept for 15 mins at room temperature (RT). This solution was added stepwise to cells and gently mixed. Cells were incubated at 37°C overnight, and the medium was replaced by fresh complete medium. Then cells were split a 1:50 into selective medium in the following day. Plasmid for KO were pSPCas9n-SERPINA3N-A, pSPCas9n-SERPINA3N-B

3.16 RNA extraction and Reverse transcription quantitative polymerase chain reaction (RT-qPCR)

After removing the medium, un-infected and prion infected cell lines were washed in PBS and pellet at 12000 rpm for 5 minutes. Cell pellets were resuspended in 1mL TRIzol reagent (Ambion, Life Technologies) following manufacturer's instructions and store at -80°C until further processing. Total RNA was extracted with PureLink[®] RNA Mini Kit (Life Technologies) and on-column DNA digestion was performed using PureLink DNase Set (Life Technologies). RNA was checked for concentration and purity on a NanoDrop 2000 spectrophotometer (Thermo Scientific). For the total RNA from one hemisphere of mouse whole brain tissue, the tissue was homogenized with Stainless Steel Beads 5 mm in Tissue Lyser II (Qiagen), in TRIzol reagent (Invitrogen) following manufacturer's instructions. RNA was extracted with PureLink RNA Mini Kit (Life Technologies) and on-column DNA digestion was performed using PureLink DNase Set (Life Technologies).

cDNA was obtained starting from 3µg of total RNA with 50µM Oligo(dT)20, 10mM dNTP mix, 5X First Strand Buffer, 0.1M DTT, 40 U RNase inhibitor and 200 U SuperScript[®] III Reverse Transcriptase (Life Technologies). A negative control was performed for each sample by omitting the reverse transcriptase (-RT control).

Gene expression assays were performed using qPCR primer sequences (*Gfap*, *Cd86*, *IL-1β*, *IL-6*, *Stat3*, *SerpinA3n*, *Gapdh*, *Tubb3* and *ActB*) and protocol as reported in Vanni et al 2017 and the relative expression ratio (fold change, FC) was calculated using $2^{-\Delta\Delta CT}$ method (Livak & Schmittgen, 2001) as reported in Vanni et al., 2018.

ΔC_T were calculated subtracting the C_T of the reference genes to the C_T of the target genes, both for “test” (prion infected cell) and “calibrator” (un-infected cells). Then, $\Delta\Delta C_T$ were obtained with the ΔC_T of each sample (both of calibrator and test) minus the mean ΔC_T of the population of calibrator samples. Fold change values smaller than 1 were converted using the equation $-1/FC$, for representation.

3.17 Pharmacokinetic

Pharmacokinetic *in vivo* studies

Compound 5 was administered orally (PO) and intravenously (IV) to C57BL/6 male mice at 10 and 3 mg/kg. Vehicle was: PEG400/Tween 80/Saline solution at 10/10/80 % in volume respectively. Three animals per each time point were treated. Blood samples and brains at 0, 15, 30, 60, 120, and 240 min after administration were collected for PO arm. Blood samples and brains at 0, 5, 15, 30, 60, 120 and 240 min after administration were collected for IV arm.

Plasma was separated from blood by centrifugation for 15 min at 1500 rpm at 4°C, collected in an Eppendorf tube and frozen (-80°C). Brain samples were homogenized in Phosphate buffered saline and then split in two aliquots kept at -80 °C until analysis. An aliquot was used for compound brain level evaluation, following the same procedure described below for plasma samples. The second aliquot was kept for protein content evaluation by bicinchoninic acid assay (BCA). Control animals treated with vehicle only were also included in the experimental protocol.

Pharmacokinetic measurements

Plasma samples were centrifuged at 21.100 x g for 15min at 4°C, while homogenized brain samples were vigorously whirled. An aliquot of each sample was extracted (1:3) with cold CH₃CN containing 200nM of an appropriate internal standard. A calibration curve was prepared in both naïve mouse plasma and naïve mouse brain homogenate over a 1nM – 10µM range. Three quality control samples were prepared by spiking the parent compound in both naïve mouse plasma and naïve brain homogenate to 20, 200 and 2000nM as final concentrations. The calibrators and quality control samples were extracted (1:3) with the same extraction solution as the plasma and brain samples. The plasma and brain samples, calibrators and quality control samples were centrifuged at 3.270 x g for 15min at 4°C. The supernatants were further diluted

(1:1) with H₂O, and analyzed by LC-MS/MS on a Waters ACQUITY UPLC/MS TQD system consisting of a Triple Quadrupole Detector (TQD) Mass Spectrometer equipped with an Electrospray Ionization interface and a Photodiode Array λ Detector from Waters Inc. (Milford, MA, USA). Electrospray ionization was applied in positive mode. Compound-dependent parameters as MRM transitions and collision energy were developed for the parent compound and the internal standard. The analyses were run on an ACQUITY UPLC BEH C₁₈ (50x1mm ID, particle size 1.7 μ m) with a KrudKatcher ULTRA HPLC In-Line Filter (0.5 μ m x 0.004in ID) at 40°C, using H₂O + 0.1% HCOOH (A) and CH₃CN + 0.1% HCOOH (B) as mobile phase at 0.1mL/min. A linear gradient was applied starting at 10%B with an initial hold for 0.5min, then 10-100%B in 3min, followed by a hold for 0.5min at 100%B. All samples (plasma and brain samples, calibrators and quality controls) were quantified by MRM peak area response factor in order to determine the levels of the parent compound in plasma. The plasma concentrations versus time were plotted and the profiles were fitted using PK Solutions Excel Application (Summit Research Service, USA) in order to determine the pharmacokinetic parameters.

3.18 Bioinformatic research on SerpinA3n promoter

The bioinformatic research focused on the analysis of SerpinA3n gene and, in particular, on its promoter. The Ensemble software (Zerbino et al., 2018) was used to find the mouse sequence of SerpinA3n, from which the gene promoter sequence was selected and analyzed with the Jaspas software (Bryne et al., 2008) to find possible Stat3 binding sites on this sequence.

3.19 Fractionation protocol for cellular lysates: Rapid Efficient And Practical (REAP) protocol

The chosen fractionation method for cellular lysates is the rapid, efficient and practical protocol (REAP) which is a two minutes non-ionic detergent-based purification technique (Suzuki, Bose, Leong-Quong, Fujita, & Riabowol, 2010).

N2a and ScN2a cells were grown as monolayers in 10 cm diameter dishes, removed from culture dishes on ice and collected in 1.5 mL micro-centrifuge tubes in 1 mL of ice-cold PBS. After centrifugation (a "pop-spin" for 10 sec in an Eppendorf tabletop microfuge), supernatants were removed from each sample and cell pellets were resuspended in 900 μ L of ice-cold 0.1% NP40 (Nonidet-P40, Sigma Aldrich) in PBS and triturated 5 times using a p1000 micropipette (Gilson, WI, USA).

300 μ L of the lysate was removed as "whole cell lysate" and kept on ice until the sonication

step. The remaining (600 μ L) material was centrifuged for 10 sec in 1.5 mL micro-centrifuge tubes and 300 μ L of the supernatant was removed as the "cytosolic fraction" and kept on ice. After the remaining supernatant was removed, the pellet was resuspended in 1 mL of ice-cold 0.1% NP40 in PBS, centrifuged for 10 sec as above and the supernatant was discarded. The pellet (~20 μ L) was resuspended in 30 μ L of ice-cold 0.1% NP40 in PBS and designated as "nuclear fraction".

Nuclear and whole cell lysates that contained DNA were sonicated (Vibra cells Ultrasonic liquid processor, amplitude 70%) 3 x 5 sec each.

Each sample was added with the inhibitor of phosphatases 1x (PhosSTOP EASYpack Roche, Sigma Aldrich, 10x) in water to avoid the possible dephosphorylation of pSTAT3 and boiled for 10 min at 100° C.

3.20 Immunofluorescence of fixed cells

N2a and ScN2a cells were seeded to semi-confluence in each well of a 24-well plate for 24 hours. After one day of incubation, the medium was removed, and the cells were fixed in 4 % of paraformaldehyde (PFA) for 20 minutes. The PFA was discharged and the cells were washed 3 times with PBS. Then, the cells were permeabilized with 0,02% of TritonX-100 in PBS for 5 minutes and then washed again 3 times with PBS. After the permeabilization step the cells were blocked in 1% Bovine Serum Albumin (BSA, Sigma-Aldrich) for 1 hour at room temperature. After the blocking the cells were incubated with primary antibody (W226 1:500, pSTAT3 Cell Signaling 1:100) in incubation buffer (1% BSA in PBS) for 1hour at room temperature. Next the cells were washed 3 times with 1% BSA and then incubated with the secondary antibody (Goat anti-mouse [G α Mo]-AlexaFluor488 or 594, Life Technologies) diluted 1:200 in the incubation buffer (1% BSA in PBS) for 1 hour at room temperature in the dark. After 2 washes in 1% BSA and 1 in PBS, the cells were incubated with 0.1-1 μ g/mL of DAPI (Life Technologies) in PBS for 10 minutes. The cells were washed 3 times in PBS and then the coverslips were mounted with a drop of Fluoromount-G (Invitrogen). The coverslips were sealed with nail polish to prevent drying and movement under the microscope.

To reveal scrapie epitopes in ScN2a cells we followed the same protocol but before the blocking step the cells were treated with PK 2,5mg/mL (15 minutes), washed 3 times in PBS and then treated with PMSF for 10minutes and GndHCL for 5 minutes and then blocked.

For the PrP^C surface staining we cultured cells to semi-confluence in each well of a 24-well plate for 24 hours. After one day of incubation, we moved cells on ice for 15 minutes and we

stained with primary Ab (W226, 1:500) in culture medium for 20 minutes, always in ice. Then, we removed medium and we washed cells with PBS 2 times. We next fixed cells with 4% PFA for 20 minutes and we washed with PBS 3 times. Then, cells were blocked with 1% BSA for 1 hour at RT and incubated with the secondary antibody (Goat anti-mouse [G α Mo]-AlexaFluor488, Life Technologies). After 2 washes in 1% BSA and 1 in PBS, the cells were incubated with 0.1-1 μ g/mL of DAPI (Life Technologies) in PBS for 10 minutes. The cells were washed 3 times in PBS and then the coverslips were mounted with a drop of Fluoromount-G (Invitrogen). For infected primary mixed cultures, we followed the protocol described by Victoria et al., 2016. Images were acquired with C1 confocal microscope (Nikon). FITC and TRITC filters were used for detection of PrP and pSTAT3 specific staining, while DAPI specific staining was acquired with 500 nm filter.

3.21 Statistical analysis

Statistical analysis was performed using GraphPad Prism 7.0 software. Normal distribution of data was assessed by D'Agostino-Pearson normality test.

For RT-qPCR analysis, differences between the ΔC_{Ts} of prion infected and uninfected cells and mouse brain homogenates were assessed with Kruskal-Wallis and Mann-Whitney test for not normally distributed data. Concerning Kruskal-Wallis test the level of significance was calculated using Dunn's multiple comparisons test between ΔC_{Ts} of prion infected and uninfected cells.

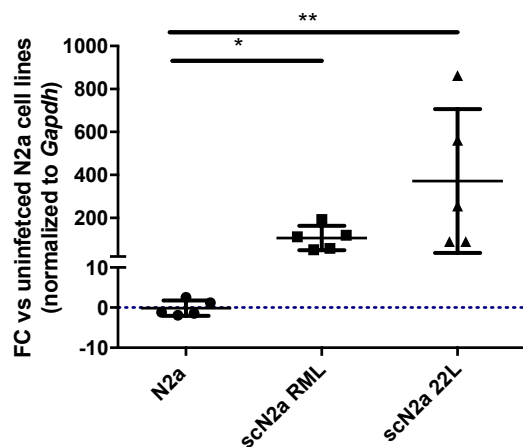
β -actin normalized Western blot signal values obtained from control and treated cells were normalized to the mean of the control samples for each experiment (in technical duplicates or triples). Groups were compared by using the non-parametric Mann-Whitney and Wilcoxon's matched pairs ranked test or Kruskal-Wallis and Friedman test with Dunn's multiple comparisons test. P-values ≤ 0.05 were considered as statistically significant.

4. RESULTS

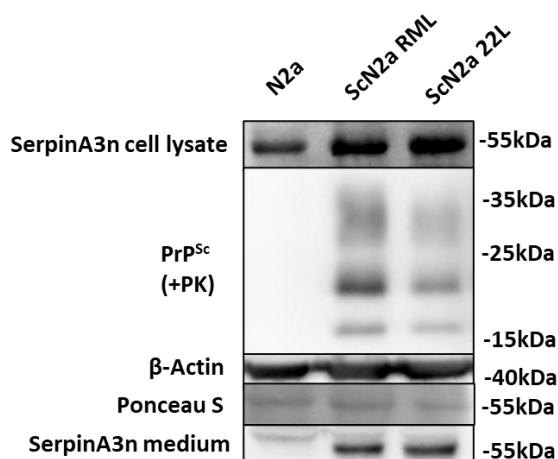
4.1 SerpinA3n expression in uninfected and prion-infected cell lines

We first analysed the expression of SerpinA3n transcript and protein in N2a and GT1 prion infected cells. At transcript levels, SerpinA3n is highly upregulated in both RML and 22L infected N2a and GT1 cells compared to uninfected ones (**Figure 1a, 2a**). Since SerpinA3n is mainly secreted (Gueugneau et al., 2018; Sergi et al., 2018), we performed Western Blot on conditioned medium collected from both prion-infected and un-infected N2a and GT1 cell lines observing a statistically significant increase of extracellular SerpinA3n in the medium of RML and 22L infected N2a (**Figure 1b, c**) and GT1 cells (**Figure 2b, c**). Nevertheless, we also appreciated an increased signal of intracellular SerpinA3n in both RML and 22L infected N2a (**Figure 1b**) and GT1 (**Figure 2b**) compared to uninfected cells.

a)



b)



c)

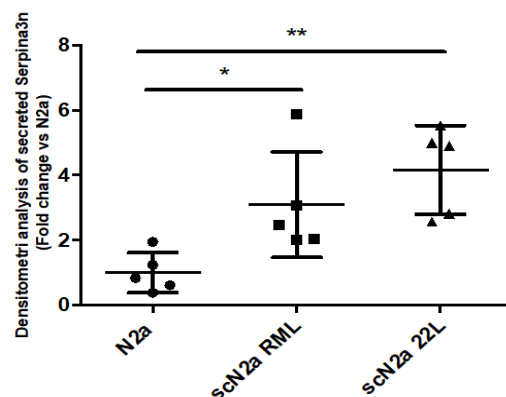
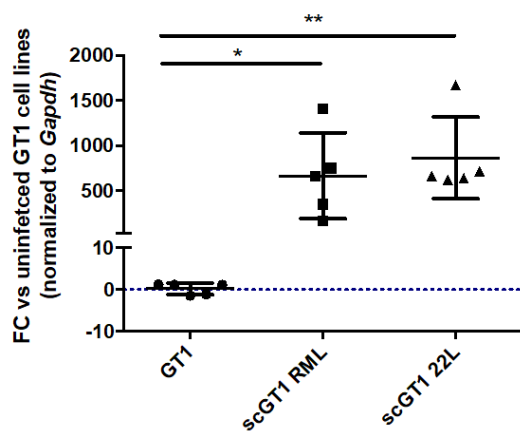
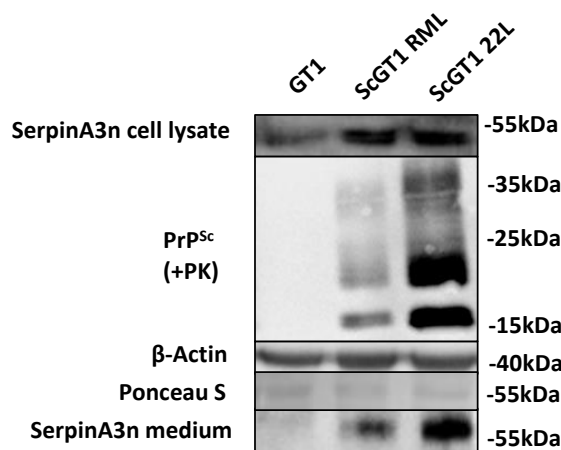


Figure 1. SerpinA3n expression in uninfected and prion infected N2a cell lines. a) Gene expression analysis of SerpinA3n transcript normalized against β -actin between uninfected and prion-infected (with RML and 22L prion strains) N2a cell lines. b) Representative Western Blot image of intracellular SerpinA3n, PrP^{Sc}, β -actin and secreted SerpinA3n. PonceauS staining on membrane was performed to verify the loading amount. c) Densitometric analysis of western blot signals from secreted SerpinA3n between uninfected and prion infected (RML and 22L) N2a cell lines. N=5 biological replicates Kruskal-Wallis test, Dunnett's multiple comparisons * $p < 0.05$ ** $p < 0.01$

a)



b)



c)

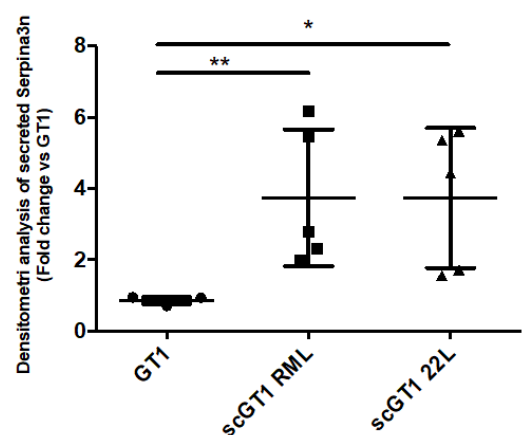


Figure 2. SerpinA3n expression in uninfected and prion infected GT1 cell lines. a) Gene expression analysis of SerpinA3n transcript normalized against β -actin between uninfected and prion-infected (with RML and 22L prion strains) GT1 cell lines. b) Representative Western Blot image of intracellular SerpinA3n, PrP^{Sc}, β -actin and secreted SerpinA3n. PonceauS staining on membrane was performed to verify the loading amount. c) Densitometric analysis of western blot signals from secreted SerpinA3n between uninfected and prion infected (RML and 22L) GT1 cell lines. N=5 biological replicates Kruskal-Wallis test, Dunnett's multiple comparisons * $p < 0.05$ ** $p < 0.01$

SerpinA3n, PrP^{Sc}, β -actin and secreted SerpinA3n. PonceauS staining on membrane was performed to verify the loading amount. **c)** Densitometric analysis of western blot signals from secreted SerpinA3n between uninfected and prion infected (RML and 22L) GT1 cell lines. N=5 biological replicates Kruskal-Wallis test, Dunnett's multiple comparisons * $p < 0.05$ ** $p < 0.01$

4.2 Structure based virtual screening

Firstly, we conducted a structure based virtual screening (SBVS) campaign to identify novel SERPINA3 binders able to inhibit the protein function. To do so, we docked a virtual library of ~15,000 compounds against the sB/sC pocket. Such pocket is located in the interface of the sheets B and C and it has been found for the first time in the plasminogen activator inhibitor 1 (PAI). Due to high structural similarity among the Serpin's family, it has been proposed that the sB/sC pocket is also present in SerpinA3n (S. H. Li et al., 2013). After a visual inspection of the best scored compounds, we selected 19 structurally diverse compounds (compounds A-U) for biological assays.

4.3 MTT analysis and acute cell treatment of first library (A-U)

Before starting the evaluation of the potential anti-prion efficacy, we determined the effect of compounds of the library (A-U) at 20 μ M concentration on cell viability using MTT assay. We set the toxicity threshold at 70% of cell viability compared to vehicle treated cells, discarding compound A (**Figure 3a**). Then, their ability to reduce the level of the resistant PrP^{Sc} in prion-infected cells was determined by Western blotting densitometric analysis. Relative amounts of PK-resistant PrP^{Sc} were measured comparing to untreated ScGT1-RML cells, observing a significant reduction of prion accumulation after the treatment with compound F, G and H (**Figure 4a, b**); however, when we repeated the experiment, we obtained lower reduction in the prion clearance using this dose, so we decided to test the molecules at a higher concentration. Thus, ScGT1 RML were treated with a higher dose of the F, G and H (40 μ M) and the MTT assay revealed the toxicity of the compound F (**Figure 3b**), so we next treated cells with G and H at 40 μ M appreciating a high anti-prion effect in all the experiments performed (**Figure 4c**).

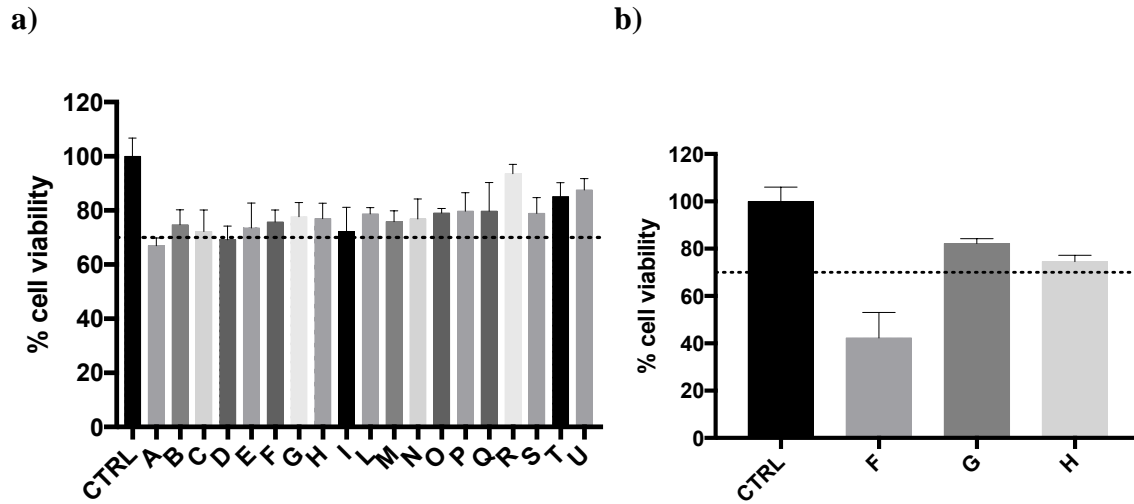
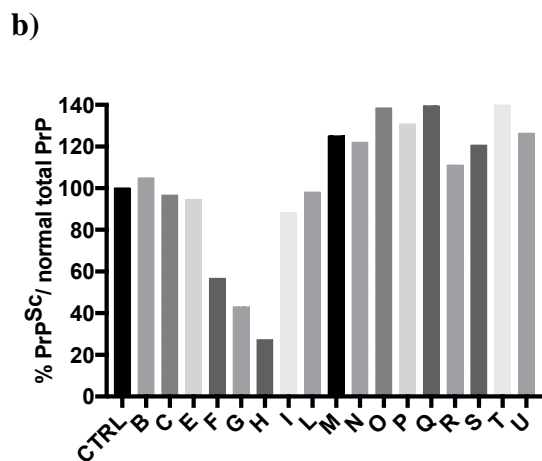
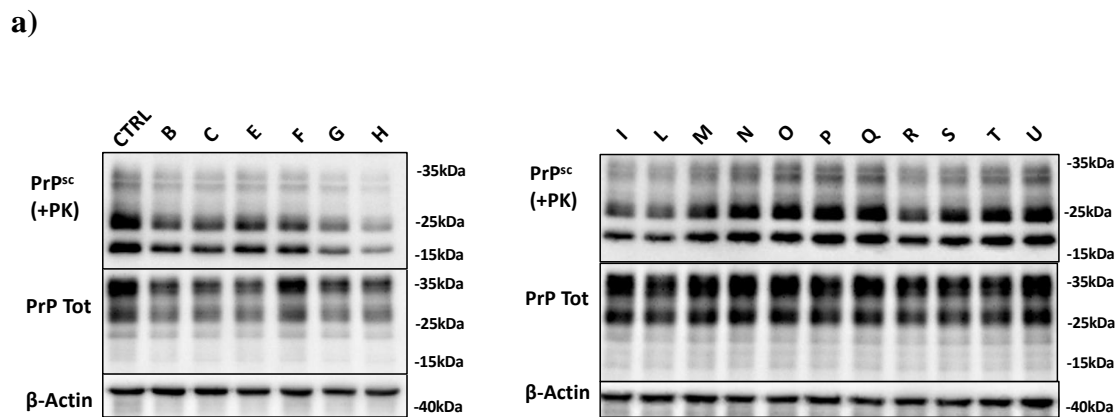


Figure 3. Viability of RML ScGT1 cell line treated with the first library of molecules. MTT analysis of ScGT1 RML treated with the vehicle (CTRL) or the drug (compounds A-U). a) 20µM b) 40µM



c)

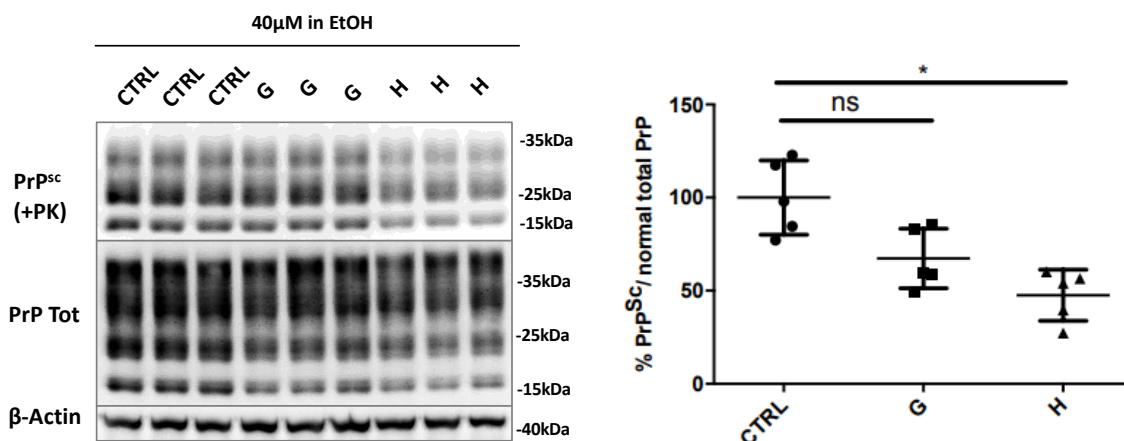


Figure 4. RML ScGT1 cell line treated with the first library of molecules. Western blotting analysis of PrP^{Sc} in lysates from ScGT1 treated with the vehicle (CTRL) or the drug (compounds A-U) at 20µM (a) and 40µM (b). Molecular weight is represented on the right (kDa). β-actin was used as proteins loading control and to normalize the expression level of PrP^{Sc} for densitometric analysis. Statical significance was performed by Friedman test with Dunn's multiple comparison. *P < 0.05 (N=5)

4.4 Identification of the second library of compounds

We found that the most active compounds tested in MTT assay (i.e. G and H) share a common scaffold based on 5-aminopyrazole core. This indicates that this heterocycle might be important for the ligand binding and, therefore, we decided to further explore new compounds bearing the 5-aminopyrazole scaffold. A ligand-based similarity search on our in-house virtual library of ~15,000 compounds (Savardi et al., 2020) resulted in the identification of eight new compounds tested in MTT assay. Compound 5 was found the most active compound and the proposed binding mode is depicted in **Figure 5**. The 4-trifluoromethoxy-phenyl moiety finds room in the small idrophobic pocket formed by Phe 198, Leu223, Leu226, Met 196, Leu242 and Trp194. The 5-aminopyrazole core is located at the entrance of the sB/sC pocket. Finally, the piperidine moiety is exposed to the solvent, interacting through an H-bond with the Glu195 (**Figure 5**).

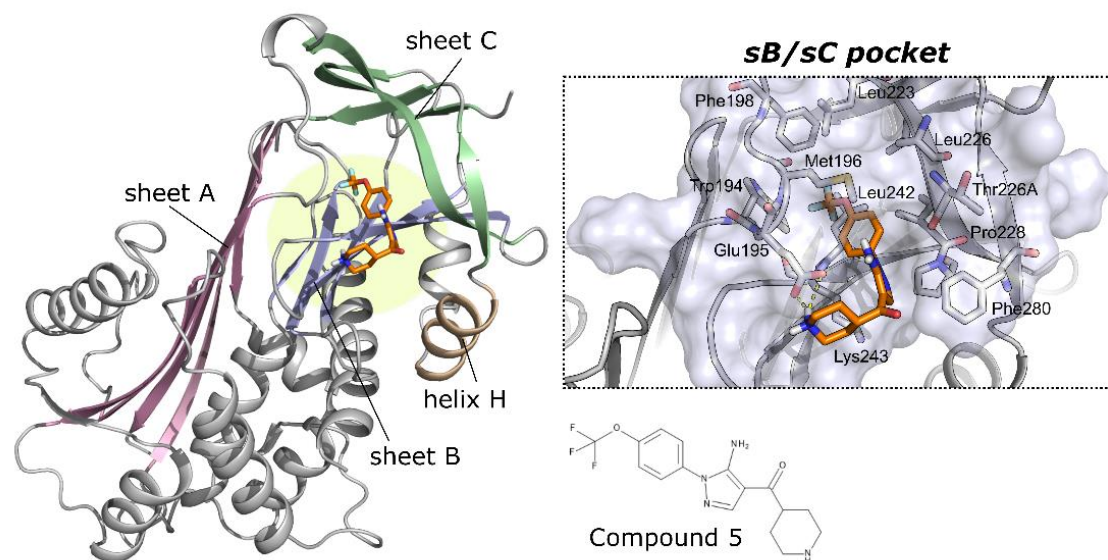


Figure 5. Binding mode of compound 5. Left: the structure of SerpinA3n (pdb: 1AS4) is shown in cartoon style, with sheet A in pink, sheet B in light blue, sheet C in green, and the helix H in sand. The compound 5 is shown in orange sticks. The sB/sC pocket is highlighted with a lemon circle. Right: the sB/sC pocket is represented in grey surface and the bound compound 5 in orange sticks. Residues in the binding pocket are shown in grey sticks.

4.5 MTT analysis and acute cell treatment of second library (1-8)

For what concern the second library (1-8), after MTT assay we discarded compound 3 from the evaluation of anti-prion efficacy, due to its toxicity (**Figure 6**). So, we next treated ScGT1-RML cells with the other compounds and we evaluated which molecules showed the higher anti-prion activity. Western blotting analysis revealed that only the compound 5 was able to decrease efficiently PrP^{Sc} amount (**Figure 7a, b**). Therefore, we choose it as the hit compound for next experiments.

We repeated the acute treatment with compound 5 in six independent experiments on different cell lines (GT1 RML- and 22L-infected and N2a RML- and 22L-infected) obtaining a PrP^{Sc} amount decreased in all cases. Particularly, we obtained an average 55% PrP^{Sc} reduction in ScGT1 RML, 35% in ScGT1 22L, 60% in ScN2a RML cell and 85% in ScN2a 22L (**Figure 8, 9**). These results indicated that compound 5 was able to decrease the amount of PrP^{Sc} regardless of the cell line used, underlying its role in PrP^{Sc} inhibition via SerpinA3n inhibition and not via PrP inhibition. Moreover, strain-independent compound 5 anti-prion effect highlights its potential to be used in clinic.

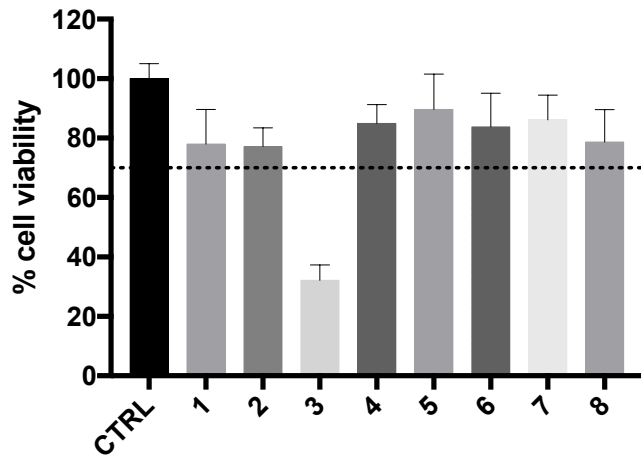
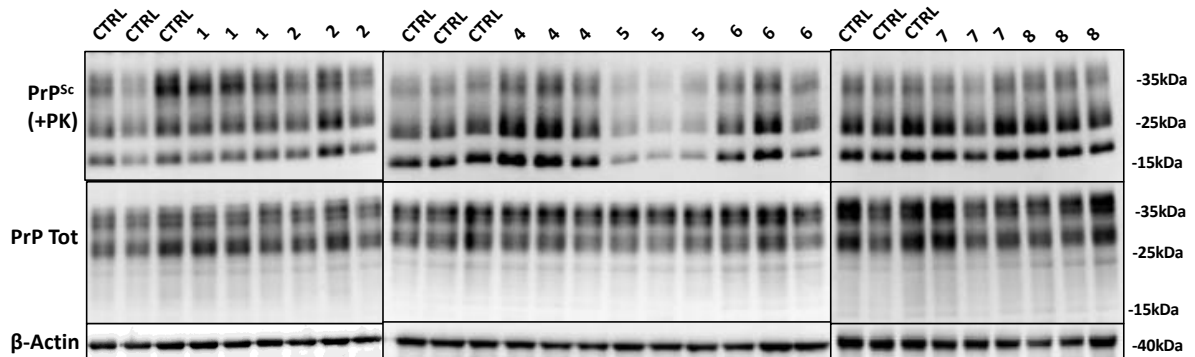


Figure 6. Viability of RML ScGT1 cell line treated with the second library of molecules. MTT analysis of ScGT1 RML treated with the vehicle (CTRL) or the drug (compounds 1-8) at 20 μ M concentration.

a)



b)

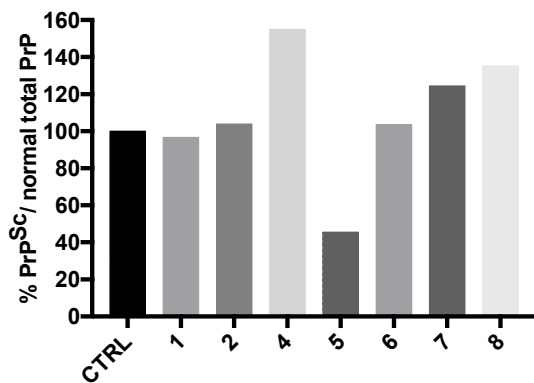


Figure 7. RML ScGT1 cell line treated with the second library of molecules. a) Western blotting analysis of PrP^{Sc} in lysates from ScGT1 treated with the vehicle (CTRL) or the drug (compounds 1-8). The experiment has been performed in triplicates. Molecular weight is represented on the right (kDa). β -actin was used as proteins loading control and to normalize the expression level of PrP^{Sc} for densitometric analysis (b).

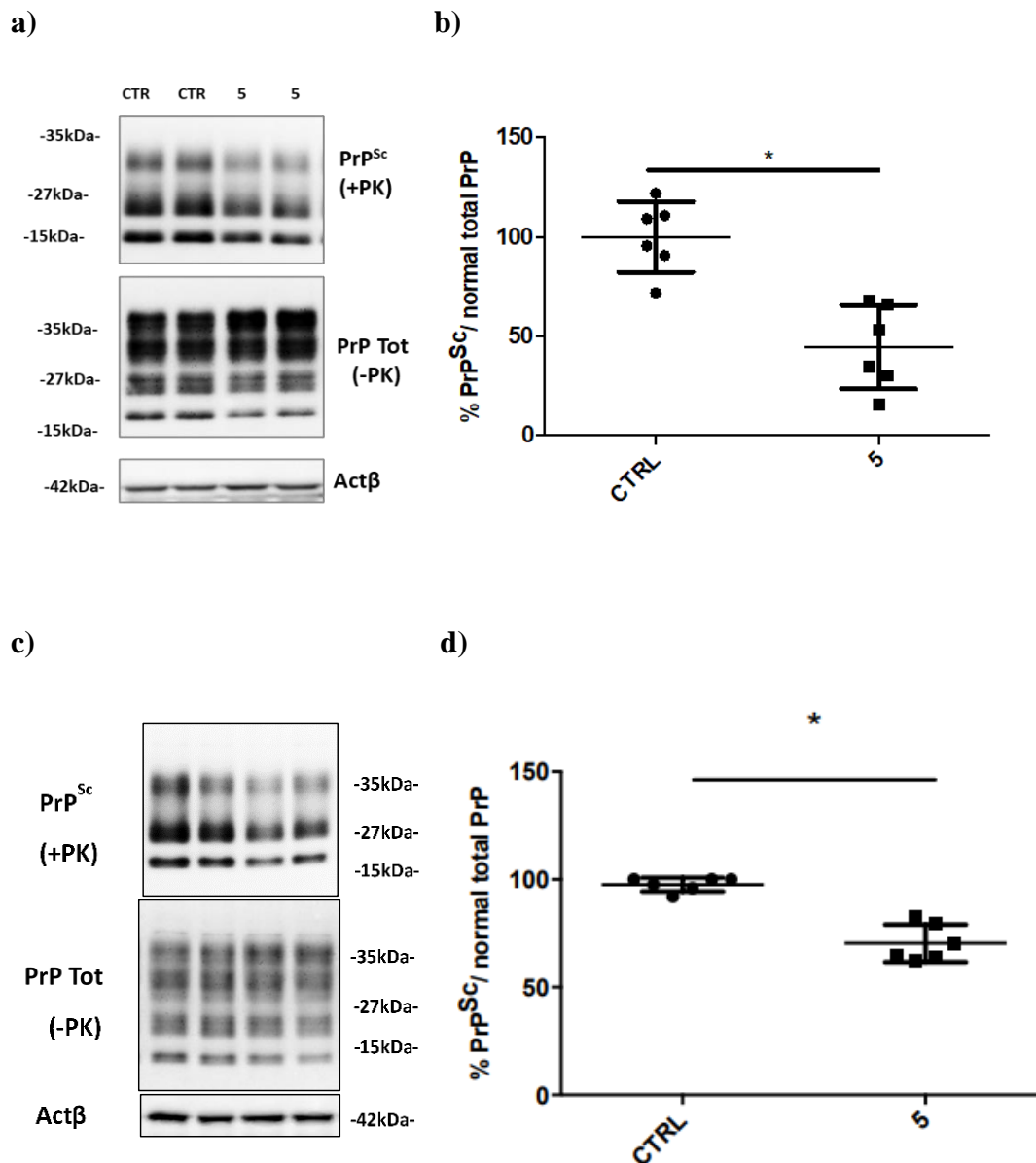


Figure 8. RML- and 22L-infected GT1 cell line treated with compound 5 Western blotting analysis of PrP^{Sc} in lysates from ScGT1 RML (a,b) and 22L (c,d) treated with the vehicle (CTRL) or the drug (compound 5). The experiment has been performed in duplicates 6. β -actin was used as protein loading

control and to normalize the expression level of PrP^{Sc} for densitometric analysis. Statistical significance was performed by Wilcoxon matched-pairs signed rank test, *p < 0.05 N=6.

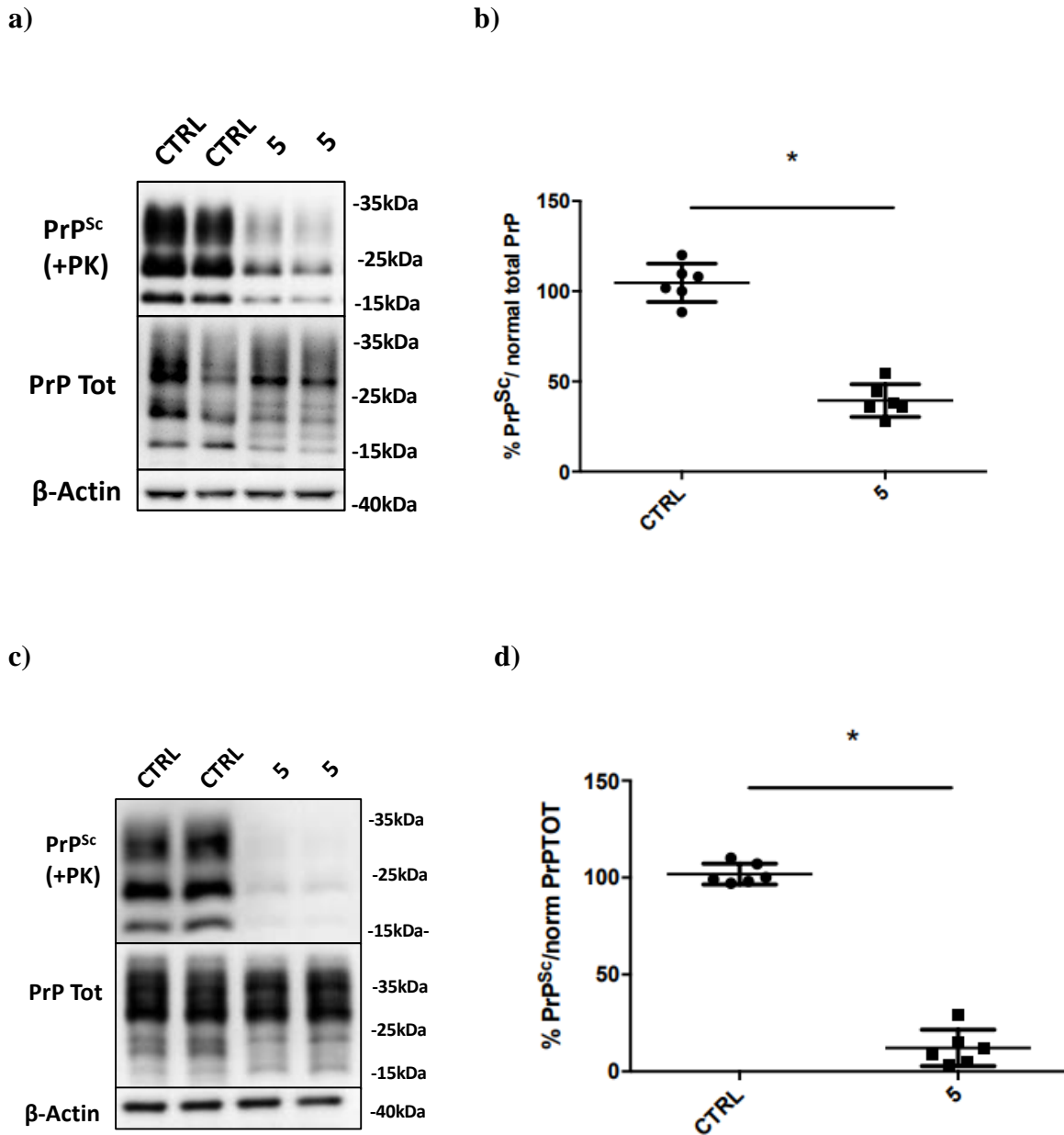
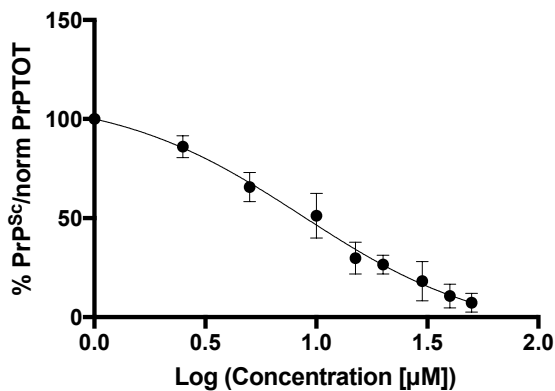


Figure 9. RML- and 22L-infected N2a cell line treated with compound 5. a) Western blotting analysis of PrP^{Sc} in lysates from ScN2a RML (a,b) and 22L (c,d) treated with the vehicle (CTRL) or the drug (compound 5). The experiment has been performed in duplicates. Molecular weight is represented on the right (kDa). β-actin was used as protein loading control and to normalize the expression level of PrP^{Sc} for densitometric analysis. Statistical significance was performed by Wilcoxon matched-pairs signed rank test, *p < 0.05 N=6

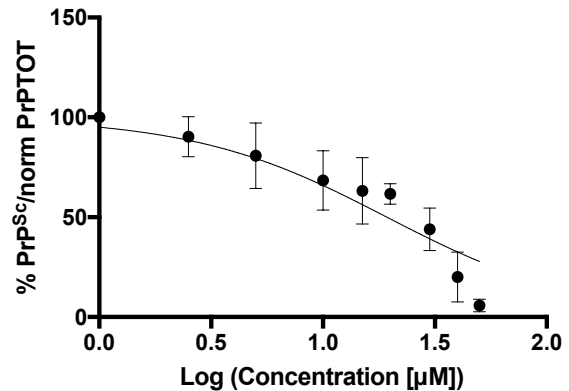
IC₅₀ of compound 5 in both N2a and GT1 prion infected cell lines revealed a range of prion clearance efficacy between 6 and 19 μ M. Indeed, we observed that the effect of compound 5 was prion strain- and cell line-independent since we obtained the highest IC₅₀ in GT1 22L-infected cells and the lowest IC₅₀ in N2a 22L-infected cells (**Figure 10**). These results are in line with the idea that the compound acts on SerpinA3n. The observed differences in PrP^{Sc} clearance are probably due to the different PrP^{Sc} amount in the cell lines used.

We also investigated compound 5 PrP^{Sc} reduction by the means of immunofluorescence in ScN2a RML cell lines, showing that compound 5 treated cells presented a decreased signal of PrP^{Sc} compared to untreated cells after PK digestion and GndHcl treatment to display the scrapie epitopes (**Figure 11**).

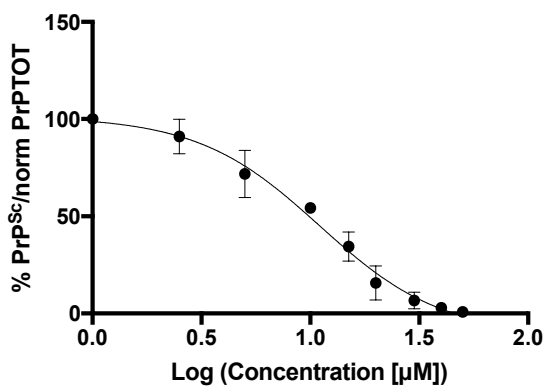
a)



b)



c)



d)

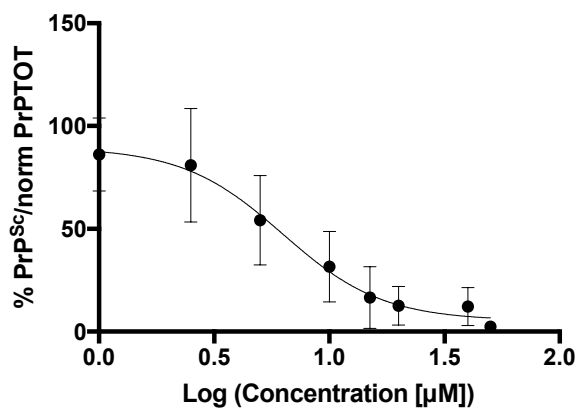


Figure 10. IC50 of compound 5 on RML- and 22L-infected GT1 and N2a cell lines. a) RML-infected GT1 cells IC50=8.64 μ M; b) 22L-infected GT1 cells IC50=19.3 μ M; c) RML-infected N2a cells IC50=11.2 μ M; d) 22L-infected N2a cells IC50=6.27 μ M. Each graph is the representation of three different experiments.

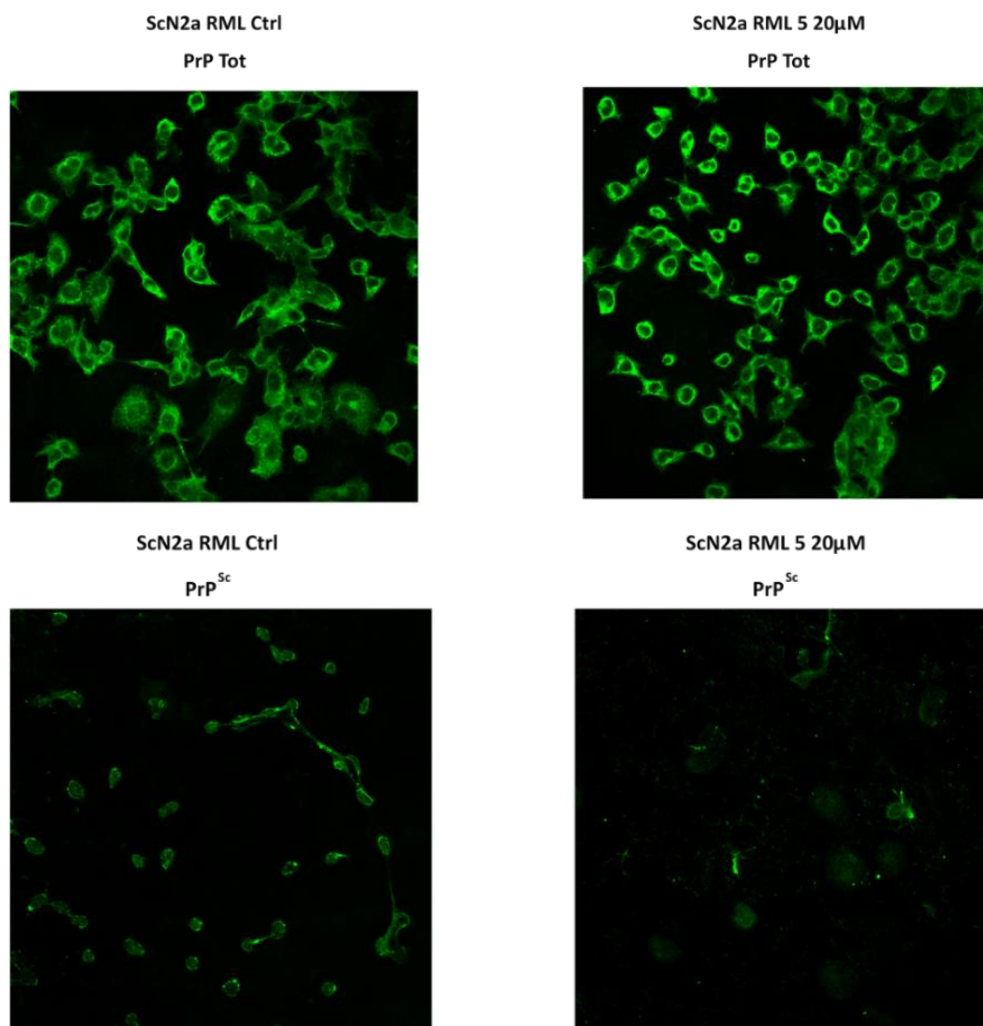


Figure 11. Immunofluorescence of RML-infected N2a cell line treated with compound 5 at 20 μ M concentration. Immunofluorescence staining of Total PrP and PrP^{Sc} in cells treated with compound 5 compared with ctrl cells (treated with vehicle only, DMSO 20 μ M). The upper panels represent the same staining for the total PrP in cells treated and untreated, while in the panels below is represented the amount of PrP^{Sc} which results lower if compared to ctrl cells, confirming the ability of the compound 5 in decreasing the accumulation of PrP^{Sc}.

4.6 Chronic treatment of ScGT1 and ScN2a cell lines with compound 5

We next chronically treated both RML and 22L-infected GT1 and N2a cell lines with compound 5 every 5 days for several passages. As shown, an 80-90% of reduction in PrP^{Sc} levels was observed from the first passage and was maintained for all the subsequent ones in all treated cell lines infected with the two prion strains (**Figure 12 and 13**). The results highlighted that compound 5 is able to slow down prion replication across passages under repeated administration.

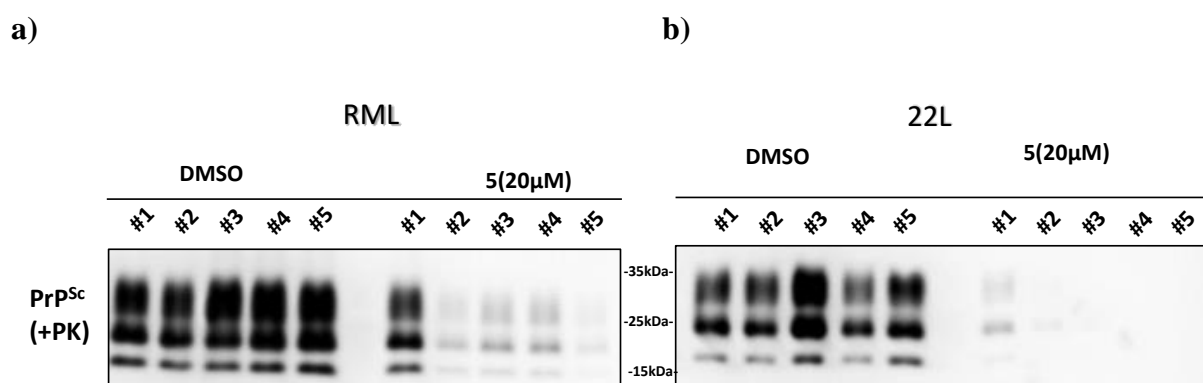


Figure 12. Chronic treatment of ScN2a cell line with SerpinA3n inhibitor 5. Western blotting analysis of PrP^{Sc} in lysates from RML-infected **a)** or 22L-infected **b)** N2a cells treated with vehicle (DMSO) or the drug (compound 5) at 20 μM for several passages. Molecular weight is represented between the two panels (kDa).

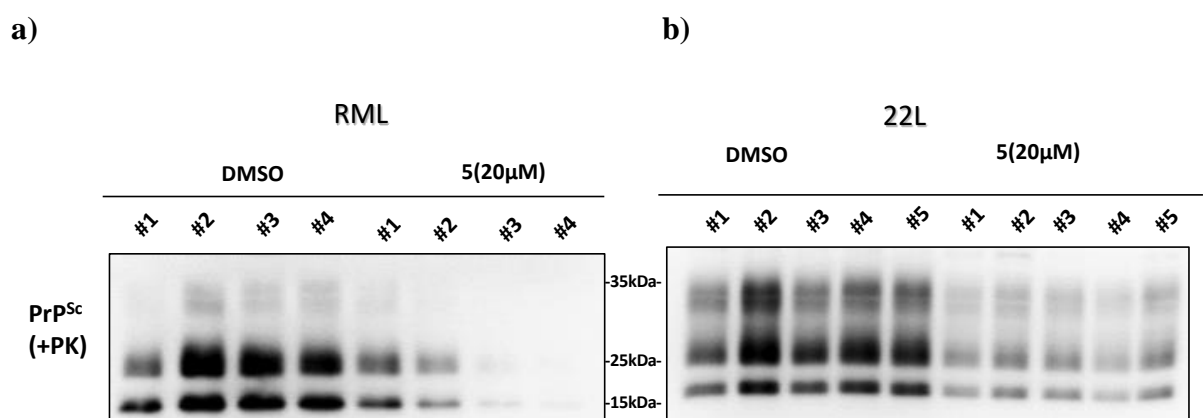


Figure 13. Chronic treatment of ScGT1 cell line with SerpinA3n inhibitor 5. Western blotting analysis of PrP^{Sc} in lysates from RML-infected **a)** or 22L-infected **b)** GT1 treated with vehicle (DMSO) or the drug (compound 5) at 20 μM for several passages. Molecular weight is represented between the two panels (kDa).

4.7 *De novo* infection of GT1 cell line and treatment with compound 5

Next, we treated *de novo* RML-infected GT1 cells in parallel with and without compound 5. We first observed the appearance of prion in GT1 cells after challenging them with RML prions, which were stable for all the passages. Moreover, we observed that *de novo* prion-infected and simultaneously compound 5-treated cells, showed a delayed appearance of prion accumulation compared to control cells (**Figure 14**).

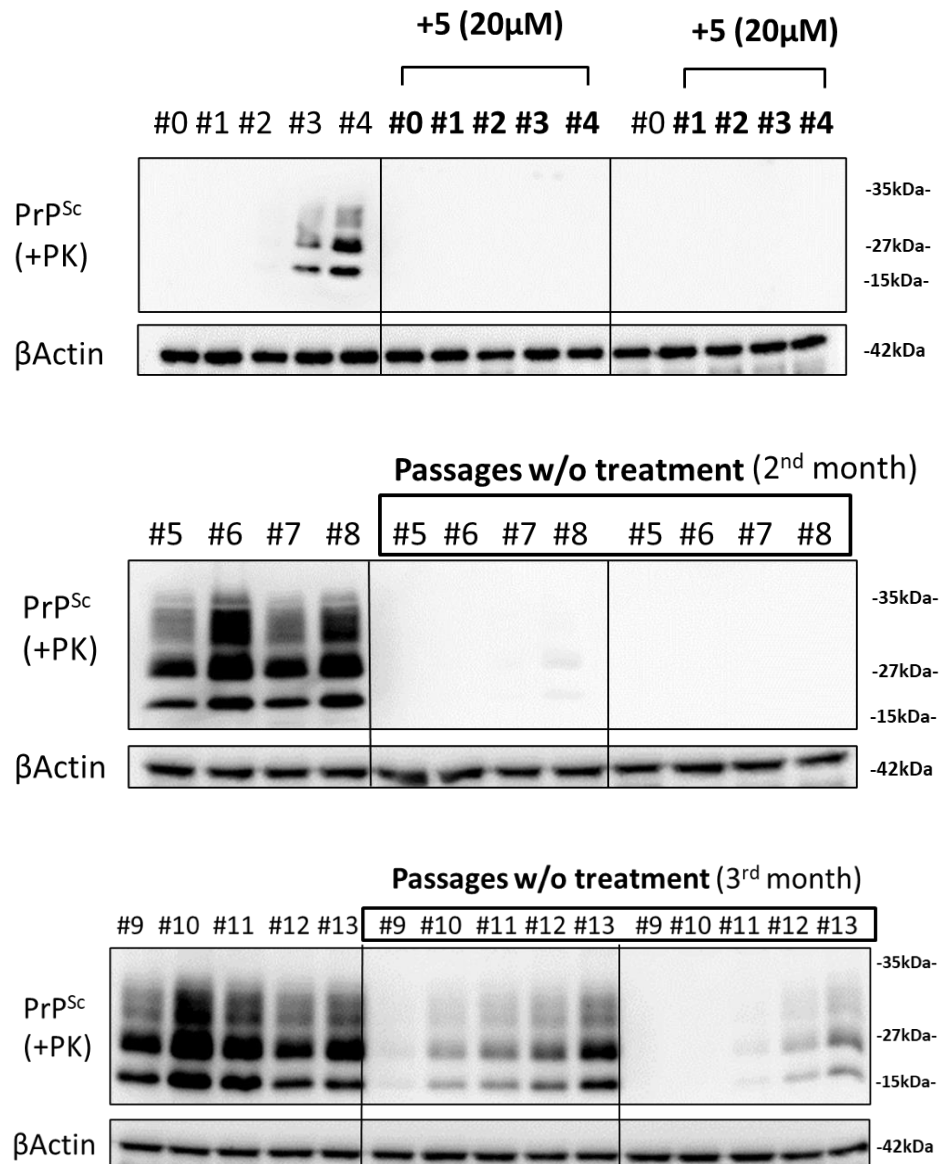


Figure 14. *De novo* infection of GT1 cell line and treatment with SerpinA3n inhibitor 5. Western blotting analysis of PrP^{Sc} in lysates from *de novo* infected GT1 cell line treated with vehicle (DMSO) or the drug (compound 5) for several passages and western blotting analysis of PrP^{Sc} in lysates from *de novo* infected GT1 treated with compound 5 after stopping of treatment compared to cells never treated. Molecular weight is represented on the right (kDa).

4.8 Investigation of *in vitro* effect of compound 5 on prion fibril formation

To exclude possible compound 5 off-target effects on the prion protein itself, we performed an RT-QuIC assay. As showed in **Figure 15**, the addition of compound 5 to recombinant mouse PrP and ScN2a derived seed does not affect fibrils formation, suggesting that the compound is not able to bind neither PrP^C nor PrP^{Sc} and it is able to exert its anti-prion activity without a direct interaction with either PrP^C or PrP^{Sc}

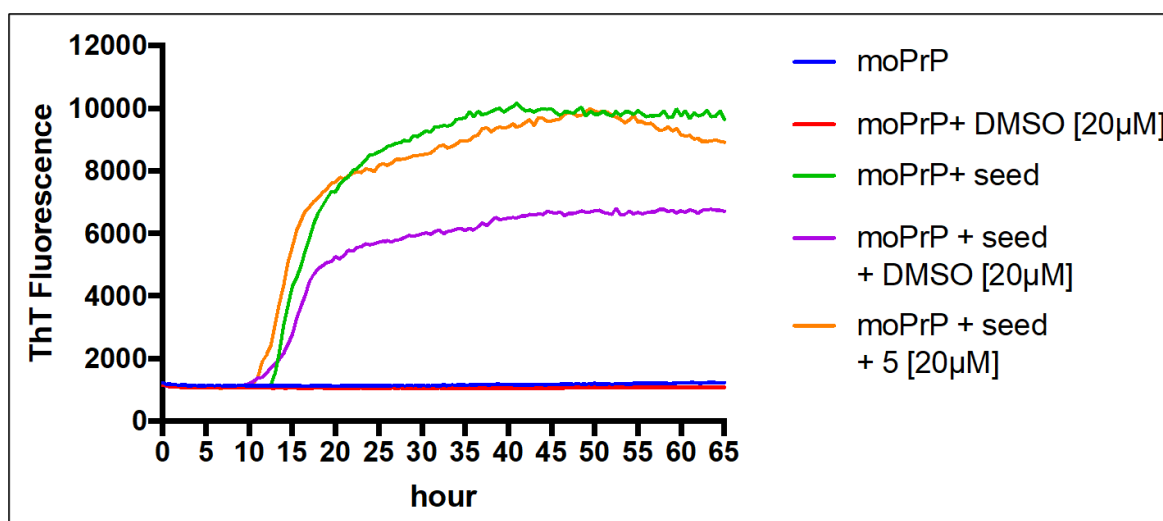


Figure 15. RT-QuIC analysis of PrP-compound5 interaction. RT-QuIC technique to analyze and exclude the possible interaction of the compound 5 with the PrP^C or PrP^{Sc} (N=2)

4.9 Investigation of PrP localization after compound 5 treatment

To further investigate compound 5 specificity, we set up an immunofluorescence experiment on compound 5 treated N2a cells to exclude any possible biological interaction with PrP. In this case, we wanted to observe whether compound 5 treatment was able to induce a shift of PrP^C from the plasma membrane to the inner compartments, hiding the substrate necessary for PrP^C to PrP^{Sc} conversion. We observed that compound 5 treated N2a cells displayed a similar PrP^C and total PrP localization compared to untreated cells (**Figure 16**), indicating that the compound was not able to induce a PrP shift to other cellular compartments.

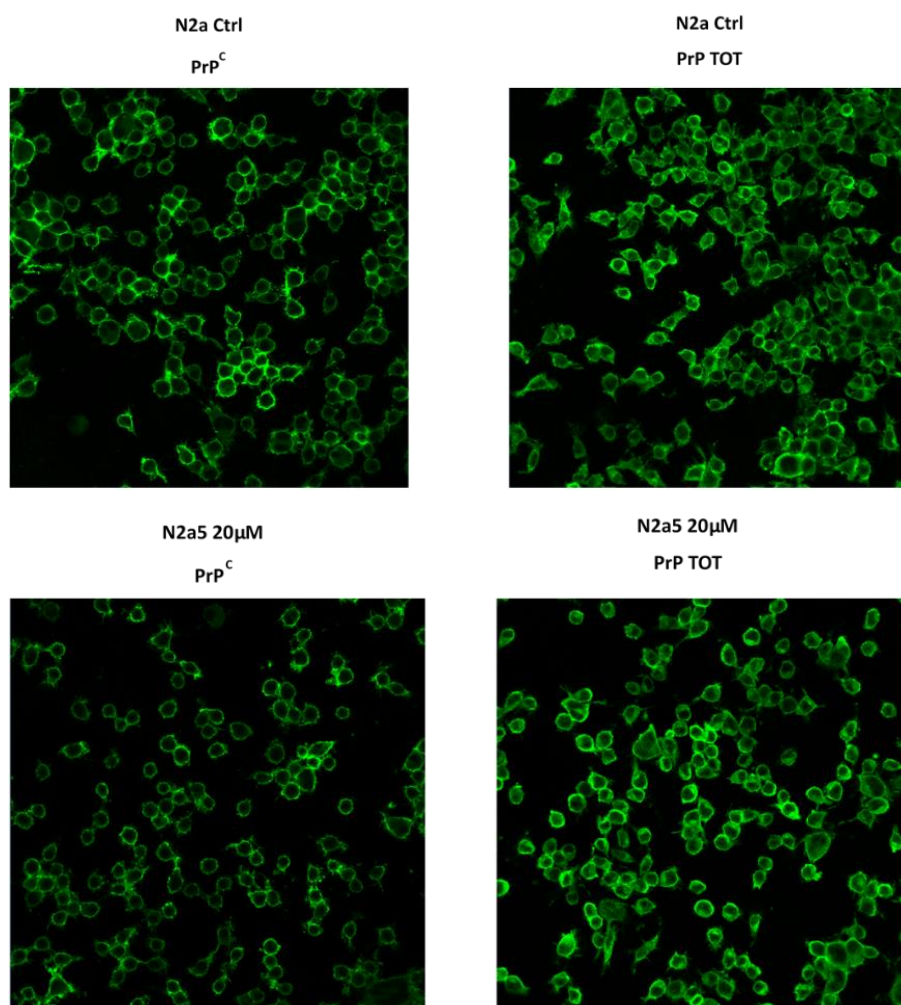


Figure 16. Immunofluorescence of Total PrP and surface PrP^C in N2a cell line treated with compound 5. Immunofluorescence staining of Total PrP and surface PrP^C in N2a cells treated with compound 5 compared with ctrl cells (treated with vehicle only, DMSO 20μM). The panels represent the same staining for surface PrP^C and the Total PrP in N2a cells both treated and untreated with compound 5, indicating that the localization of PrP^C on the membrane is not affected by the treatment.

4.10 Binding specificity of compound 5 for SerpinA3n

To assess compound 5 specificity to SerpinA3n, we treated ScN2a RML cells with compound 5 and an anti-SerpinA3n antibody. We observed that compound 5 and antibody treated cells displayed a reduced amount of PrP^{Sc} compared to control cells (**Figure 17**). Then, we generated ScN2a RML cells knock-out for SerpinA3n. First of all, we observed that all of the obtained clones showed a reduced or absent PrP^{Sc} signal compared to normal ScN2a cells, underlying a SerpinA3n role played in PrP accumulation and replication (**Figure 18 a**). Since some SerpinA3n KO ScN2a RML clones showed a remaining signal of PrP^{Sc}, we treated one of them

(clone 5) with compound 5. As expected, compound 5 was not able to reduce PrP^{Sc} accumulation in SerpinA3n devoid ScN2a RML cells (**Figure 18 b**), suggesting again that the compound acts on PrP^{Sc} clearance via a specific SerpinA3n inhibition.

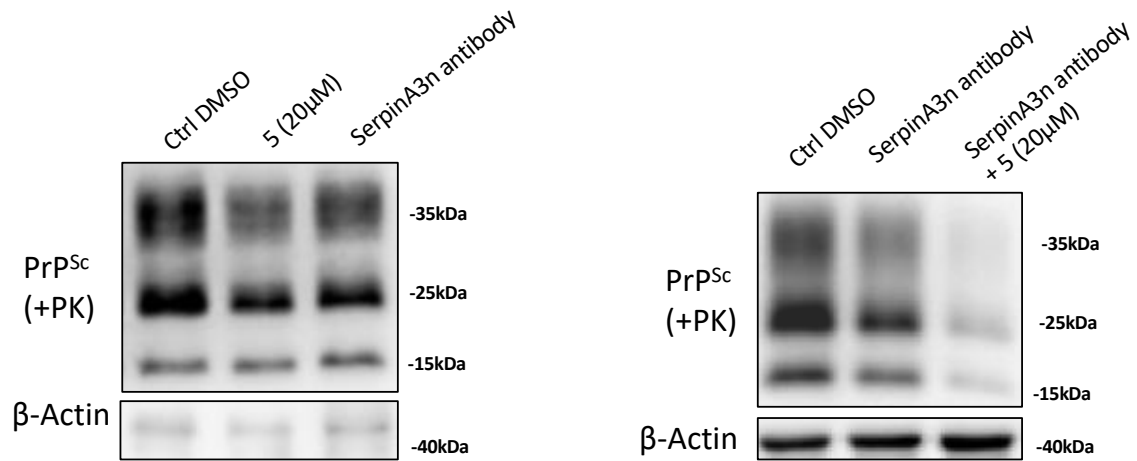
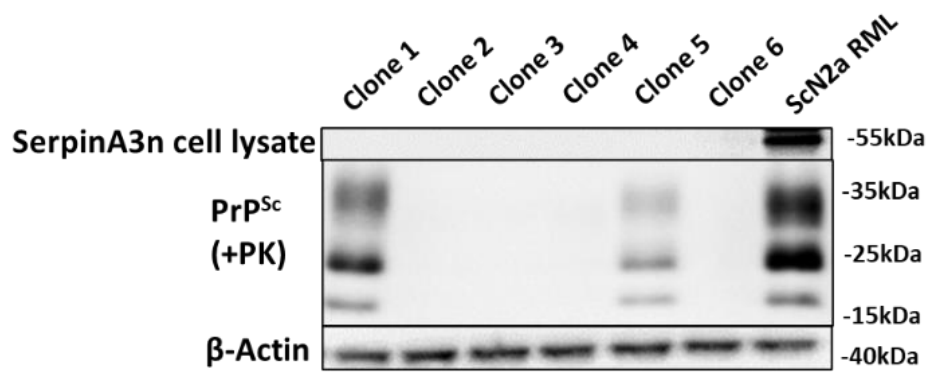


Figure 17. Specificity of compound 5 effect in decreasing of PrP^{Sc} with Anti-SerpinA3n antibody. Western blotting analysis of PrP^{Sc} on RML-infected N2a cells after the treatment with Anti-SerpinA3n antibody (R&D System) and compound 5 to confirm compound 5 specificity to SerpinA3n in decreasing PrP^{Sc}. Molecular weight is represented on the right (kDa).

a)



b)

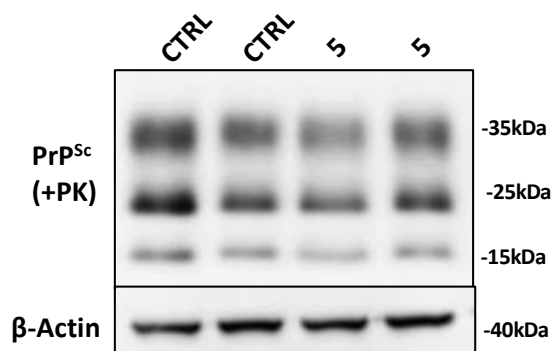


Figure 18. Treatment of ScN2a RML cell line knock-out for SerpinA3n. Western blotting analysis of PrP^{Sc} after the treatment with compound 5 in RML-infected N2a cell line knock-out for SerpinA3n to confirm the compound 5 specificity to SerpinA3n in decreasing PrP^{Sc}. **a)** Western blotting analysis of PrP^{Sc} signal in different clones of RML-infected N2a cells knock-out for SerpinA3n; **b)** treatment with compound 5 of clone 5 of RML-infected N2a cells knock-out for SerpinA3n with a residual signal of PrP^{Sc}. Molecular weight is represented on the right (kDa).

4.11 SerpinA3n genetic inhibition

As a complementary approach, we decided to decrease SerpinA3n levels in our cell line models using shRNA approach in order to silence *SerpinA3N* gene expression.

Indeed, being a single-stranded RNA molecule, shRNA can be delivered to cells on a DNA plasmid, ensuring continuous expression over time and avoiding the need of regular dosing. In addition, it has been shown that single stranded RNAs have less “off-target” effects compared to double-stranded RNAs and reduced propensity to elicit immune response activation, inflammation and toxicity (Aguilar, S., et al., 2017). Our data showed a reduction of PrP^{Sc} accumulation (around 50%) after SerpinA3n inhibition compared to un-transfected ScN2a RML (**Figure 19**).

Taken together, these data suggest us that compound 5 is directed towards SerpinA3n inhibition since, the results obtained from specific inhibition of SerpinA3n (SerpinA3n KO cells, shRNA and Anti-SerpinA3n antibody) gave us the same results in decreasing PrP^{Sc} accumulation.

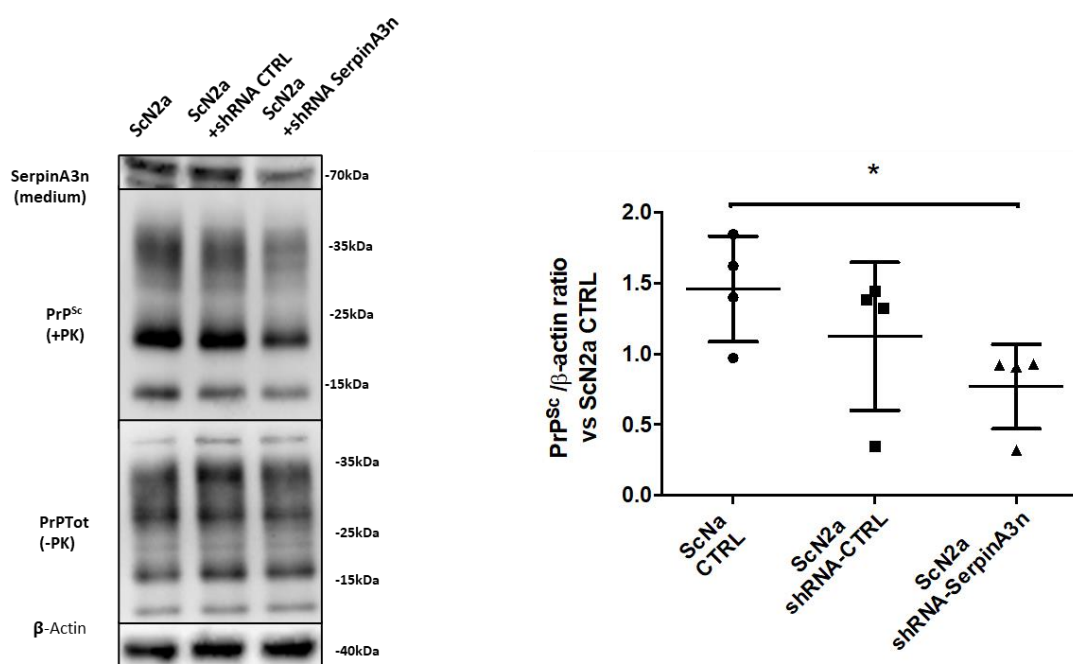


Figure 19. SerpinA3n genetic inhibition. Western blotting analysis and quantification of PrP^{Sc} on RML-infected N2a cells after the treatment with shRNA for SerpinA3n to confirm compound 5 specificity to SerpinA3n in decreasing PrP^{Sc}. Statistical analysis was made by Prism software and Kruskal-Wallis test with Dunn's multiple comparison was applied. Molecular weight is represented on the right (kDa) N=4.

4.12 Pharmacokinetic of compound 5

Due to the encouraging results obtained with *in vitro* compound 5 treatment, we decided to test the efficacy of this molecule also *in vivo*, performing a pharmacokinetic profile of this compound.

All animals treated with the two different route of administrations displayed normal behaviour without side effects for the entire period of experiments. Compound 5 showed fast and moderate exposure ($C_{max} = 206 \text{ ng/mL P.O. and } C_{max} = 549 \text{ ng/mL I.V. at } 5 \text{ min}$) and high clearance in plasma (791 mL/min/kg). The exposure (AUC) over the time interval 0-4 hours was 12192 min*ng/mL, resulting in a ca. 26% oral bioavailability, calculated over the same time interval (**Figure 20** and **Table 1**). Only negligible amount (very low levels) of compound was measured in the brain after IV and PO administration, very close to the limit of quantification (5nM).

Mouse PK Profile

Plasma

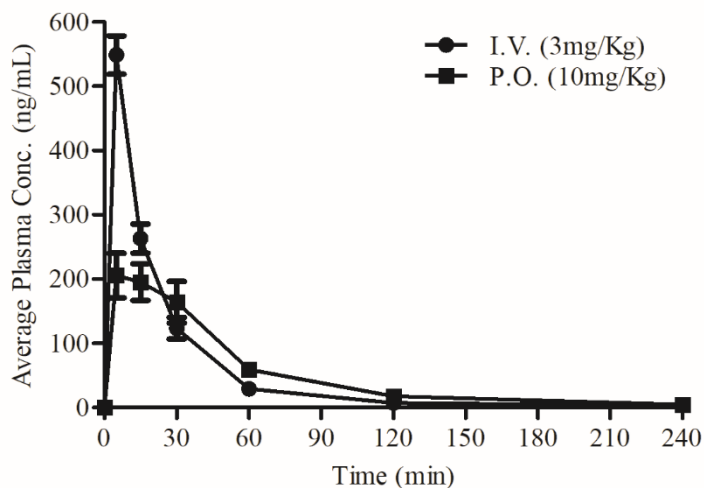


Figure 20. Pharmacokinetic profile of compound 5. Pharmacokinetic profile of compound 5 in plasma following intravenous (*I.V.*) and oral (*P.O.*) administration to male C57BL/6 mice ($n=3$ per dose).

Pharmacokinetic Parameters		
Parameter	<i>I.V.</i>	<i>P.O.</i>
Dose (mg/Kg)	3	10
C_{max} [ng/mL (μM)] (obs)	549 (1.55)	206 (0.58)
T_{max} (min) (obs)	5	5
AUC [min*ng/mL ($\mu M \cdot h$)] (calc)	14192 (0.67)	12192 (0.57)
$t_{1/2}$ (min) (elimination phase) (calc)	98	65
V_D (mL/Kg) (calc)	29000	74291
CL (mL/min/Kg) (calc)	205	791

Table 1. The observed and calculated pharmacokinetic parameters of Compound5 following intravenous (*I.V.*) and oral (*P.O.*) administration to male C57BL/6 mice. The AUC was calculated based on the time interval $t=0-240$ min.

4.13 Analysis of SerpinA3n and Jak/Stat3 pathway relationship in prion diseases development

4.13.1 Immortalized prion-infected cell lines evaluation

Bioinformatic research of Stat3 binding sites on SerpinA3n promoter

Given the presence of STAT binding on ACT (SERPINA3) sequence (C. Baker et al., 2007), we decided to investigate the presence of STAT3 binding sites in the promoter sequence of SerpinA3n gene. Thus, we took the SerpinA3n promoter sequence (**Figure 21 a**) taking advantage of the Ensembl website (Zerbino et al., 2018) and then, through Jaspar website (Bryne et al., 2008) we searched for the STAT3 binding sites on SerpinA3n promoter and we found at least three different STAT3 binding sites (**Figure 21 b**).

a)

```
>NC_000078.6:104406600-104407401 Mus musculus strain C57BL/6J chromosome 12, GRCm38.p6 C57BL/6J
CAGTCTGTTTCATTTCCAGTCTGAGCACAGACAGCTTGCCATGCCAGCATTTCCTAAGAGGAGGGAG
GAGCCCTTGATGGGAATAAATAGGCTTTAATGTGCACTGGGGACAACATGCCAGGCAAGCGGCAACCCCTG
AACATCGGGAGTCAGCTATCACAGAGGCTGGCAGCTGGCTGGTTTCAGCTCTGTAGGTAAGCCAGGAT
TCCTTGACTCCAGGGACAGAGAAGGAACCTTCCAGGACTGTGCGGTACTGGCTACTGCCTGCAACCTGT
GTTTGTGGGGGTGGGGCAAGGGCTTTGGCTGAGATACTGGCTTACAATCAGGGAACTTTCTTGGGTTCA
TAAATCTTCTCTCCGGTCAGTTTCTTCCCTGTGGAAGATACAGATGCTGTGGTCTCTGCTCGTGGAG
AGTAAATGGAGCCTGCTTCTGACTCCAAGGGGGGGGGAGGTTTAGAGACATGTCTAGCTTGCATGCT
GCAGTCATAGCTAGGGTGAGACCGGACTTTGCAGAGTCACTGTTGGGGAGGTGGCAGCTCTGCCTTGCT
CACATCACAGAAGAGATGCCTGGGGGGTTGGGACTCCACTTCCCTCTTAGATACCAGATCCCTAGGCAA
GCAGAGGGGCTTCCCTCAACTAGGGAAGCAAAGATGGCTCAGTCACTGAGCCACGTCTCCTGCTGTAT
GAACCGAGCAGCCTCTTTCTCTGAAATATTTTGGTGCAAATATTGTTAGTGCTTTTCAAAGAAA
TGGTTGCATCGGACTGAAAATAAATCAGCCA
```

b)

Matrix ID	Name	Score	Relative score	Sequence ID	Start
MA0144.1	Stat3	9.7277	0.866899507453	NC_000078.6:104406600-104407401	119
MA0144.1	Stat3	8.09812	0.83697846284	NC_000078.6:104406600-104407401	239
MA0144.1	Stat3	7.33462	0.822959722974	NC_000078.6:104406600-104407401	266

Figure 21. Bioinformatic analysis of STAT3 binding sites on SerpinA3n promoter.

a) SerpinA3n promoter sequence from Ensembl. The promoter coordinates are 104,406,600-104407401, on chromosome 12 b) Bioinformatic Jaspar results for functional binding sites of STAT3 on SerpinA3n promoter

RT-qPCR reference genes selection

To elucidate a possible involvement of the JAK/STAT3 pathway in prion infected cells, we analyzed the expression levels of the genes involved in this signaling cascade, correlating the significant overexpression of *SerpinA3n* to the upregulation of different cytokines, in particular of IL-6 and IL-1 β .

cDNA for N2a, ScN2a 22L and RML was obtained by 8 different batches of cells.

The normalization against *Gapdh*, *Actb* and *Tubb3* was performed to avoid variations among the samples and experiment executions and the differences in terms of quantity cDNA between the samples caused by pipetting errors.

In literature, the vast majority of RT-qPCR experiments use glyceraldehyde-3-phosphate deshydrogenase (*Gapdh*), β -Actin and β -Tubb3 as internal references to normalize results, since they are found to be constitutively expressed in different cell types. However, variations of their mRNA level were observed under certain experimental conditions, thus we checked for their expression level among infected and control cells, observing similar expression profiles in all the analyzed groups.

RT-qPCR results

A strong upregulation of *SerpinA3n* was found in both ScN2a 22L and ScN2a RML cells, with a P value of 0.0002 and a fold change of almost 450 in ScN2a RML and up to 480 in ScN2a 22L. Similar results were obtained against all the reference genes. Regarding un-infected N2a cells, *SerpinA3n* mRNA was found at very low levels and in some cases not even detectable. Then, we evaluated *IL-1 β* and *IL-6* expression level, observing a significant upregulation of these transcripts in both 22L- and RML-infected N2a cells, with a fold change of 6 and 4 respectively and a P value of 0.0002.

Thereafter, we evaluated the mRNA expression of *Stat3* which showed an upregulation of almost 3 folds in both ScN2a 22L and ScN2a RML respect to control cells, with a P value around 0.0001 and 0.0002 (**Figure 22**).

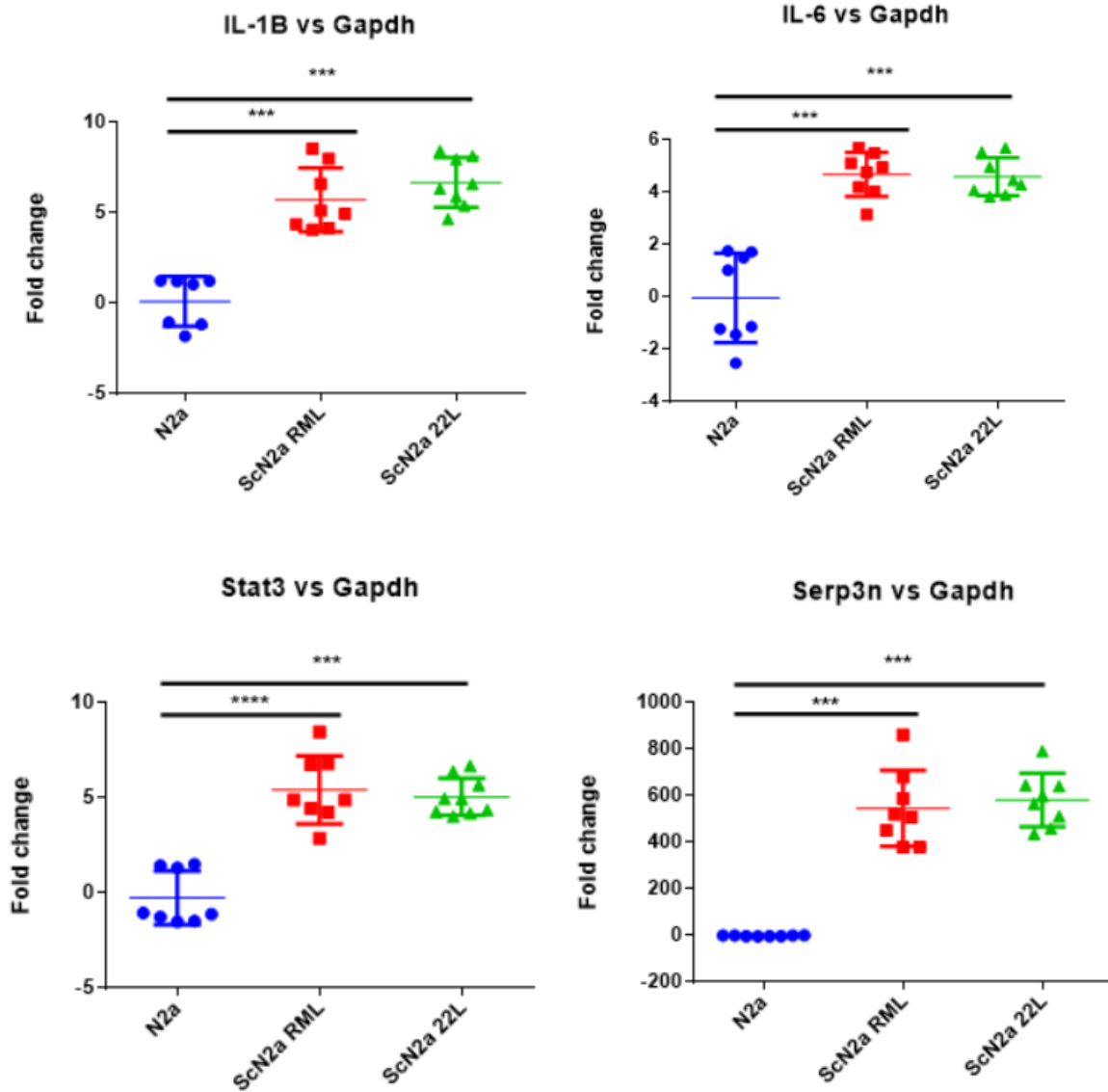


Figure 22. RT-qPCR analysis of the mRNA expression of SerpinA3n, IL-1B, IL-6 and Stat3 in N2a, ScN2a RML and ScN2a 22L mouse cells normalized against Gapdh.

Fold changes (FC) are calculated using the $2^{-\Delta\Delta C_T}$ classical method: first ΔC_T is calculated as the difference between the C_T of the target gene and the C_T of the housekeeping gene to normalize the C_T value of N2a, ScN2a RML and ScN2a 22L cells. $\Delta\Delta C_T$ is calculated as the difference between ΔC_T of prion infected cell and ΔC_T of uninfected cells. FC are represented with the Mann-Whitney test (non-parametric) and the significance is given according to the statistical criteria of P value, with a P value < 0.05 considered significant. ***P value \leq 0.0003, ****p value < 0.0001. N2a (n = 8), ScN2a RML (n = 8), ScN2a 22L (n = 8).

Western blot analysis

Later, we moved to the analysis of the protein expression of all the players involved in the suggested pathway. Firstly, we evaluated the differential expression of phosphorylated-STAT3 (pStat3) compared to Total STAT3 (Stat3 tot), to see if there were any differences between prion infected and uninfected cells. Western Blot analysis revealed a higher amount of pSTAT3 in ScN2a RML and 22L cells, whereas a lower protein concentration was found in N2a cells (**Figure 23a**).

The densitometric analysis showed the differential expression of the normalized pSTAT3 in the three cell groups (**Figure 23b**).

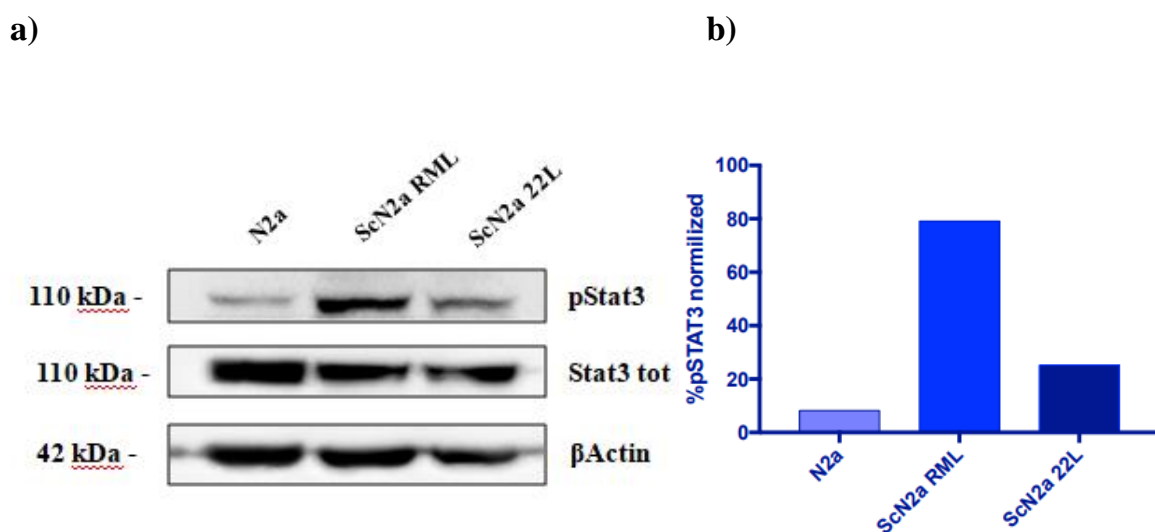


Figure 23. Western Blot analysis of whole cell lysates from N2a, ScN2a RML and 22L

a) Western Blot analysis of p-Stat3 and Stat3 tot expression with beta Actin used as a marker of the correct samples loading N=2. **b)** The graph shows the normalized pStat3 levels in N2a, ScN2a RML and ScN2a 22L cells.

Thereafter, we evaluated the expression of pSTAT3 in the three subcellular fractions (whole lysate, cytosolic and nuclear fractions) of N2a, ScN2a RML and ScN2a 22L cells, taking advantage of the REAP protocol, since the shift of pStat3 from cytoplasm to the nucleus indicates the activation of the JAK/STAT3 pathway.

pSTAT3 cellular compartmentalization was examined by comparing the cytoplasmic and nuclear level between infected and uninfected cells (**Figure 24a, b**).

Concerning ScN2a RML cells, we found higher phosphorylation of Stat3 protein in the whole and nuclear fraction compared to control cells.

To ensure the efficacy of the protocol used to separate the subcellular compartments, we assessed the level of Nup62 and β Tubb3, respectively used as the nuclear and cytosolic marker. Nup62 was found in the whole and nuclear fractions, while β Tubb3 in the whole lysate and in the cytosolic one, confirming the proper separation of the different cellular compartments (**Figure 24a**).

Concerning ScN2a 22L, we firstly tried to fractionate the three cellular compartments using the same REAP protocol used for the N2a and ScN2a RML, as described in the materials and methods section. However, Western blot analysis revealed that this procedure was not effective in separating the different cell fractions for the 22L-infected N2a, showing that both pSTAT3 and Nup62 were present in the whole and in the cytosolic fractions (**Figure 24a**).

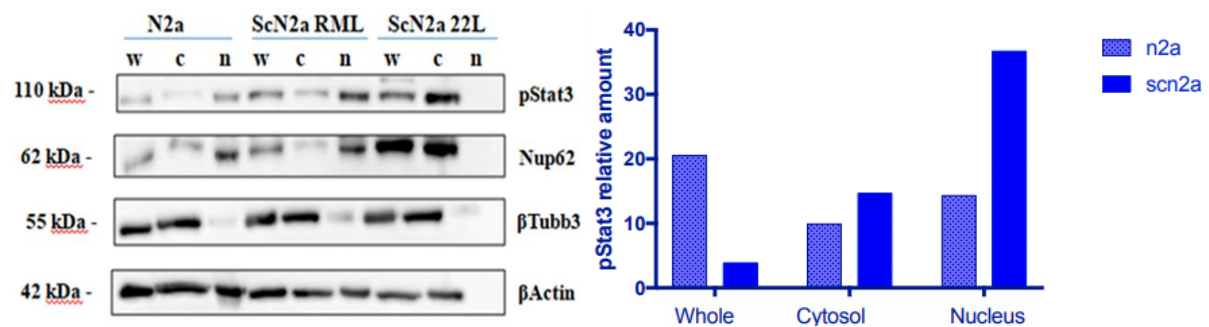


Figure 24. Western Blot analysis on N2a, ScN2a RML and 22L after REAP fractionation protocol.

a) Western Blot analysis of pStat3 expression, with Nup62 used as a nuclear marker, β -Tubb3 as a cytosolic marker and β -Actin as a marker of the correct samples loading.
b) The graph shows pStat3 relative amount in N2a and ScN2a RML cells in the three subcellular fractions.

Immunofluorescence

Since WB analysis allowed the separation of the nuclear fraction only in N2a and N2a RML-infected cells, we proceeded by performing immunofluorescence analysis in N2a, RML- and 22L-infected N2a cells to better evaluate the distribution of phosphorylated Stat3 protein. In particular, we wanted to analyze the cytosol to nuclear translocation of pStat3 since it is the key event in the activation of the JAK/STAT3 pathway, which is necessary to modulate SerpinA3n expression.

As shown, it is possible to observe that controls (N2a) are characterized by a higher amount of pStat3 at the membrane level, while both strains of prion infected cells show a more diffused signal between the membrane and the nuclear sites, indicating a possible activation of the signaling cascade (**Figure 25**).

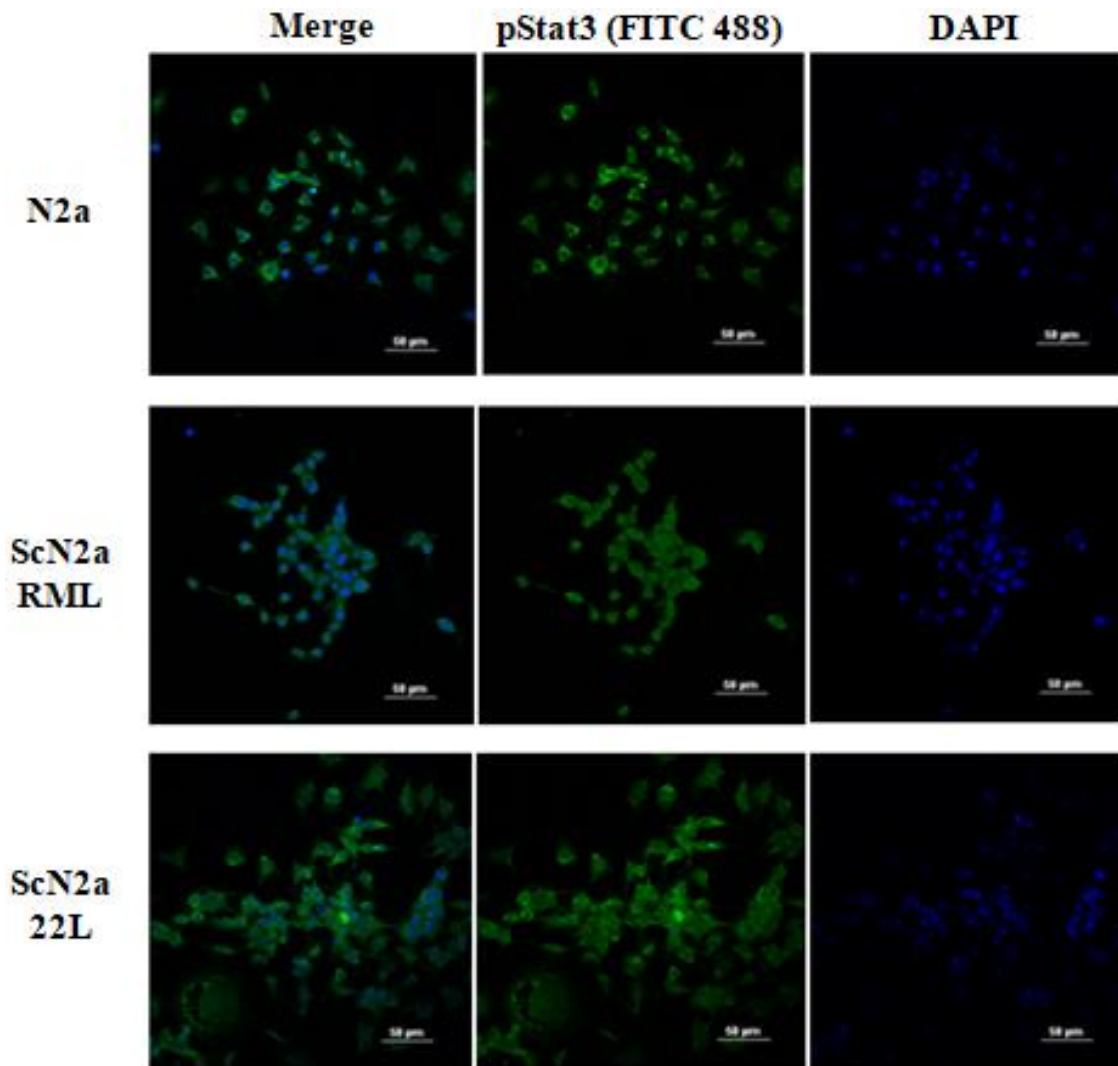


Figure 25. Immunofluorescence of pStat3 in N2a, ScN2a RML and ScN2a 22L cells. pSTAT3 localization was detected by means of IF. N2a, ScN2a RML and 22L infected have been stained for anti-pSTAT3 antibody (Cell Signaling 1:100) and detected through Alexa-fluor Goat-anti mouse-488 as secondary antibody. Nuclei have been stained with DAPI (1µg/mL).

4.13.2 FVB primary mixed culture evaluation

To further investigate the role of JAK/STAT3 pathway in SerpinA3n upregulation upon prion infection, we moved to primary mixed culture experiments in order to study both glial and neuronal cells. Since we supposed that the pathway is activated upon prion infection, inducing SerpinA3n upregulation, we analyzed JAK/STAT3 pathway components in *de novo* infected primary hippocampal cells from p2 FVB mouse brains (Victoria et al., 2016).

RT-qPCR results

We first analyzed the activation of the glial cells upon prion infection. Results showed that cells infected with prions presented a slight activation of microglia at the beginning of the process (7dpi) which increases at 21 dpi, as showed by the upregulation of the *CD86* marker. Concerning the astrocytes, the activation of this population seems to appear only at the beginning of the process, as indicated by a slight upregulation of the Glial Fibrillary Acidic Protein (*GFAP*) used as an astrocytic marker.

Then, we analysed the expression of *Il-1 β* and *Il-6*, known to be produced upon prion infection by glial cells (Aguzzi & Zhu, 2017; Campbell et al., 1994; Van Everbroeck et al., 2002) observing an upregulation of both transcripts at 14 and 21 dpi.

Later, we evaluated *STAT3* expression observing an upregulation of the *STAT3* mRNA at 14 and 21dpi. Finally, we observed a *SerpinA3n* transcript overexpression at 14 and 21 dpi (**Figure 26**).

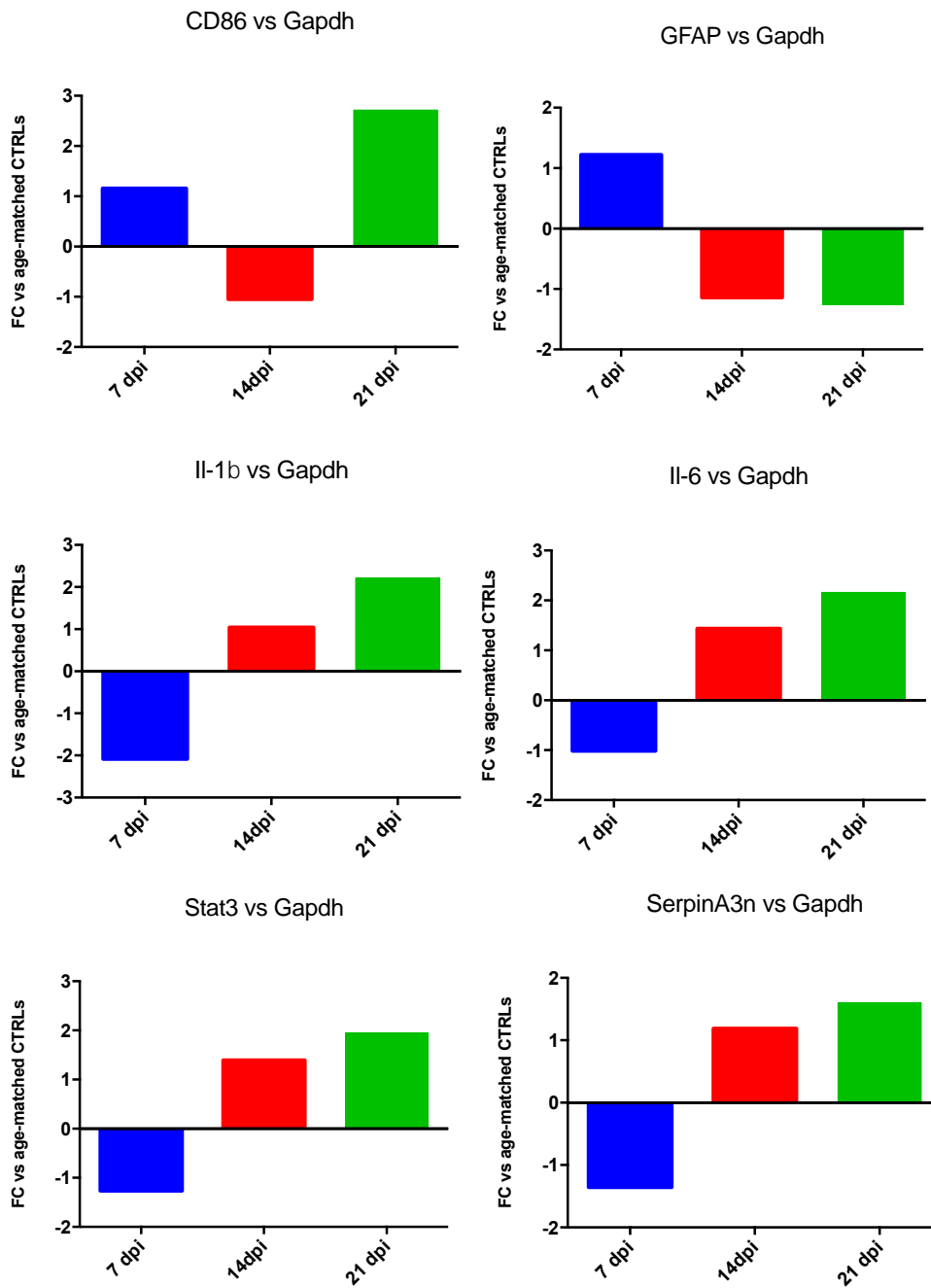


Figure 26. RT-qPCR analysis of the mRNA expression of *CD86*, *Gfap*, *IL-1β*, *IL-6*, *Stat3* *SerpinA3n* in FVB primary mixed culture at three different time points. Fold changes (FC) are calculated using the $2^{-\Delta\Delta C_T}$ classical method: first ΔC_T is calculated as the difference between the C_T of the target gene and the C_T of the housekeeping gene to normalize the C_T value of. $\Delta\Delta C_T$ is calculated as the difference between ΔC_T of prion infected cells and ΔC_T of uninfected ones. *Gapdh* was used to normalize results.

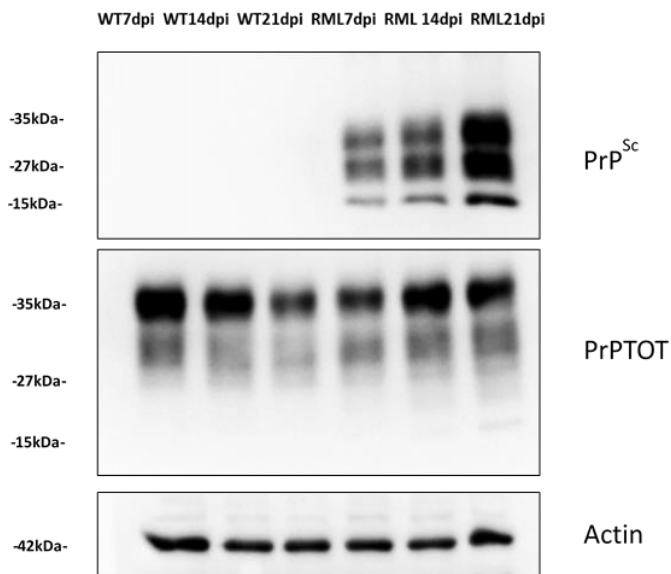
Western blot analysis

After the mRNA evaluation, we moved to the analysis of the protein level. To begin, we firstly assessed the infection protocol used, evaluating the presence of PK-resistant PrP isoforms (PrP^{Sc}) through WB analysis, as signal of PrP infection.

As showed in **Figure 27**, hippocampal primary cells infected with RML prions presented the typical banding pattern of the PrP^{Sc} after the PK treatment, whereas uninfected cells were totally devoid of the signal. Moreover, we observed the accumulation of prions after 7 days post infection, with a progressive increased signal over time.

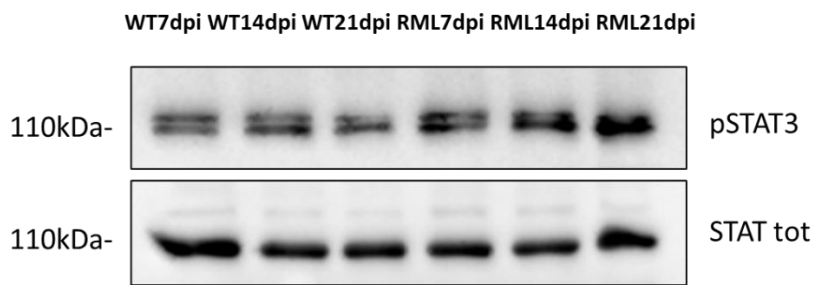
Established the infection, we evaluated the presence of PrP^{Sc} aggregates by the means of the immunofluorescence, using a previous published protocol (Victoria et al., 2016). As showed in **Figure 28**, infected cells present an increasing accumulation of PrP^{Sc} aggregates over time, as indicated by the white arrows.

a)



We then analysed the levels of the main players of the JAK/STAT3 cascade and we observed a higher pSTAT3 levels upon prion infection, at all the time points, suggesting us that prion infection in primary hippocampal cells induces JAK/STAT3 activation (**Figure 29**).

a)



b)

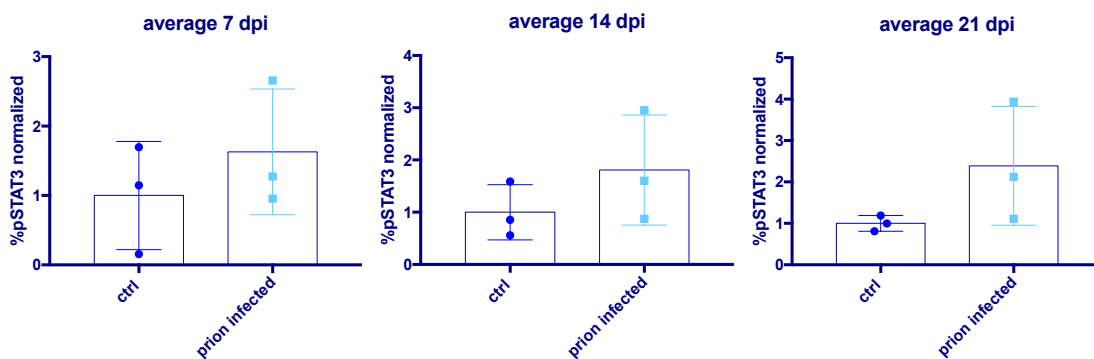
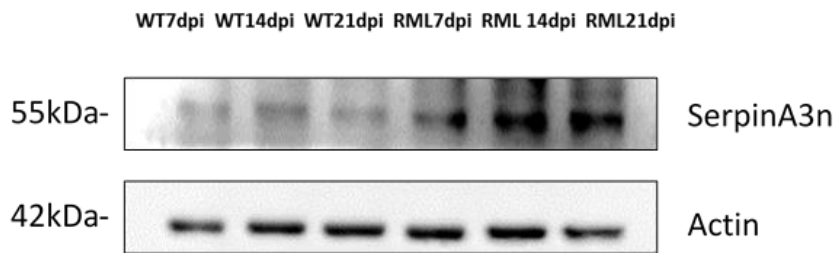


Figure 29. Western Blot analysis of pStat3 and total Stat3 expression in infected and uninfected primary mixed culture cells. a) Western Blot analysis of pSTAT3/total STAT3 expression in both infected and uninfected cells. b) The graph shows the ratio of pSTAT3 on total STAT3 in controls (ctrl) and prion infected cells. At all the time points pSTAT3 signal in infected cells is higher compared to the one coming from controls. Statistical analysis was performed by Wilcoxon matched-pairs signed rank test (N=3).

We then analyzed SerpinA3n induction by the activation of the JAK/STAT3 pathway, confirming RT-qPCR results. As expected, we observed an increased SerpinA3n signal in all infected cells compared to control samples (**Figure 30**).

a)



b)

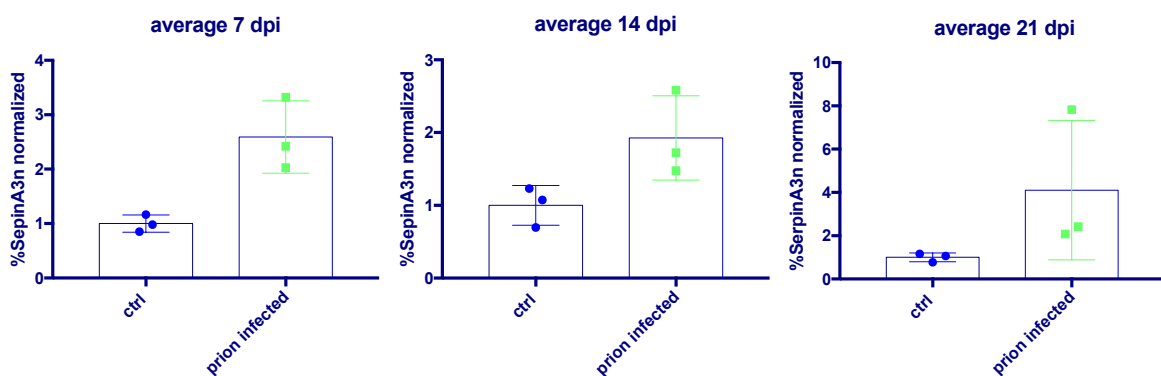
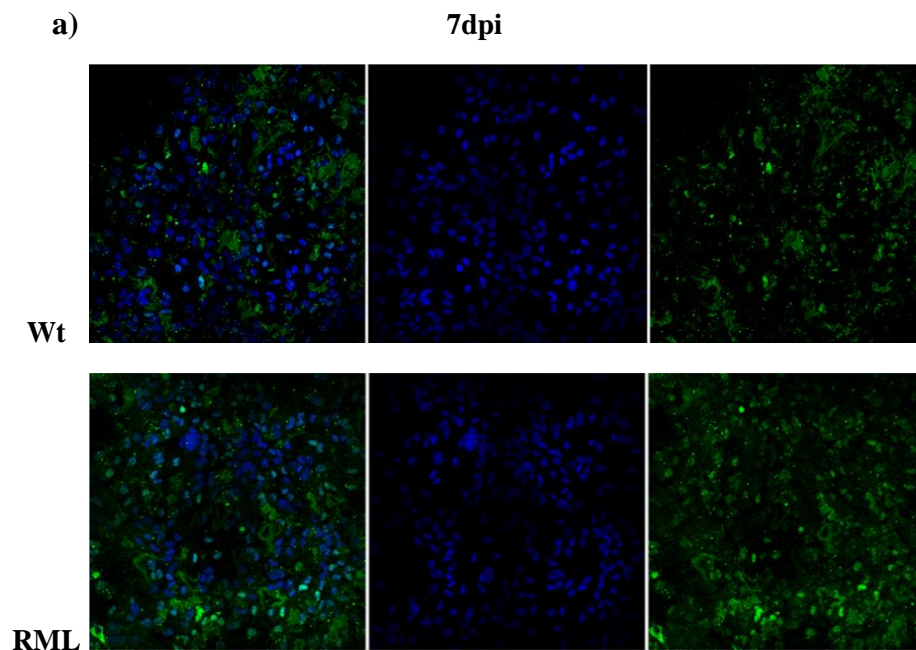


Figure 30. Western Blot analysis of SerpinA3n expression in infected and uninfected primary mixed culture cells. a) Western Blot analysis of SerpinA3n expression in both infected and uninfected cells, with β -Actin as a marker of the correct samples loading. b) The graph shows the ratio of SerpinA3n on β -Actin in controls (ctrl) and prion infected cells. At all the time points SerpinA3n signal in infected cells is higher compared to the one coming from controls. Statistical analysis was performed by Wilcoxon matched-pairs signed rank test (N=3).

Immunofluorescence

We performed immunofluorescence experiment to evaluate whether pSTAT3 was not only increased but also delocalized in different compartments in prion infected cells, possibly with a higher presence into the nucleus.

As shown in **Figure 31**, we obtained, as observed in immortalized cell lines, a higher signal of pSTAT3 in all the infected cells compared to uninfected ones. In particular, at 14 days post-infection, we observed a strong and diffuse signal in infected cells.



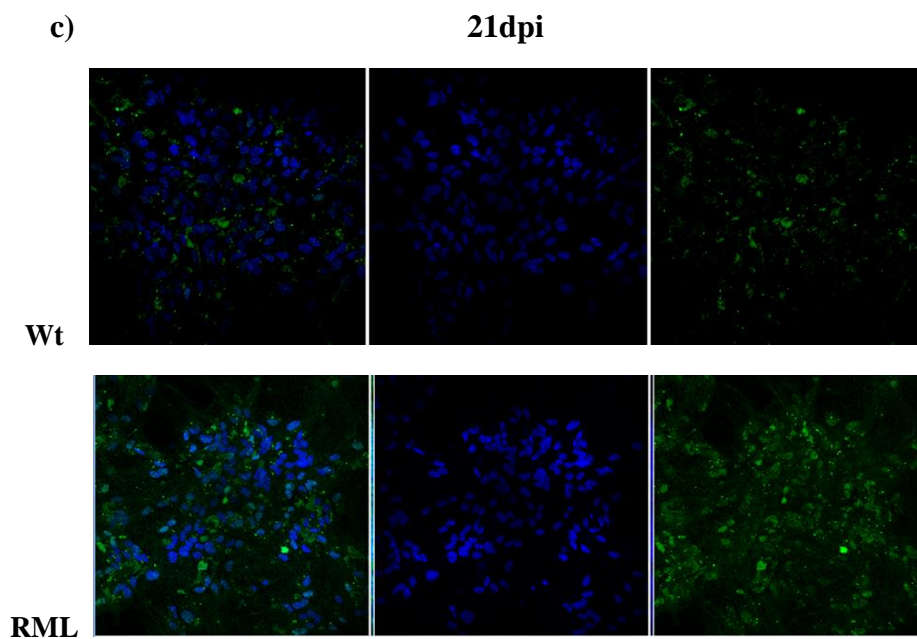
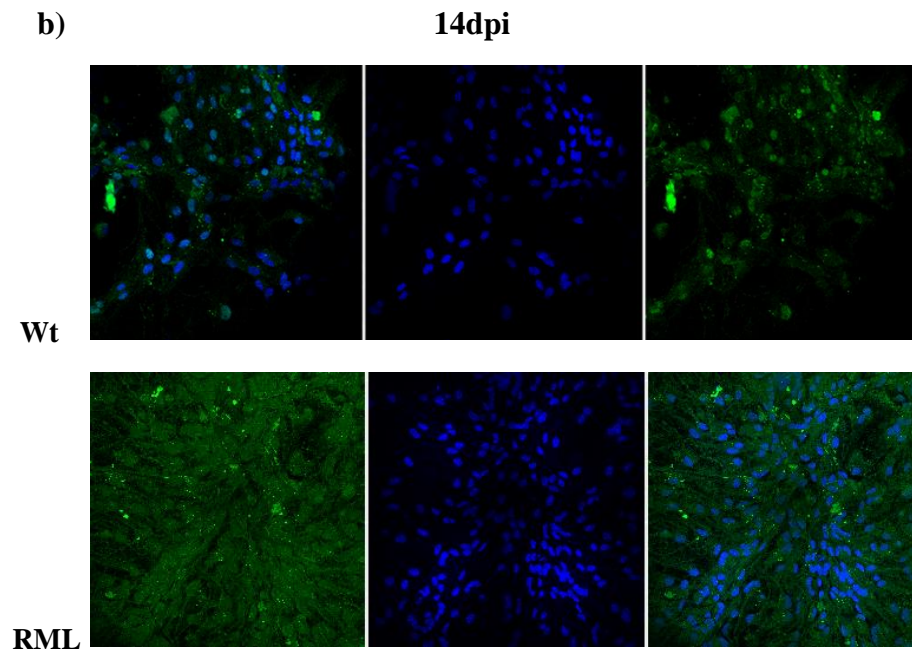


Figure 31. Immunofluorescence of pSTAT3 levels in infected primary cells. Primary mixed culture cells were stained with pSTAT3 (Cell Signaling) 1:100 and Goat anti-mouse [GoMo]-AlexaFluor 488 (Life Technologies) as secondary antibody to evaluate the localization of the protein in infected cells (RML) and uninfected cells (WT), at the three different time points: **a)** 7dpi **b)** 14dpi and **c)** 21dpi. Nuclei have been stained with DAPI (1 μ g/mL).

4.13.3 Mouse brains evaluation

RT-qPCR results

To deeply investigate the role of JAK/STAT3 pathway in *Serpina3n* upregulation upon prion infection, we took advantage of an *in vivo* model of prion disorders. We homogenized brains of CD1 RML-infected mice sacrificed at 3 months and 5 months post-infection and then we analyzed the expression levels of the genes involved in this signaling cascade.

cDNA was obtained from 16 different samples, 8 prion-infected and 8 control brain homogenates. In particular we analyzed 4 RML-infected brain homogenates at 3 months post infection (3mpi) and 4 at 5 months post infection (5mpi) with the relative age matched controls. As for the immortalized cell lines and primary mixed cultures, mRNA expression was normalized against *Gapdh*, β -*Actin* and β -*Tubb3*.

We analyzed the glial activation upon prion infection evaluating the expression of *GFAP* and *CD86*, as marker for glial population. Results showed that prion-infected mice presented a significant upregulation of both transcripts only at 5mpi (**Figure 32**). These results indicate that the activation of glial cells becomes consistent after a long period of incubation, explaining the variability of results obtained in the primary mixed culture cells.

Then, we analysed the expression of the two interleukins produced upon prion infection by glial cells, *Il-1 β* and *IL-6*, and we found again a significant upregulation of both mRNAs at 5mpi, but also a significant upregulation of *IL-6* at 3mpi (**Figure 32**).

Later, we evaluated also the expression level of *STAT3*, observing an upregulation of the *STAT3* mRNA at 5mpi, and *Serpina3n* which also becomes statistically significant upregulated at 5mpi (**Figure 32**).

The absence of statistically significant results in the group of mice at 3mpi infection would probably rely on to the presence of a mouse devoid of PrP^{Sc} signal, which was equally included into the analysis.

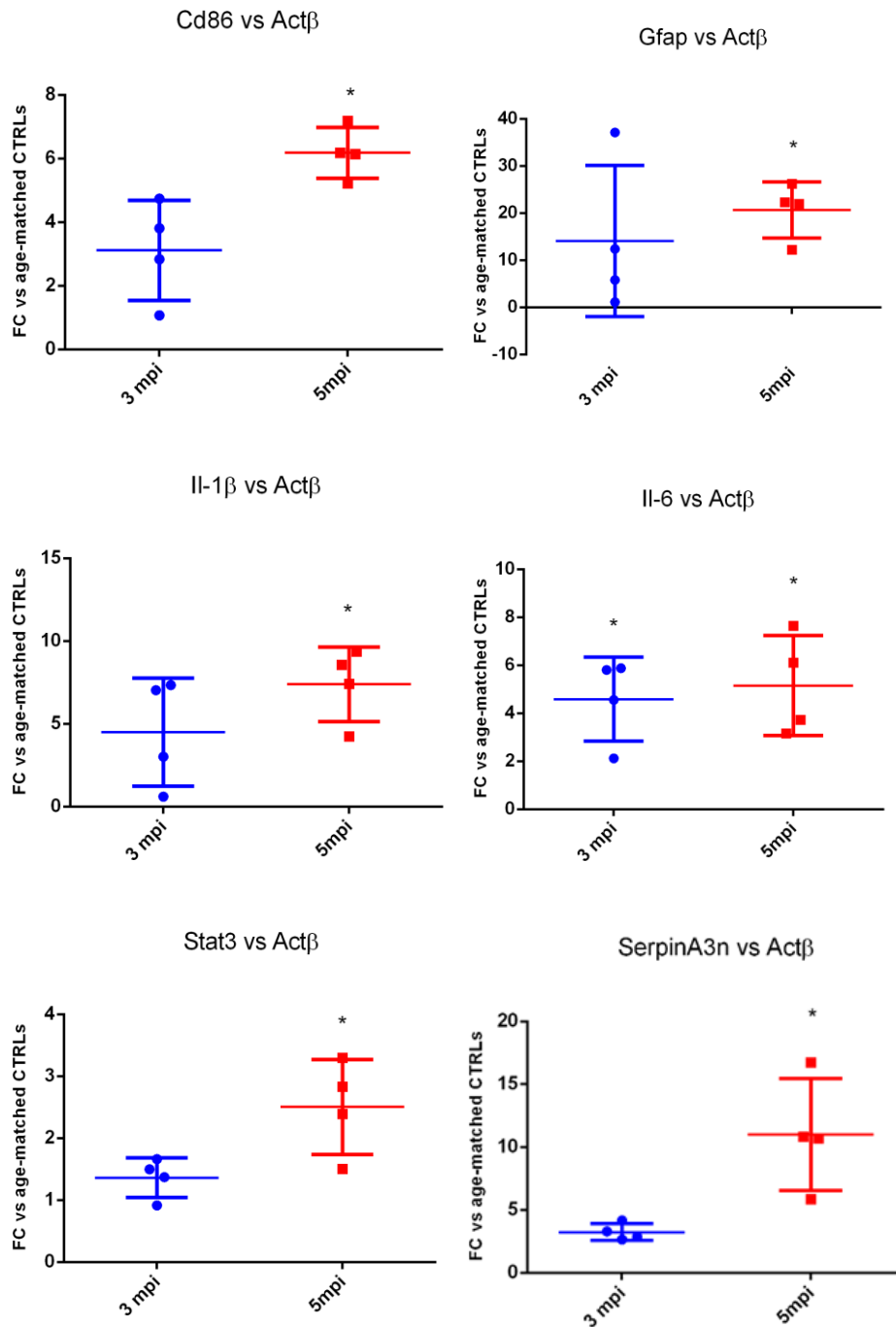


Figure 32. RT-qPCR analysis of the mRNA expression of *Gfap*, *Cd86*, *Il-1β*, *Il-6*, *STAT3* and *SerpinA3n* in CD1 mice RML-infected and uninfected normalized against β -Actin.

Fold changes (FC) are calculated using the $2^{-\Delta\Delta C_T}$ classical method: first ΔC_T is calculated as the difference between the C_T of the target gene and the C_T of the housekeeping gene to normalize the C_T value of RML infected and uninfected mice (two different time points, n=4 for each group). $\Delta\Delta C_T$ is calculated as the difference between ΔC_T of prion infected brain homogenates and ΔC_T of uninfected ones. FC are represented with the Mann-Withney test and the significance is given according to the statistical criteria of P value, with a P value < 0.05 considered significant. *P value < 0.05.

Western blot analysis

Then, we performed WB analysis to analyze the signal for PrP^{Sc}, GFAP, pSTAT3, STAT ToT and SerpinA3n in infected mouse brains. We wanted to investigate whether pSTAT3 levels were upregulated in infected mouse brains compared to uninfected ones, to confirm our idea of STAT3 involvement in SerpinA3n expression, as consequence of prion infection.

We used 8 mouse brain homogenates, 4 infected with RML prions and 4 not infected and for each group two were sacrificed 3 months post infection (3mpi) and other two 5 months post infection (5mpi).

As expected, the appearance of the typical PrP^{Sc} banding pattern was observed only in RML brain homogenates (**Figure 33**).

Since astrogliosis is one of the main hallmarks of prion diseases, we found that GFAP signal was higher in all infected mice compared to controls, as shown in **Figure 33**, confirming that prion infection induces astrocytes reactivity.

To analyze JAK/STAT3 pathway activation, as shown in the **Figure 33**, we used anti-pSTAT3 antibody, observing signals coming only from mice infected with RML prions.

Due to the absence of pSTAT3 signal in WT mouse brains, we evaluated the presence of total STAT3, observing a similar expression level in all the samples. These results indicated us that pSTAT3 overexpression is closely related to prion infection.

Collectively, these results suggested us, again, that the pathway of JAK/STAT3 can be activated upon prion infection.

Therefore, we moved on analyzing SerpinA3n levels upon pathway activation, to confirm our hypothesis. As shown in Western Blot analysis, even SerpinA3n levels were upregulated only in RML-infected brain homogenates. In particular, the lower band corresponding to the precise molecular weight of SerpinA3n protein was barely detectable in not-infected brain homogenates (**Figure 33**).

Thus, these results suggested us that JAK/STAT3 signaling cascade can be the one involved in SerpinA3n overexpression upon prion infection.

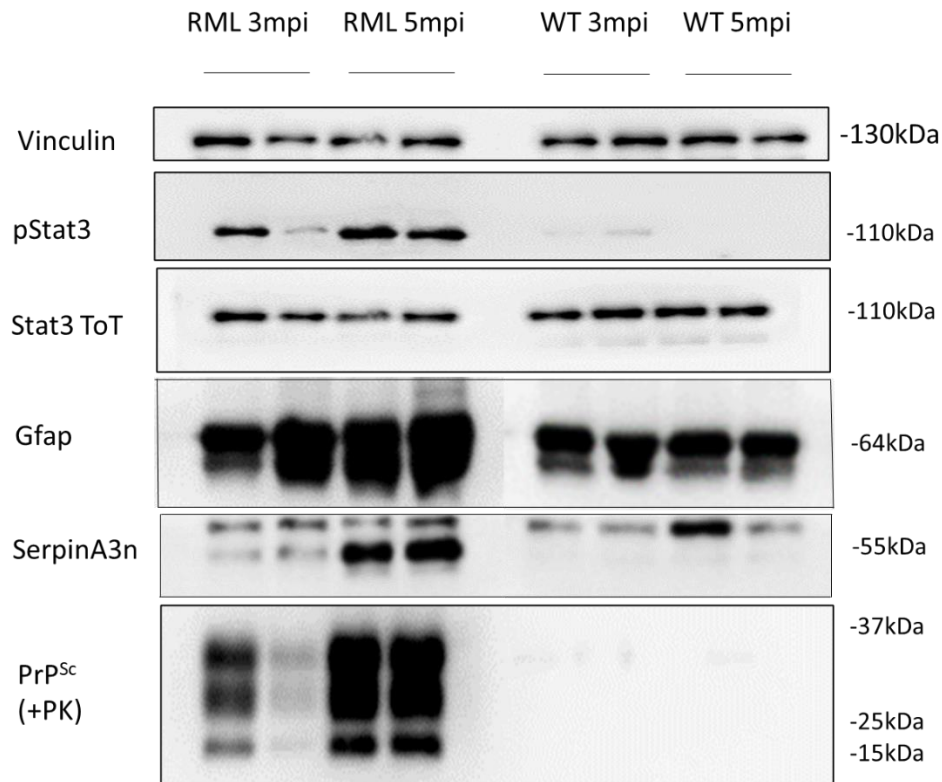


Figure 33. Western Blot analysis of RML-infected and uninfected mouse brain homogenates. Western blot analysis of PrP^{Sc}, SerpinA3n, GFAP, total STAT3 (Stat3 ToT) and phosphorylated STAT3 (pStat3) to evaluate the activation of the JAK/STAT3 signalling cascade in the upregulation of SerpinA3n after prion infection. Vinculin is used as a loading control. Molecular weights (kDa) are represented on the right of the image.

5. DISCUSSION

5.1 SerpinA3n inhibitors

Having identified SERPINA3 highly upregulated in prion infected mice, macaques, and humans (Barbisin et al., 2014; Chen et al., 2017; Vanni et al., 2017), we selected a library of inhibitors of this protein with the aim of interfering with the process of prion conversion and accumulation.

Indeed, despite all active efforts for these disorders, there are currently no drugs available.

To date, drug discovery aimed to identify useful compounds for prion disorders treatment followed the so-called ‘small molecule design’, whose rationale relies in the ability of a given compound to interfere with either PrP^C or PrP^{Sc}, hampering the pathogenic conversion. However, despite a huge number of compound libraries has been generated, all these molecules failed to prove significant therapeutic effect when administered to humans (Colini Baldeschi et al., 2020).

Thus, for the first time, we propose a novel not-PrP targeted therapeutic strategy to treat prion and, likely, prion-like disorders.

Indeed, our strategy is direct towards the inhibition of protease inhibitors, in this case SERPINA3/SerpinA3n, that may be responsible for defective prion clearance.

The aim is to reduce protein conversion and/or accumulation without interfering with the cellular or misfolded prion protein. This strategy could also be applied to treat other diseases such as AD, PD and other prion-like neurodegenerative diseases that share the same misfolding mechanism. Indeed, it has recently been shown that SERPINA3 is upregulated also in AD samples (Vanni et al., 2017).

Since the evaluation of anti-prion molecule efficacy is prevalently focused on cell-based *in vitro* screening (Moda, Bolognesi, & Legname, 2019), we took advantage of two immortalized cell-based models of prion infection, N2a and GT1 RML- or 22L-infected cells (Vilette, 2008). Our tested molecules have been selected to specifically inhibit the activity of the serine-protease inhibitor SERPINA3/SerpinA3n.

Our hypothesis is that in prion-infected subjects, the up-regulation of SERPINA3/SerpinA3n leads to the inhibition of the target protease(s) that, in physiological conditions, would degrade the aberrant PrP^{Sc} isoform. Thus, using inhibitors of these serpins we could restore protease(s) activity, leading to PrP^{Sc} clearance and slowing down the disease progression.

Among the first library of 19 compounds (A-U), we *in vitro* selected compound H as the one showing a higher anti-prion activity. Given its high effective concentration, we screened a second library of 8 structural compound H-analogs, selecting compound 5 as the most effective one. Indeed, our SerpinA3n-directed ‘hit compound’ demonstrated a strong inhibition of PrP^{Sc} accumulation in all *in vitro* experiments, confirming that SerpinA3n plays a key role in prion replication.

However, even if we demonstrated that SerpinA3n is certainly involved in prion accumulation process and that Compound 5 is able to induce prion clearance, we lack a direct demonstration of the Compound5-SerpinA3n specific binding.

Indeed, we tried to demonstrate the specific binding of Compound 5 to SerpinA3n *in silico* and *in vitro*, as showed by SerpinA3n-KO ScN2a RML cells treatment, but we were aware that a specific assay to assess this binding was needed.

Thus, we purified a recombinant SerpinA3n protein and we used it to set up some experiments to test its functionality. In particular, we incubated the recombinant protein with one of its known target proteases (Chymotrypsin), to see if SerpinA3n was able to block its activity or not. We used WB analysis to evaluate the results coming from the incubation of the recombinant SerpinA3n and the Chymotrypsin and the results coming from the incubation of SerpinA3n isolated from N2a cells overexpressing SerpinA3n and the same protease.

What we found was that the recombinant protein was not functional, since it was being degraded by the action of Chymotrypsin, when incubated together (see **Appendix, Figure 1**), while SerpinA3n isolated from N2a conditioned medium presented a higher band when incubated with the target protease, meaning that it was able to bait the protease into its structure, inhibiting its activity, and to form the complex, as stated by the mechanism of inhibition of serpins (see **paragraph 1.7.1**).

For this reason, we could not perform a direct assay to establish the Compound5-SerpinA3n direct binding; thus, we are now trying to set up a new procedure to produce a functional recombinant SerpinA3n, to be used for this purpose.

However, encouraged by the promising results obtained *in vitro* in the prion clearance, we decided to try the efficacy of the Compound also *in vivo*.

Unfortunately, *in vivo* compound 5 testing showed a poor pharmacokinetic profile, demonstrating a low brain concentration and a fast plasma clearance.

Thus, we are now planning the design of new libraries of molecules based on compound 5 structure with increased *in vivo* capacities.

However, all together, these results suggest us that our novel not-PrP targeted anti-prion strategy could represent the most promising way to pave the way for innovative anti-prion, and prion-like, therapies.

Importantly, the up-regulation of SerpinA3n has been detected also at a pre-symptomatic stage in prion-infection (Vanni et al., 2017). Therefore, together with the improvement of more sensitive pre-symptomatic diagnostic tools for prion disorders (Zanusso, Monaco, Pocchiari, & Caughey, 2016), compound 5-based therapies could be used to delay symptoms appearance increasing patients' life expectancy.

So far, no inhibitors against SERPINA3 or SerpinA3n have been developed for neurodegenerative disorders. A SERPINA3/SerpinA3n directed therapeutic strategy has limited to the use of SerpinA3n itself as protease-inhibitor (Haile et al., 2015) or about inhibitors of other components of the serpin family (Jacobsen et al., 2008). Indeed, SerpinA3n itself has been used to inhibit granzyme- β activity in a mouse model of Multiple Sclerosis, showing reduced axonal and neuronal injury (Haile et al., 2015). For what concerns the use of other serpin inhibitors to treat neurodegeneration, a small molecule inhibitor (PAZ-417) of SERPINE1, has been shown to partially block amyloid deposition in a mouse model of AD (Jacobsen et al., 2008).

Therefore, it is the first time in which the use of molecules that specifically inhibit SerpinA3n is proposed to treat prion disorders and, likely, other neurodegenerative diseases.

5.2 The JAK/STAT3 pathway

In the last years, different studies have reported a role of SERPINA3/SerpinA3n in prion disorders; indeed, it has been demonstrated that these serpins are particularly upregulated in several models of prion diseases, like BSE-infected cynomolgus macaques, prion-infected mice but also in human samples (Barbisin et al., 2014; Chen et al., 2017; Vanni et al., 2017). However, the molecular mechanism at the basis of SERPINA3/SerpinA3n up-regulation has not been investigated yet. Thus, we focused on the identification of the cellular process that correlates prion infection and SERPINA3/SerpinA3n appearance.

One of the main hallmarks of prion diseases is the activation of glial cells upon prion infection with the consequent production of many inflammatory mediators, as cytokines and chemokines. The exact role for glial cells in prion diseases is still not completely understood,

but it seems to take part in the degeneration of prion-infected brain tissues (Aguzzi & Zhu, 2017).

Serpina3n is mainly produced by the astrocytes in the brain, thus the activation of glial cells upon prion infection, can explain its upregulation during the course of the disease. However, it remains to understand the peculiar signalling pathway involved in this process.

Among the inflammatory mediators produced after prion infection, Interleukin-6 (Il-6) is the one related to astrocytes activation (Chiang, Stalder, Samimi, & Campbell, 1994). Many studies reported that IL-6 can induce the activation of the JAK/STAT3 pathway, which has been already correlated to different inflammatory responses, including astrogliosis (Ceyzeriat et al., 2016). Indeed, it has been reported that activated STAT3 is present in reactive astrocytes involved in acute brain injury and neurodegenerative disorders, among which prion diseases (Ben Haim et al., 2015; Na et al., 2007). Moreover, in 2007 Baker et al. discovered STAT binding sites on SERPINA3 promoter sequence, suggesting us a possible correlation between SERPINA3 and the JAK/STAT3 pathway.

Supported by literature data, we wondered if this signalling cascade would be the one linking prion infection and SerpinA3n upregulation.

Firstly, we searched for the presence of possible STAT3 binding sites on SerpinA3n promoter, since no data are available about that, and we found at least three possible binding sites of this transcription factor.

Then, we moved to the analysis of the pathway activation in prion infected immortalized cell lines and we started from a transcriptional analysis of the different cascade components, observing that cells chronically infected with prions presented increased mRNA expression levels of *Il-1β*, *Il-6*, *Stat3*, and as already demonstrated, *Serpina3n*.

Later, we analysed protein levels, since the activation of this pathway is characterized by the phosphorylation of STAT3 and its consequent shift into the nucleus of cells, necessary for the activation of target genes transcription.

We found that prion infected cells presented higher amount of phosphorylated STAT3, compared to uninfected ones. Moreover, separating the different cellular fractions we observed that pSTAT3 was prevalently present into the nucleus of infected cells, indicating a pathway activation during prion infection.

However, our cellular model lack of glial cells, which represent the key players in this pathway. Thus, we decide to take advantage of a more complex prion disease model, using hippocampal primary mixed cell cultures.

After *de novo* RML-prion infection of these cells, we evaluated the expression of those genes involved in the pathway, analysing in this case also the activation of the glial cells (*Gfap* and *Cd86* were used as astrocytic and microglial marker, respectively).

We found that in prion infected cells the majority of the genes were upregulated at 14- and 21-days post infection (dpi), while *Gfap* and *Cd86* showed an overexpression immediately after the infection (7dpi) and, only *Cd86* was upregulated again at 21 dpi. At protein levels, we found that both pSTAT3 and SerpinA3n were increased in infected cells compared to controls.

However, since we could maintain cells in culture only up to 30 days, this limited time window was probably not sufficient to analyse properly the effect of prion infection on JAK/STAT3 pathway.

So, we decided to move on RML- infected CD1 mouse brain homogenates to have a more reliable model. We found that all the pathway related genes were upregulated in prion-infected mouse brains compared to un-infected ones, with statistically significant differences at the end stage of the disease (5mpi). Moreover, at the protein level we found higher level of STAT3 phosphorylation, GFAP and SerpinA3 in all infected mice.

All together, these data suggested that prion infection is able to activate glial cells, which induce the secretion of many inflammatory mediators, such as IL-6, which can lead to the activation of JAK/STAT3 pathway, as observed by an increase phosphorylation of STAT3 in prion infected models, where also SerpinA3n is overexpressed. Thus, we claim that the JAK/STAT3 pathway could be responsible for SerpinA3n overexpression during prion infection.

To further analyse the involvement of this pathway on SerpinA3n overexpression in prion diseases, we performed LPS treatment on immortalized cell lines to induce inflammation and activate the same signalling cascade (Greenhill et al., 2011).

Indeed, we wondered that whether SerpinA3n is an acute phase gene, expressed as a consequence of an inflammatory response, we should observe its upregulation and JAK/STAT3 pathway activation upon LPS-induced inflammation, as demonstrated during prion infection.

To assess this question, we left in culture LPS-treated N2a cells (1µg/mL) for 6 and 24 h before collecting cells and conditioned media. Then, we analysed treated and untreated cells by the means of RT-qPCR and WB, evaluating STAT3 and released SerpinA3n levels.

Interestingly, we found increased levels of both STAT3 and SerpinA3n at the transcription (**Figure 2, Appendix**) and protein level (**Figure 3 and 4, Appendix**), suggesting us that LPS acts as prions, inducing an inflammatory response and activating JAK/STAT3 pathway.

However, it has been shown that LPS-induced inflammatory response is dependent on Toll-Like Receptor (TLR) 4 interaction (Greenhill et al., 2011), a receptor expressed by lymphoid or myeloid cells and microglia in murine CNS (Vaure & Liu, 2014).

Thus, since we used N2a cells to induce the LPS inflammation, we evaluated whether TLR4 was expressed in our cell model; indeed, through Western Blot analysis we observed that TLR4 is also expressed in N2a cells (see **Figure 5, Appendix**).

Concluding, we hypothesised that prion infection induces an inflammatory response in the cells (as LPS does), leading to IL-6 production and JAK/STAT3 activation, with the consequent SerpinA3n overexpression.

Of course, other experiments are needed to deeply investigate the detailed mechanism responsible for JAK/STAT3 pathway activation, as the analysis of the JAKs involved in the phosphorylation of STAT3 and the soluble and/or the membrane bound receptors recognized by IL-6. Moreover, we wondered to use inhibitors of the pathway, as SOCS3, or downregulate STAT3 itself to observe what happen to SerpinA3n expression.

6.CONCLUSIONS

For our work we started from the observation of a great overexpression of the serine protease inhibitor SerpinA3n, the murine orthologue of human SERPINA3, in several models of prion diseases. Prion diseases are characterized by a progressive conversion and accumulation of misfolded prion protein into the brain, which leads to vacuolation, gliosis and neuronal death. To date, all the therapeutic strategies developed for prion disorders were based on the interference of the PrP^C-PrP^{Sc} conversion mechanism.

However, no effective therapies have been found yet and new therapeutic interventions are needed. Thus, we decided to focus our attention on prion related SerpinA3n overexpression.

Indeed, being SerpinA3n a protease inhibitor, we supposed that it could be involved in the development of the pathology, through the inhibition of the protease(s) involved in prion clearance. To test our hypothesis, we used SerpinA3n inhibitors to evaluate PrP^{Sc} accumulation upon treatment; interestingly, we found that one of these inhibitors was able to induce prion clearance, confirming our idea.

Thus, we concluded that SerpinA3n plays a crucial role in prion disease development since it possibly blocks the activity of the protease (s) involved in the clearance of the aberrant prion protein. As far as we know, this is the first time that SerpinA3n is targeted to clear prions and we propose a novel, promising and not-PrP targeted therapeutic strategy to treat prion diseases, which might be applied also for other neurodegenerative disorders.

Moreover, since no data are available regarding the relationship between SerpinA3n overexpression and prion accumulation, we tried to unravel the molecular mechanism at the basis of this event. Indeed, being SerpinA3n an acute phase gene prevalently expressed by brain astrocytes, we suggested that prion infection induces an inflammatory response which stimulates glial cells to release many inflammatory mediators to counteract the infection, as Il-1 β and Il-6. Given that Il-6 has been proposed as activator of the JAK/STAT3 pathway, which has been showed to induce the transcription of several acute phase genes, we investigated its activation in different *in vitro* models of prion diseases.

Analysing the principal components of the cascade (Il-6, Gfap, Stat3) and SerpinA3n expression at the transcriptional and protein level, we observed the activation of the pathway in all the *in vitro* models used; thus, we propose this signalling cascade as the one responsible of SerpinA3n overexpression upon prion infection.

7. APPENDIX

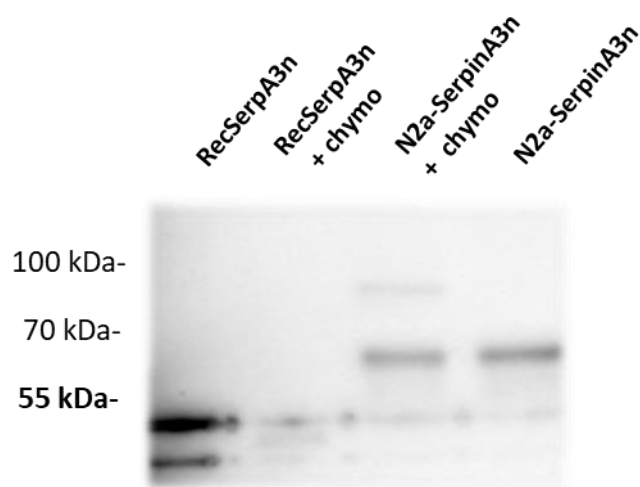


Figure 1. Recombinant SerpinA3n in complex with Chymotrypsin. As shown in the WB recombinant SerpinA3n shows a double band that is degraded when it is incubated with the protease target (Chymotrypsin), indicating that the function of the SerpinA3n RCL is impaired in the recombinant protein. As control we used medium of N2a overexpressing SerpinA3n in complex with Chymotrypsin. In this case, SerpinA3n is able to block the activity of the protease, forming a complex with a higher molecular weight, around 100kDa

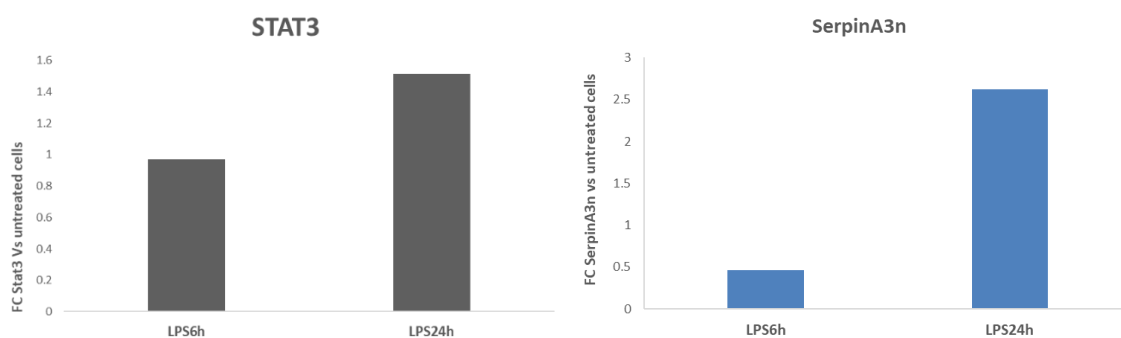


Figure 2. RT-qPCR of *STAT3* and *SerpA3n* in N2a cells treated with LPS. Both *STAT3* and *SerpA3n* transcripts are upregulated in N2a cells treated with LPS for 24 hours compared to Ctrl cells (N2a untreated).

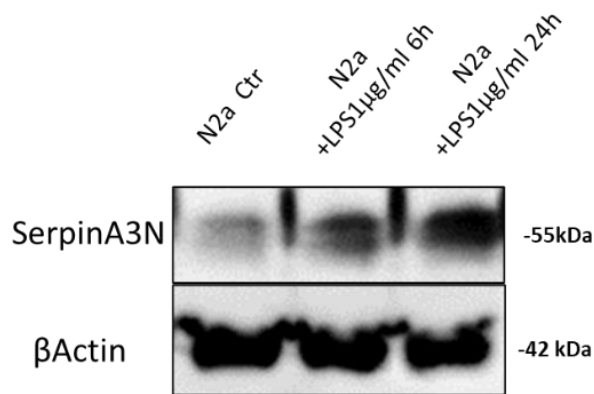


Figure 3. Western Blot analysis of SerpinA3n expression in N2a treated with LPS. SerpinA3n level is higher in N2a cells treated with LPS (1 µg/mL) compared to untreated N2a and it increases over time, with a higher level after 24 hours of treatment. β-Actin is used as control for sample loading. Molecular weights are represented on the right of the image.

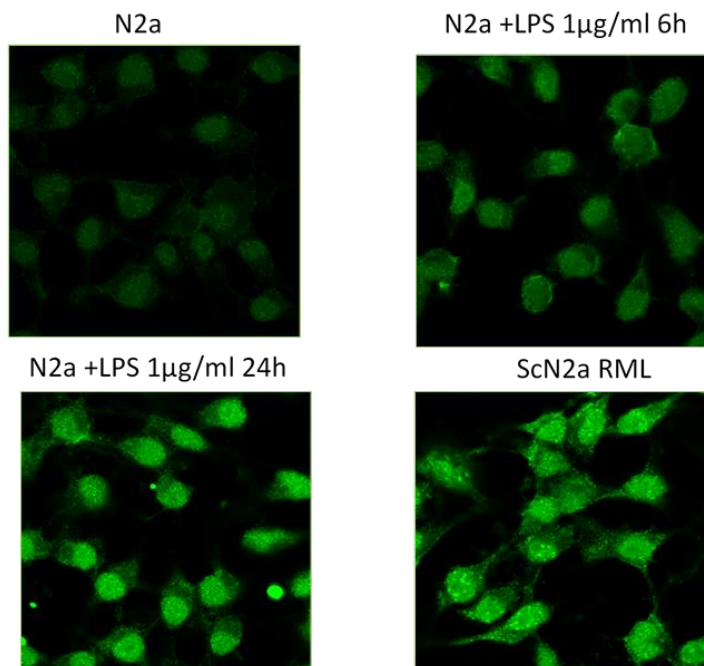


Figure 4. Immunofluorescence of pSTAT3 in N2a and ScN2a cells. Immunofluorescence of pSTAT3 signal in N2a cells treated with LPS (1 µg/mL) and untreated, compared to ScN2a cells. Cells were stained with pSTAT3 (Cell Signaling 1:100) and Goat anti-mouse [GαMo]-AlexaFluor 488 (Life Technologies) as secondary antibody to evaluate the localization of the protein. pSTAT3 signal appears to be higher in the nuclei of N2a cells treated with LPS both after 6h or 24h of treatment compared to

untreated cells (N2a) and particularly after 24h of treatment the signal is similar to the one present in the ScN2a cells.

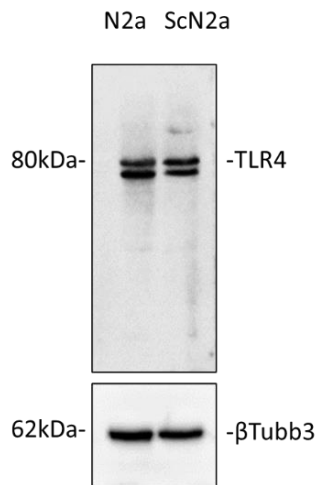


Figure 5. Western Blot analysis of TLR4 expression in N2a and ScN2a RML cell lines. Western Blot analysis reveals that both N2a and ScN2a RML cells express TLR4. β -Tubulin3 has been used as a marker of the correct sample loading. Molecular weights are represented on the left of the image.

8. BIBLIOGRAPHY

- Abid, K., & Soto, C. (2006). The intriguing prion disorders. *Cell Mol Life Sci*, *63*(19-20), 2342-2351. doi:10.1007/s00018-006-6140-5
- Abraham, C. R., Selkoe, D. J., & Potter, H. (1988). Immunochemical identification of the serine protease inhibitor alpha 1-antichymotrypsin in the brain amyloid deposits of Alzheimer's disease. *Cell*, *52*(4), 487-501. doi:10.1016/0092-8674(88)90462-x
- Acevedo-Morantes, C. Y., & Wille, H. (2014). The structure of human prions: from biology to structural models-considerations and pitfalls. *Viruses*, *6*(10), 3875-3892. doi:10.3390/v6103875
- Adjou, K. T., Privat, N., Demart, S., Deslys, J. P., Seman, M., Hauw, J. J., & Dormont, D. (2000). MS-8209, an amphotericin B analogue, delays the appearance of spongiosis, astrogliosis and PrPres accumulation in the brain of scrapie-infected hamsters. *J Comp Pathol*, *122*(1), 3-8. doi:10.1053/jcpa.1999.0338
- Aguzzi, A. (1996). Between cows and monkeys. *Nature*, *381*(6585), 734. doi:10.1038/381734a0
- Aguzzi, A., Baumann, F., & Bremer, J. (2008). The prion's elusive reason for being. *Annu Rev Neurosci*, *31*, 439-477. doi:10.1146/annurev.neuro.31.060407.125620
- Aguzzi, A., Glatzel, M., Montrasio, F., Prinz, M., & Heppner, F. L. (2001). Interventional strategies against prion diseases. *Nat Rev Neurosci*, *2*(10), 745-749. doi:10.1038/35094590
- Aguzzi, A., & Weissmann, C. (1996). Spongiform encephalopathies: a suspicious signature. *Nature*, *383*(6602), 666-667. doi:10.1038/383666a0
- Aguzzi, A., & Zhu, C. (2017). Microglia in prion diseases. *J Clin Invest*, *127*(9), 3230-3239. doi:10.1172/JCI90605
- Altmeyden, H. C., Prox, J., Krasemann, S., Puig, B., Kruszewski, K., Dohler, F., . . . Glatzel, M. (2015). The sheddase ADAM10 is a potent modulator of prion disease. *Elife*, *4*. doi:10.7554/eLife.04260
- Altmeyden, H. C., Puig, B., Dohler, F., Thurm, D. K., Falker, C., Krasemann, S., & Glatzel, M. (2012). Proteolytic processing of the prion protein in health and disease. *Am J Neurodegener Dis*, *1*(1), 15-31.
- Amin, L., Nguyen, X. T., Rolle, I. G., D'Este, E., Giachin, G., Tran, T. H., . . . Legname, G. (2016). Characterization of prion protein function by focal neurite stimulation. *J Cell Sci*, *129*(20), 3878-3891. doi:10.1242/jcs.183137
- Amor, S., Peferoen, L. A., Vogel, D. Y., Breur, M., van der Valk, P., Baker, D., & van Noort, J. M. (2014). Inflammation in neurodegenerative diseases--an update. *Immunology*, *142*(2), 151-166. doi:10.1111/imm.12233
- Ang, L. S., Boivin, W. A., Williams, S. J., Zhao, H., Abraham, T., Carmine-Simmen, K., . . . Granville, D. J. (2011). Serpina3n attenuates granzyme B-mediated decorin cleavage and rupture in a murine model of aortic aneurysm. *Cell Death Dis*, *2*, e209. doi:10.1038/cddis.2011.88
- Arata, H., Takashima, H., Hirano, R., Tomimitsu, H., Machigashira, K., Izumi, K., . . . Arimura, K. (2006). Early clinical signs and imaging findings in Gerstmann-Straussler-Scheinker syndrome (Pro102Leu). *Neurology*, *66*(11), 1672-1678. doi:10.1212/01.wnl.0000218211.85675.18
- Asante, E. A., Gowland, I., Linehan, J. M., Mahal, S. P., & Collinge, J. (2002). Expression pattern of a mini human PrP gene promoter in transgenic mice. *Neurobiol Dis*, *10*(1), 1-7. doi:10.1006/nbdi.2002.0486
- Aslam, M. S., & Yuan, L. (2019). Serpina3n: Potential drug and challenges, mini review. *J Drug Target*, *1-11*. doi:10.1080/1061186X.2019.1693576
- Atarashi, R., Satoh, K., Sano, K., Fuse, T., Yamaguchi, N., Ishibashi, D., . . . Nishida, N. (2011). Ultrasensitive human prion detection in cerebrospinal fluid by real-time quaking-induced conversion. *Nat Med*, *17*(2), 175-178. doi:10.1038/nm.2294

- Atarashi, R., Wilham, J. M., Christensen, L., Hughson, A. G., Moore, R. A., Johnson, L. M., . . . Caughey, B. (2008). Simplified ultrasensitive prion detection by recombinant PrP conversion with shaking. *Nat Methods*, *5*(3), 211-212. doi:10.1038/nmeth0308-211
- Avar, M., Heinzer, D., Steinke, N., Dogancay, B., Moos, R., Luga, S., . . . Aguzzi, A. (2020). Prion infection, transmission, and cytopathology modeled in a low-biohazard human cell line. *Life Sci Alliance*, *3*(8). doi:10.26508/lsa.202000814
- Baker, C., Belbin, O., Kalsheker, N., & Morgan, K. (2007). SERPINA3 (aka alpha-1-antichymotrypsin). *Front Biosci*, *12*, 2821-2835. doi:10.2741/2275
- Baker, C. A., Lu, Z. Y., Zaitsev, I., & Manuelidis, L. (1999). Microglial activation varies in different models of Creutzfeldt-Jakob disease. *J Virol*, *73*(6), 5089-5097. doi:10.1128/JVI.73.6.5089-5097.1999
- Baker, C. A., Martin, D., & Manuelidis, L. (2002). Microglia from Creutzfeldt-Jakob disease-infected brains are infectious and show specific mRNA activation profiles. *J Virol*, *76*(21), 10905-10913. doi:10.1128/jvi.76.21.10905-10913.2002
- Bakkebo, M. K., Mouillet-Richard, S., Espenes, A., Goldmann, W., Tatzelt, J., & Tranulis, M. A. (2015). The Cellular Prion Protein: A Player in Immunological Quiescence. *Front Immunol*, *6*, 450. doi:10.3389/fimmu.2015.00450
- Ballmer, B. A., Moos, R., Liberali, P., Pelkmans, L., Hornemann, S., & Aguzzi, A. (2017). Modifiers of prion protein biogenesis and recycling identified by a highly parallel endocytosis kinetics assay. *J Biol Chem*, *292*(20), 8356-8368. doi:10.1074/jbc.M116.773283
- Barbisin, M., Vanni, S., Schmadicke, A. C., Montag, J., Motzkus, D., Opitz, L., . . . Legname, G. (2014). Gene expression profiling of brains from bovine spongiform encephalopathy (BSE)-infected cynomolgus macaques. *BMC Genomics*, *15*, 434. doi:10.1186/1471-2164-15-434
- Barreca, M. L., Iraci, N., Biggi, S., Cecchetti, V., & Biasini, E. (2018). Pharmacological Agents Targeting the Cellular Prion Protein. *Pathogens*, *7*(1). doi:10.3390/pathogens7010027
- Barria, M. A., Balachandran, A., Morita, M., Kitamoto, T., Barron, R., Manson, J., . . . Head, M. W. (2014). Molecular barriers to zoonotic transmission of prions. *Emerg Infect Dis*, *20*(1), 88-97. doi:10.3201/eid2001.130858
- Barria, M. A., Gonzalez-Romero, D., & Soto, C. (2012). Cyclic amplification of prion protein misfolding. *Methods Mol Biol*, *849*, 199-212. doi:10.1007/978-1-61779-551-0_14
- Bartz, J. C., Aiken, J. M., & Bessen, R. A. (2004). Delay in onset of prion disease for the HY strain of transmissible mink encephalopathy as a result of prior peripheral inoculation with the replication-deficient DY strain. *Journal of General Virology*, *85*, 265-273. doi:10.1099/vir.0.19394-0
- Bartz, J. C., Bessen, R. A., McKenzie, D., Marsh, R. F., & Aiken, J. M. (2000). Adaptation and selection of prion protein strain conformations following interspecies transmission of transmissible mink encephalopathy. *J Virol*, *74*(12), 5542-5547. doi:10.1128/jvi.74.12.5542-5547.2000
- Bate, C., Nolan, W., McHale-Owen, H., & Williams, A. (2016). Sialic Acid within the Glycosylphosphatidylinositol Anchor Targets the Cellular Prion Protein to Synapses. *J Biol Chem*, *291*(33), 17093-17101. doi:10.1074/jbc.M116.731117
- Baylis, M., & Goldmann, W. (2004). The genetics of scrapie in sheep and goats. *Curr Mol Med*, *4*(4), 385-396. doi:10.2174/1566524043360672
- Belay, E. D. (1999). Transmissible spongiform encephalopathies in humans. *Annu Rev Microbiol*, *53*, 283-314. doi:10.1146/annurev.micro.53.1.283
- Ben Haim, L., Ceyzeriat, K., Carrillo-de Sauvage, M. A., Aubry, F., Auregan, G., Guillermier, M., . . . Escartin, C. (2015). The JAK/STAT3 pathway is a common inducer of astrocyte reactivity in Alzheimer's and Huntington's diseases. *J Neurosci*, *35*(6), 2817-2829. doi:10.1523/JNEUROSCI.3516-14.2015
- Bender, H., Noyes, N., Annis, J. L., Hitpas, A., Mollnow, L., Croak, K., . . . Zabel, M. (2019). PrPC knockdown by liposome-siRNA-peptide complexes (LSPCs) prolongs survival and normal

- behavior of prion-infected mice immunotolerant to treatment. *PLoS One*, 14(7), e0219995. doi:10.1371/journal.pone.0219995
- Benetti, F., Biarnes, X., Attanasio, F., Giachin, G., Rizzarelli, E., & Legname, G. (2014). Structural determinants in prion protein folding and stability. *J Mol Biol*, 426(22), 3796-3810. doi:10.1016/j.jmb.2014.09.017
- Benetti, F., Gustincich, S., & Legname, G. (2012). Gene expression profiling and therapeutic interventions in neurodegenerative diseases: a comprehensive study on potentiality and limits. *Expert Opin Drug Discov*, 7(3), 245-259. doi:10.1517/17460441.2012.659661
- Benetti, F., & Legname, G. (2015). New insights into structural determinants of prion protein folding and stability. *Prion*, 9(2), 119-124. doi:10.1080/19336896.2015.1022023
- Beranger, F., Mange, A., Goud, B., & Lehmann, S. (2002). Stimulation of PrP(C) retrograde transport toward the endoplasmic reticulum increases accumulation of PrP(Sc) in prion-infected cells. *J Biol Chem*, 277(41), 38972-38977. doi:10.1074/jbc.M205110200
- Bistaffa, E., Moda, F., Virgilio, T., Campagnani, I., De Luca, C. M. G., Rossi, M., . . . Legname, G. (2019). Synthetic Prion Selection and Adaptation. *Mol Neurobiol*, 56(4), 2978-2989. doi:10.1007/s12035-018-1279-2
- Bolton, D. C., McKinley, M. P., & Prusiner, S. B. (1982). Identification of a protein that purifies with the scrapie prion. *Science*, 218(4579), 1309-1311. doi:10.1126/science.6815801
- Bolton, D. C., McKinley, M. P., & Prusiner, S. B. (1984). Molecular characteristics of the major scrapie prion protein. *Biochemistry*, 23(25), 5898-5906. doi:10.1021/bi00320a002
- Bons, N., Mestre-Frances, N., Belli, P., Cathala, F., Gajdusek, D. C., & Brown, P. (1999). Natural and experimental oral infection of nonhuman primates by bovine spongiform encephalopathy agents. *Proc Natl Acad Sci U S A*, 96(7), 4046-4051. doi:10.1073/pnas.96.7.4046
- Brandner, S., & Jaunmuktane, Z. (2017). Prion disease: experimental models and reality. *Acta Neuropathol*, 133(2), 197-222. doi:10.1007/s00401-017-1670-5
- Bremer, J., Baumann, F., Tiberi, C., Wessig, C., Fischer, H., Schwarz, P., . . . Aguzzi, A. (2010). Axonal prion protein is required for peripheral myelin maintenance. *Nat Neurosci*, 13(3), 310-318. doi:10.1038/nn.2483
- Brown, D. R., Schmidt, B., & Kretzschmar, H. A. (1996). Role of microglia and host prion protein in neurotoxicity of a prion protein fragment. *Nature*, 380(6572), 345-347. doi:10.1038/380345a0
- Brown, D. R., Schulz-Schaeffer, W. J., Schmidt, B., & Kretzschmar, H. A. (1997). Prion protein-deficient cells show altered response to oxidative stress due to decreased SOD-1 activity. *Exp Neurol*, 146(1), 104-112. doi:10.1006/exnr.1997.6505
- Brown, K., & Mastrianni, J. A. (2010). The prion diseases. *J Geriatr Psychiatry Neurol*, 23(4), 277-298. doi:10.1177/0891988710383576
- Bruce, M., Chree, A., McConnell, I., Foster, J., Pearson, G., & Fraser, H. (1994). Transmission of bovine spongiform encephalopathy and scrapie to mice: strain variation and the species barrier. *Philos Trans R Soc Lond B Biol Sci*, 343(1306), 405-411. doi:10.1098/rstb.1994.0036
- Bruce, M. E., & Fraser, H. (1991). Scrapie strain variation and its implications. *Curr Top Microbiol Immunol*, 172, 125-138. doi:10.1007/978-3-642-76540-7_8
- Bruce, M. E., Will, R. G., Ironside, J. W., McConnell, I., Drummond, D., Suttie, A., . . . Bostock, C. J. (1997). Transmissions to mice indicate that 'new variant' CJD is caused by the BSE agent. *Nature*, 389(6650), 498-501. doi:10.1038/39057
- Brummelkamp, T. R., Bernards, R., & Agami, R. (2002). A system for stable expression of short interfering RNAs in mammalian cells. *Science*, 296(5567), 550-553. doi:10.1126/science.1068999
- Bryne, J. C., Valen, E., Tang, M. H., Marstrand, T., Winther, O., da Piedade, I., . . . Sandelin, A. (2008). JASPAR, the open access database of transcription factor-binding profiles: new content and tools in the 2008 update. *Nucleic Acids Res*, 36(Database issue), D102-106. doi:10.1093/nar/gkm955

- Budka, H. (2003). Neuropathology of prion diseases. *Br Med Bull*, *66*, 121-130. doi:10.1093/bmb/66.1.121
- Budka, H., Aguzzi, A., Brown, P., Brucher, J. M., Bugiani, O., Gullotta, F., . . . et al. (1995). Neuropathological diagnostic criteria for Creutzfeldt-Jakob disease (CJD) and other human spongiform encephalopathies (prion diseases). *Brain Pathol*, *5*(4), 459-466. doi:10.1111/j.1750-3639.1995.tb00625.x
- Bueler, H., Aguzzi, A., Sailer, A., Greiner, R. A., Autenried, P., Aguet, M., & Weissmann, C. (1993). Mice devoid of PrP are resistant to scrapie. *Cell*, *73*(7), 1339-1347. doi:10.1016/0092-8674(93)90360-3
- Bueler, H., Fischer, M., Lang, Y., Bluethmann, H., Lipp, H. P., DeArmond, S. J., . . . Weissmann, C. (1992). Normal development and behaviour of mice lacking the neuronal cell-surface PrP protein. *Nature*, *356*(6370), 577-582. doi:10.1038/356577a0
- Burda, J. E., & Sofroniew, M. V. (2014). Reactive gliosis and the multicellular response to CNS damage and disease. *Neuron*, *81*(2), 229-248. doi:10.1016/j.neuron.2013.12.034
- Campbell, I. L. (1998). Structural and functional impact of the transgenic expression of cytokines in the CNS. *Ann N Y Acad Sci*, *840*, 83-96. doi:10.1111/j.1749-6632.1998.tb09552.x
- Campbell, I. L., Abraham, C. R., Masliah, E., Kemper, P., Inglis, J. D., Oldstone, M. B., & Mucke, L. (1993). Neurologic disease induced in transgenic mice by cerebral overexpression of interleukin 6. *Proc Natl Acad Sci U S A*, *90*(21), 10061-10065. doi:10.1073/pnas.90.21.10061
- Campbell, I. L., Eddleston, M., Kemper, P., Oldstone, M. B., & Hobbs, M. V. (1994). Activation of cerebral cytokine gene expression and its correlation with onset of reactive astrocyte and acute-phase response gene expression in scrapie. *J Virol*, *68*(4), 2383-2387. doi:10.1128/JVI.68.4.2383-2387.1994
- Campbell, I. L., Erta, M., Lim, S. L., Frausto, R., May, U., Rose-John, S., . . . Hidalgo, J. (2014). Trans-signaling is a dominant mechanism for the pathogenic actions of interleukin-6 in the brain. *J Neurosci*, *34*(7), 2503-2513. doi:10.1523/JNEUROSCI.2830-13.2014
- Campbell, I. L., Hofer, M. J., & Pagenstecher, A. (2010). Transgenic models for cytokine-induced neurological disease. *Biochim Biophys Acta*, *1802*(10), 903-917. doi:10.1016/j.bbadis.2009.10.004
- Cao, L. L., Pei, X. F., Qiao, X., Yu, J., Ye, H., Xi, C. L., . . . Gong, Z. L. (2018). SERPINA3 Silencing Inhibits the Migration, Invasion, and Liver Metastasis of Colon Cancer Cells. *Dig Dis Sci*, *63*(9), 2309-2319. doi:10.1007/s10620-018-5137-x
- Carroll, J. A., Groveman, B. R., Williams, K., Moore, R., Race, B., & Haigh, C. L. (2020). Prion protein N1 cleavage peptides stimulate microglial interaction with surrounding cells. *Sci Rep*, *10*(1), 6654. doi:10.1038/s41598-020-63472-z
- Carroll, J. A., Striebel, J. F., Race, B., Phillips, K., & Chesebro, B. (2015). Prion infection of mouse brain reveals multiple new upregulated genes involved in neuroinflammation or signal transduction. *J Virol*, *89*(4), 2388-2404. doi:10.1128/JVI.02952-14
- Castle, A. R., & Gill, A. C. (2017). Physiological Functions of the Cellular Prion Protein. *Front Mol Biosci*, *4*, 19. doi:10.3389/fmolb.2017.00019
- Caughey, B., Orru, C. D., Groveman, B. R., Hughson, A. G., Manca, M., Raymond, L. D., . . . Kraus, A. (2017). Amplified Detection of Prions and Other Amyloids by RT-QuIC in Diagnostics and the Evaluation of Therapeutics and Disinfectants. *Prog Mol Biol Transl Sci*, *150*, 375-388. doi:10.1016/bs.pmbts.2017.06.003
- Cavaliere, P., Torrent, J., Prigent, S., Granata, V., Pauwels, K., Pastore, A., . . . Zagari, A. (2013). Binding of methylene blue to a surface cleft inhibits the oligomerization and fibrillization of prion protein. *Biochim Biophys Acta*, *1832*(1), 20-28. doi:10.1016/j.bbadis.2012.09.005
- Ceyzeriat, K., Abjean, L., Carrillo-de Sauvage, M. A., Ben Haim, L., & Escartin, C. (2016). The complex STATes of astrocyte reactivity: How are they controlled by the JAK-STAT3 pathway? *Neuroscience*, *330*, 205-218. doi:10.1016/j.neuroscience.2016.05.043

- Chandler, R. L. (1961). Encephalopathy in mice produced by inoculation with scrapie brain material. *Lancet*, *1*(7191), 1378-1379. doi:10.1016/s0140-6736(61)92008-6
- Chen, C., Xu, X. F., Zhang, R. Q., Ma, Y., Lv, Y., Li, J. L., . . . Dong, X. P. (2017). Remarkable increases of alpha1-antichymotrypsin in brain tissues of rodents during prion infection. *Prion*, *11*(5), 338-351. doi:10.1080/19336896.2017.1349590
- Chesebro, B., Race, B., Meade-White, K., Lacasse, R., Race, R., Klingeborn, M., . . . Jeffrey, M. (2010). Fatal transmissible amyloid encephalopathy: a new type of prion disease associated with lack of prion protein membrane anchoring. *PLoS Pathog*, *6*(3), e1000800. doi:10.1371/journal.ppat.1000800
- Chiang, C. S., Stalder, A., Samimi, A., & Campbell, I. L. (1994). Reactive gliosis as a consequence of interleukin-6 expression in the brain: studies in transgenic mice. *Dev Neurosci*, *16*(3-4), 212-221. doi:10.1159/000112109
- Chiriboga, C. A., Swoboda, K. J., Darras, B. T., Iannaccone, S. T., Montes, J., De Vivo, D. C., . . . Bishop, K. M. (2016). Results from a phase 1 study of nusinersen (ISIS-SMN(Rx)) in children with spinal muscular atrophy. *Neurology*, *86*(10), 890-897. doi:10.1212/WNL.0000000000002445
- Cho, H. J. (1976). Is the scrapie agent a virus? *Nature*, *262*(5567), 411-412. doi:10.1038/262411a0
- Clarke, M. C., & Haig, D. A. (1970). Evidence for the multiplication of scrapie agent in cell culture. *Nature*, *225*(5227), 100-101. doi:10.1038/225100a0
- Coitinho, A. S., Lopes, M. H., Hajj, G. N., Rossato, J. I., Freitas, A. R., Castro, C. C., . . . Martins, V. R. (2007). Short-term memory formation and long-term memory consolidation are enhanced by cellular prion association to stress-inducible protein 1. *Neurobiol Dis*, *26*(1), 282-290. doi:10.1016/j.nbd.2007.01.005
- Colby, D. W., & Prusiner, S. B. (2011). Prions. *Cold Spring Harb Perspect Biol*, *3*(1), a006833. doi:10.1101/cshperspect.a006833
- Colini Baldeschi, A., Vanni, S., Zattoni, M., & Legname, G. (2020). Novel regulators of PrP(C) expression as potential therapeutic targets in prion diseases. *Expert Opin Ther Targets*, *24*(8), 759-776. doi:10.1080/14728222.2020.1782384
- Collinge, J. (2001). Prion diseases of humans and animals: their causes and molecular basis. *Annu Rev Neurosci*, *24*, 519-550. doi:10.1146/annurev.neuro.24.1.519
- Collinge, J., Gorham, M., Hudson, F., Kennedy, A., Keogh, G., Pal, S., . . . Darbyshire, J. (2009). Safety and efficacy of quinacrine in human prion disease (PRION-1 study): a patient-preference trial. *Lancet Neurol*, *8*(4), 334-344. doi:10.1016/S1474-4422(09)70049-3
- Collinge, J., Sidle, K. C., Meads, J., Ironside, J., & Hill, A. F. (1996). Molecular analysis of prion strain variation and the aetiology of 'new variant' CJD. *Nature*, *383*(6602), 685-690. doi:10.1038/383685a0
- Collinge, J., Whitfield, J., McKintosh, E., Beck, J., Mead, S., Thomas, D. J., & Alpers, M. P. (2006). Kuru in the 21st century--an acquired human prion disease with very long incubation periods. *Lancet*, *367*(9528), 2068-2074. doi:10.1016/S0140-6736(06)68930-7
- Collinge, J., Whittington, M. A., Sidle, K. C., Smith, C. J., Palmer, M. S., Clarke, A. R., & Jefferys, J. G. (1994). Prion protein is necessary for normal synaptic function. *Nature*, *370*(6487), 295-297. doi:10.1038/370295a0
- Collins, S., Boyd, A., Fletcher, A., Gonzales, M. F., McLean, C. A., & Masters, C. L. (2000). Recent advances in the pre-mortem diagnosis of Creutzfeldt-Jakob disease. *J Clin Neurosci*, *7*(3), 195-202. doi:10.1054/jocn.1999.0191
- Collins, S., McLean, C. A., & Masters, C. L. (2001). Gerstmann-Straussler-Scheinker syndrome, fatal familial insomnia, and kuru: a review of these less common human transmissible spongiform encephalopathies. *J Clin Neurosci*, *8*(5), 387-397. doi:10.1054/jocn.2001.0919
- Cronier, S., Laude, H., & Peyrin, J. M. (2004). Prions can infect primary cultured neurons and astrocytes and promote neuronal cell death. *Proc Natl Acad Sci U S A*, *101*(33), 12271-12276. doi:10.1073/pnas.0402725101

- Dandoy-Dron, F., Benboudjema, L., Guillo, F., Jaegly, A., Jasmin, C., Dormont, D., . . . Dron, M. (2000). Enhanced levels of scrapie responsive gene mRNA in BSE-infected mouse brain. *Brain Res Mol Brain Res*, *76*(1), 173-179. doi:10.1016/s0169-328x(00)00028-0
- Darnell, J. E., Jr. (1997). STATs and gene regulation. *Science*, *277*(5332), 1630-1635. doi:10.1126/science.277.5332.1630
- Das, S., & Potter, H. (1995). Expression of the Alzheimer amyloid-promoting factor antichymotrypsin is induced in human astrocytes by IL-1. *Neuron*, *14*(2), 447-456. doi:10.1016/0896-6273(95)90300-3
- Dery, M. A., Jodoin, J., Ursini-Siegel, J., Aleynikova, O., Ferrario, C., Hassan, S., . . . LeBlanc, A. C. (2013). Endoplasmic reticulum stress induces PRNP prion protein gene expression in breast cancer. *Breast Cancer Res*, *15*(2), R22. doi:10.1186/bcr3398
- Donofrio, G., Heppner, F. L., Polymenidou, M., Musahl, C., & Aguzzi, A. (2005). Paracrine inhibition of prion propagation by anti-PrP single-chain Fv miniantibodies. *J Virol*, *79*(13), 8330-8338. doi:10.1128/JVI.79.13.8330-8338.2005
- Duan, J., Dixon, S. L., Lowrie, J. F., & Sherman, W. (2010). Analysis and comparison of 2D fingerprints: insights into database screening performance using eight fingerprint methods. *J Mol Graph Model*, *29*(2), 157-170. doi:10.1016/j.jmglm.2010.05.008
- Duffy, P., Wolf, J., Collins, G., DeVoe, A. G., Streeten, B., & Cowen, D. (1974). Letter: Possible person-to-person transmission of Creutzfeldt-Jakob disease. *N Engl J Med*, *290*(12), 692-693.
- Eiden, M., Hoffmann, C., Balkema-Buschmann, A., Muller, M., Baumgartner, K., & Groschup, M. H. (2010). Biochemical and immunohistochemical characterization of feline spongiform encephalopathy in a German captive cheetah. *J Gen Virol*, *91*(Pt 11), 2874-2883. doi:10.1099/vir.0.022103-0
- Falsig, J., Julius, C., Margalith, I., Schwarz, P., Heppner, F. L., & Aguzzi, A. (2008). A versatile prion replication assay in organotypic brain slices. *Nat Neurosci*, *11*(1), 109-117. doi:10.1038/nn2028
- Fassbender, K., Walter, S., Kuhl, S., Landmann, R., Ishii, K., Bertsch, T., . . . Beyreuther, K. (2004). The LPS receptor (CD14) links innate immunity with Alzheimer's disease. *FASEB J*, *18*(1), 203-205. doi:10.1096/fj.03-0364fje
- Fillman, S. G., Sinclair, D., Fung, S. J., Webster, M. J., & Shannon Weickert, C. (2014). Markers of inflammation and stress distinguish subsets of individuals with schizophrenia and bipolar disorder. *Transl Psychiatry*, *4*, e365. doi:10.1038/tp.2014.8
- Fire, A., Xu, S., Montgomery, M. K., Kostas, S. A., Driver, S. E., & Mello, C. C. (1998). Potent and specific genetic interference by double-stranded RNA in *Caenorhabditis elegans*. *Nature*, *391*(6669), 806-811. doi:10.1038/35888
- Forsyth, S., Horvath, A., & Coughlin, P. (2003). A review and comparison of the murine alpha1-antitrypsin and alpha1-antichymotrypsin multigene clusters with the human clade A serpins. *Genomics*, *81*(3), 336-345. doi:10.1016/s0888-7543(02)00041-1
- Fraser, H., & Dickinson, A. G. (1973). Scrapie in mice. Agent-strain differences in the distribution and intensity of grey matter vacuolation. *J Comp Pathol*, *83*(1), 29-40. doi:10.1016/0021-9975(73)90024-8
- Fraser, P. E., Nguyen, J. T., McLachlan, D. R., Abraham, C. R., & Kirschner, D. A. (1993). Alpha 1-antichymotrypsin binding to Alzheimer A beta peptides is sequence specific and induces fibril disaggregation in vitro. *J Neurochem*, *61*(1), 298-305. doi:10.1111/j.1471-4159.1993.tb03568.x
- Friesner, R. A., Banks, J. L., Murphy, R. B., Halgren, T. A., Klicic, J. J., Mainz, D. T., . . . Shenkin, P. S. (2004). Glide: a new approach for rapid, accurate docking and scoring. 1. Method and assessment of docking accuracy. *J Med Chem*, *47*(7), 1739-1749. doi:10.1021/jm0306430
- Gajdusek, D. C., Gibbs, C. J., & Alpers, M. (1966). Experimental transmission of a Kuru-like syndrome to chimpanzees. *Nature*, *209*(5025), 794-796. doi:10.1038/209794a0

- Gajdusek, D. C., & Zigas, V. (1957). Degenerative disease of the central nervous system in New Guinea; the endemic occurrence of kuru in the native population. *N Engl J Med*, *257*(20), 974-978. doi:10.1056/NEJM195711142572005
- Gasperini, L., Meneghetti, E., Pastore, B., Benetti, F., & Legname, G. (2015). Prion protein and copper cooperatively protect neurons by modulating NMDA receptor through S-nitrosylation. *Antioxid Redox Signal*, *22*(9), 772-784. doi:10.1089/ars.2014.6032
- Gauczynski, S., Peyrin, J. M., Haik, S., Leucht, C., Hundt, C., Rieger, R., . . . Weiss, S. (2001). The 37-kDa/67-kDa laminin receptor acts as the cell-surface receptor for the cellular prion protein. *EMBO J*, *20*(21), 5863-5875. doi:10.1093/emboj/20.21.5863
- Geschwind, M. D. (2015). Prion Diseases. *Continuum (Minneapolis, Minn)*, *21*(6 Neuroinfectious Disease), 1612-1638. doi:10.1212/CON.0000000000000251
- Gettins, P. G., & Olson, S. T. (2016). Inhibitory serpins. New insights into their folding, polymerization, regulation and clearance. *Biochem J*, *473*(15), 2273-2293. doi:10.1042/BCJ20160014
- Gibbs, C. J., Jr., Gajdusek, D. C., Asher, D. M., Alpers, M. P., Beck, E., Daniel, P. M., & Matthews, W. B. (1968). Creutzfeldt-Jakob disease (spongiform encephalopathy): transmission to the chimpanzee. *Science*, *161*(3839), 388-389. doi:10.1126/science.161.3839.388
- Giri, R. K., Young, R., Pitstick, R., DeArmond, S. J., Prusiner, S. B., & Carlson, G. A. (2006). Prion infection of mouse neurospheres. *Proc Natl Acad Sci U S A*, *103*(10), 3875-3880. doi:10.1073/pnas.0510902103
- Glatzel, M., Abela, E., Maissen, M., & Aguzzi, A. (2003). Extraneural pathologic prion protein in sporadic Creutzfeldt-Jakob disease. *N Engl J Med*, *349*(19), 1812-1820. doi:10.1056/NEJMoa030351
- Glynn, C., Sawaya, M. R., Ge, P., Gallagher-Jones, M., Short, C. W., Bowman, R., . . . Rodriguez, J. A. (2020). Cryo-EM structure of a human prion fibril with a hydrophobic, protease-resistant core. *Nat Struct Mol Biol*, *27*(5), 417-423. doi:10.1038/s41594-020-0403-y
- Goedert, M., Spillantini, M. G., & Crowther, R. A. (1991). Tau proteins and neurofibrillary degeneration. *Brain Pathol*, *1*(4), 279-286. doi:10.1111/j.1750-3639.1991.tb00671.x
- Goel, S., Desai, K., Macapinlac, M., Wadler, S., Goldberg, G., Fields, A., . . . Mani, S. (2006). A phase I safety and dose escalation trial of docetaxel combined with GEM231, a second generation antisense oligonucleotide targeting protein kinase A R1alpha in patients with advanced solid cancers. *Invest New Drugs*, *24*(2), 125-134. doi:10.1007/s10637-006-2378-x
- Goold, R., Rabbanian, S., Sutton, L., Andre, R., Arora, P., Moonga, J., . . . Tabrizi, S. J. (2011). Rapid cell-surface prion protein conversion revealed using a novel cell system. *Nat Commun*, *2*, 281. doi:10.1038/ncomms1282
- Gopalan, S. M., Wilczynska, K. M., Konik, B. S., Bryan, L., & Kordula, T. (2006). Astrocyte-specific expression of the alpha1-antichymotrypsin and glial fibrillary acidic protein genes requires activator protein-1. *J Biol Chem*, *281*(4), 1956-1963. doi:10.1074/jbc.M510935200
- Graner, E., Mercadante, A. F., Zanata, S. M., Forlenza, O. V., Cabral, A. L., Veiga, S. S., . . . Brentani, R. R. (2000). Cellular prion protein binds laminin and mediates neurite outgrowth. *Brain Res Mol Brain Res*, *76*(1), 85-92. doi:10.1016/s0169-328x(99)00334-4
- Greenhill, C. J., Rose-John, S., Lissilaa, R., Ferlin, W., Ernst, M., Hertzog, P. J., . . . Jenkins, B. J. (2011). IL-6 trans-signaling modulates TLR4-dependent inflammatory responses via STAT3. *J Immunol*, *186*(2), 1199-1208. doi:10.4049/jimmunol.1002971
- Gueugneau, M., d'Hose, D., Barbe, C., de Barys, M., Lause, P., Maiter, D., . . . Thissen, J. P. (2018). Increased Serpina3n release into circulation during glucocorticoid-mediated muscle atrophy. *J Cachexia Sarcopenia Muscle*, *9*(5), 929-946. doi:10.1002/jcsm.12315
- Guillot-Sestier, M. V., Sunyach, C., Druon, C., Scarzello, S., & Checler, F. (2009). The alpha-secretase-derived N-terminal product of cellular prion, N1, displays neuroprotective function in vitro and in vivo. *J Biol Chem*, *284*(51), 35973-35986. doi:10.1074/jbc.M109.051086

- Guillot-Sestier, M. V., Sunyach, C., Ferreira, S. T., Marzolo, M. P., Bauer, C., Thevenet, A., & Checler, F. (2012). alpha-Secretase-derived fragment of cellular prion, N1, protects against monomeric and oligomeric amyloid beta (Abeta)-associated cell death. *J Biol Chem*, *287*(7), 5021-5032. doi:10.1074/jbc.M111.323626
- Haddon, D. J., Hughes, M. R., Antignano, F., Westaway, D., Cashman, N. R., & McNagny, K. M. (2009). Prion protein expression and release by mast cells after activation. *J Infect Dis*, *200*(5), 827-831. doi:10.1086/605022
- Haik, S., Marcon, G., Mallet, A., Tettamanti, M., Welaratne, A., Giaccone, G., . . . Tagliavini, F. (2014). Doxycycline in Creutzfeldt-Jakob disease: a phase 2, randomised, double-blind, placebo-controlled trial. *Lancet Neurol*, *13*(2), 150-158. doi:10.1016/S1474-4422(13)70307-7
- Haile, Y., Carmine-Simmen, K., Olechowski, C., Kerr, B., Bleackley, R. C., & Giuliani, F. (2015). Granzyme B-inhibitor serpin3n induces neuroprotection in vitro and in vivo. *J Neuroinflammation*, *12*, 157. doi:10.1186/s12974-015-0376-7
- Haile, Y., Simmen, K. C., Pasichnyk, D., Touret, N., Simmen, T., Lu, J. Q., . . . Giuliani, F. (2011). Granule-derived granzyme B mediates the vulnerability of human neurons to T cell-induced neurotoxicity. *J Immunol*, *187*(9), 4861-4872. doi:10.4049/jimmunol.1100943
- Hansen, H. C., Zschocke, S., Sturenburg, H. J., & Kunze, K. (1998). Clinical changes and EEG patterns preceding the onset of periodic sharp wave complexes in Creutzfeldt-Jakob disease. *Acta Neurol Scand*, *97*(2), 99-106. doi:10.1111/j.1600-0404.1998.tb00617.x
- Hardy, J. A., & Higgins, G. A. (1992). Alzheimer's disease: the amyloid cascade hypothesis. *Science*, *256*(5054), 184-185. doi:10.1126/science.1566067
- Head, M. W., Yull, H. M., Toro, K., Keller, E., Rozsa, C., Ironside, J. W., & Kovacs, G. G. (2015). Pathological and biochemical investigation of a woman diagnosed with genetic Creutzfeldt-Jakob disease shortly after parturition. *Neuropathol Appl Neurobiol*, *41*(5), 676-680. doi:10.1111/nan.12204
- Heinrich, P. C., Behrmann, I., Haan, S., Hermanns, H. M., Muller-Newen, G., & Schaper, F. (2003). Principles of interleukin (IL)-6-type cytokine signalling and its regulation. *Biochem J*, *374*(Pt 1), 1-20. doi:10.1042/BJ20030407
- Heit, C., Jackson, B. C., McAndrews, M., Wright, M. W., Thompson, D. C., Silverman, G. A., . . . Vasiliou, V. (2013). Update of the human and mouse SERPIN gene superfamily. *Hum Genomics*, *7*, 22. doi:10.1186/1479-7364-7-22
- Hill, A. F., Desbruslais, M., Joiner, S., Sidle, K. C., Gowland, I., Collinge, J., . . . Lantos, P. (1997). The same prion strain causes vCJD and BSE. *Nature*, *389*(6650), 448-450, 526. doi:10.1038/38925
- Horvath, A. J., Forsyth, S. L., & Coughlin, P. B. (2004). Expression patterns of murine antichymotrypsin-like genes reflect evolutionary divergence at the Serpina3 locus. *J Mol Evol*, *59*(4), 488-497. doi:10.1007/s00239-004-2640-9
- Horvath, A. J., Irving, J. A., Rossjohn, J., Law, R. H., Bottomley, S. P., Quinsey, N. S., . . . Whisstock, J. C. (2005). The murine orthologue of human antichymotrypsin: a structural paradigm for clade A3 serpins. *J Biol Chem*, *280*(52), 43168-43178. doi:10.1074/jbc.M505598200
- Houston, F., & Andreoletti, O. (2018). The zoonotic potential of animal prion diseases. *Handb Clin Neurol*, *153*, 447-462. doi:10.1016/B978-0-444-63945-5.00025-8
- Hu, W., Nessler, S., Hemmer, B., Eagar, T. N., Kane, L. P., Leliveld, S. R., . . . Stuve, O. (2010). Pharmacological prion protein silencing accelerates central nervous system autoimmune disease via T cell receptor signalling. *Brain*, *133*(Pt 2), 375-388. doi:10.1093/brain/awp298
- Hunt, L. T., & Dayhoff, M. O. (1980). A surprising new protein superfamily containing ovalbumin, antithrombin-III, and alpha 1-proteinase inhibitor. *Biochem Biophys Res Commun*, *95*(2), 864-871. doi:10.1016/0006-291x(80)90867-0
- Ianni, M., Manerba, M., Di Stefano, G., Porcellini, E., Chiappelli, M., Carbone, I., & Licastro, F. (2010). Altered glycosylation profile of purified plasma Aβ from Alzheimer's disease. *Immun Ageing*, *7 Suppl 1*, S6. doi:10.1186/1742-4933-7-S1-S6

- Igel-Egalon, A., Beringue, V., Rezaei, H., & Sibille, P. (2018). Prion Strains and Transmission Barrier Phenomena. *Pathogens*, 7(1). doi:10.3390/pathogens7010005
- Imran, M., & Mahmood, S. (2011). An overview of animal prion diseases. *Virology*, 8, 493. doi:10.1186/1743-422X-8-493
- Ironside, J. W., Sutherland, K., Bell, J. E., McCardle, L., Barrie, C., Estebeiro, K., . . . Will, R. G. (1996). A new variant of Creutzfeldt-Jakob disease: neuropathological and clinical features. *Cold Spring Harb Symp Quant Biol*, 61, 523-530.
- Irving, J. A., Pike, R. N., Lesk, A. M., & Whisstock, J. C. (2000). Phylogeny of the serpin superfamily: implications of patterns of amino acid conservation for structure and function. *Genome Res*, 10(12), 1845-1864. doi:10.1101/gr.gr-1478r
- Jacobsen, J. S., Comery, T. A., Martone, R. L., Elokdah, H., Crandall, D. L., Oganessian, A., . . . Pangalos, M. N. (2008). Enhanced clearance of Abeta in brain by sustaining the plasmin proteolysis cascade. *Proc Natl Acad Sci U S A*, 105(25), 8754-8759. doi:10.1073/pnas.0710823105
- Janciauskiene, S., Rubin, H., Lukacs, C. M., & Wright, H. T. (1998). Alzheimer's peptide Abeta1-42 binds to two beta-sheets of alpha1-antichymotrypsin and transforms it from inhibitor to substrate. *J Biol Chem*, 273(43), 28360-28364. doi:10.1074/jbc.273.43.28360
- Jung, I. H., Choi, J. H., Chung, Y. Y., Lim, G. L., Park, Y. N., & Park, S. W. (2015). Predominant Activation of JAK/STAT3 Pathway by Interleukin-6 Is Implicated in Hepatocarcinogenesis. *Neoplasia*, 17(7), 586-597. doi:10.1016/j.neo.2015.07.005
- Kalsheker, N. A. (1996). Alpha 1-antichymotrypsin. *Int J Biochem Cell Biol*, 28(9), 961-964. doi:10.1016/1357-2725(96)00032-5
- Khan, Z., & Bollu, P. C. (2020). Fatal Familial Insomnia. In *StatPearls*. Treasure Island (FL).
- Khosravani, H., Zhang, Y., Tsutsui, S., Hameed, S., Altier, C., Hamid, J., . . . Zamponi, G. W. (2008). Prion protein attenuates excitotoxicity by inhibiting NMDA receptors. *J Cell Biol*, 181(3), 551-565. doi:10.1083/jcb.200711002
- Khumalo, T., Reusch, U., Knackmuss, S., Little, M., Veale, R. B., & Weiss, S. F. (2013). Adhesion and Invasion of Breast and Oesophageal Cancer Cells Are Impeded by Anti-LRP/LR-Specific Antibody IgG1-iS18. *PLoS One*, 8(6), e66297. doi:10.1371/journal.pone.0066297
- Kimberlin, R. H. (1982). Scrapie agent: prions or virinos? *Nature*, 297(5862), 107-108. doi:10.1038/297107a0
- Kirkwood, J. K., Cunningham, A. A., Austin, A. R., Wells, G. A., & Sainsbury, A. W. (1994). Spongiform encephalopathy in a greater kudu (*Tragelaphus strepsiceros*) introduced into an affected group. *Vet Rec*, 134(7), 167-168. doi:10.1136/vr.134.7.167
- Kisseleva, T., Bhattacharya, S., Braunstein, J., & Schindler, C. W. (2002). Signaling through the JAK/STAT pathway, recent advances and future challenges. *Gene*, 285(1-2), 1-24. doi:10.1016/s0378-1119(02)00398-0
- Kocisko, D. A., Caughey, W. S., Race, R. E., Roper, G., Caughey, B., & Morrey, J. D. (2006). A porphyrin increases survival time of mice after intracerebral prion infection. *Antimicrob Agents Chemother*, 50(2), 759-761. doi:10.1128/AAC.50.2.759-761.2006
- Kocisko, D. A., Come, J. H., Priola, S. A., Chesebro, B., Raymond, G. J., Lansbury, P. T., & Caughey, B. (1994). Cell-free formation of protease-resistant prion protein. *Nature*, 370(6489), 471-474. doi:10.1038/370471a0
- Kordasiewicz, H. B., Stanek, L. M., Wancewicz, E. V., Mazur, C., McAlonis, M. M., Pytel, K. A., . . . Cleveland, D. W. (2012). Sustained therapeutic reversal of Huntington's disease by transient repression of huntingtin synthesis. *Neuron*, 74(6), 1031-1044. doi:10.1016/j.neuron.2012.05.009
- Kordula, T., Rydel, R. E., Brigham, E. F., Horn, F., Heinrich, P. C., & Travis, J. (1998). Oncostatin M and the interleukin-6 and soluble interleukin-6 receptor complex regulate alpha1-antichymotrypsin expression in human cortical astrocytes. *J Biol Chem*, 273(7), 4112-4118. doi:10.1074/jbc.273.7.4112

- Kovacs, G. G., Puopolo, M., Ladogana, A., Pocchiari, M., Budka, H., van Duijn, C., . . . Eurocjd. (2005). Genetic prion disease: the EUROCJD experience. *Hum Genet*, *118*(2), 166-174. doi:10.1007/s00439-005-0020-1
- Kovacs, G. G., Trabattoni, G., Hainfellner, J. A., Ironside, J. W., Knight, R. S., & Budka, H. (2002). Mutations of the prion protein gene phenotypic spectrum. *J Neurol*, *249*(11), 1567-1582. doi:10.1007/s00415-002-0896-9
- Krance, S. H., Luke, R., Shenouda, M., Israwi, A. R., Colpitts, S. J., Darwish, L., . . . Watts, J. C. (2020). Cellular models for discovering prion disease therapeutics: Progress and challenges. *J Neurochem*, *153*(2), 150-172. doi:10.1111/jnc.14956
- Kubler, E., Oesch, B., & Raeber, A. J. (2003). Diagnosis of prion diseases. *Br Med Bull*, *66*, 267-279. doi:10.1093/bmb/66.1.267
- Kuffer, A., Lakkaraju, A. K., Mogha, A., Petersen, S. C., Airich, K., Doucerain, C., . . . Aguzzi, A. (2016). The prion protein is an agonistic ligand of the G protein-coupled receptor Adgrg6. *Nature*, *536*(7617), 464-468. doi:10.1038/nature19312
- Kulesza, D. W., Ramji, K., Maleszewska, M., Mieczkowski, J., Dabrowski, M., Chouaib, S., & Kaminska, B. (2019). Search for novel STAT3-dependent genes reveals SERPINA3 as a new STAT3 target that regulates invasion of human melanoma cells. *Lab Invest*, *99*(11), 1607-1621. doi:10.1038/s41374-019-0288-8
- Kumar, P., Wu, H., McBride, J. L., Jung, K. E., Kim, M. H., Davidson, B. L., . . . Manjunath, N. (2007). Transvascular delivery of small interfering RNA to the central nervous system. *Nature*, *448*(7149), 39-43. doi:10.1038/nature05901
- Kuwata, K., Nishida, N., Matsumoto, T., Kamatari, Y. O., Hosokawa-Muto, J., Kodama, K., . . . Katamine, S. (2007). Hot spots in prion protein for pathogenic conversion. *Proc Natl Acad Sci U S A*, *104*(29), 11921-11926. doi:10.1073/pnas.0702671104
- Lasmezas, C. I., Deslys, J. P., Robain, O., Jaegly, A., Beringue, V., Peyrin, J. M., . . . Dormont, D. (1997). Transmission of the BSE agent to mice in the absence of detectable abnormal prion protein. *Science*, *275*(5298), 402-405. doi:10.1126/science.275.5298.402
- Law, R. H., Zhang, Q., McGowan, S., Buckle, A. M., Silverman, G. A., Wong, W., . . . Whisstock, J. C. (2006). An overview of the serpin superfamily. *Genome Biol*, *7*(5), 216. doi:10.1186/gb-2006-7-5-216
- Le, Y., Yazawa, H., Gong, W., Yu, Z., Ferrans, V. J., Murphy, P. M., & Wang, J. M. (2001). The neurotoxic prion peptide fragment PrP(106-126) is a chemotactic agonist for the G protein-coupled receptor formyl peptide receptor-like 1. *J Immunol*, *166*(3), 1448-1451. doi:10.4049/jimmunol.166.3.1448
- Leaman, D. W., Leung, S., Li, X., & Stark, G. R. (1996). Regulation of STAT-dependent pathways by growth factors and cytokines. *FASEB J*, *10*(14), 1578-1588.
- Lee, Y., Lee, S. R., Choi, S. S., Yeo, H. G., Chang, K. T., & Lee, H. J. (2014). Therapeutically targeting neuroinflammation and microglia after acute ischemic stroke. *Biomed Res Int*, *2014*, 297241. doi:10.1155/2014/297241
- Lee, Y. H., Sohn, H. J., Kim, M. J., Kim, H. J., Lee, W. Y., Yun, E. I., . . . Balachandran, A. (2013). Strain characterization of the Korean CWD cases in 2001 and 2004. *J Vet Med Sci*, *75*(1), 95-98. doi:10.1292/jvms.12-0077
- Legname, G. (2017). Elucidating the function of the prion protein. *PLoS Pathog*, *13*(8), e1006458. doi:10.1371/journal.ppat.1006458
- Legname, G., & Moda, F. (2017). The Prion Concept and Synthetic Prions. *Prog Mol Biol Transl Sci*, *150*, 147-156. doi:10.1016/bs.pmbts.2017.06.002
- Lewis, P. A., Properzi, F., Prodromidou, K., Clarke, A. R., Collinge, J., & Jackson, G. S. (2006). Removal of the glycosylphosphatidylinositol anchor from PrP(Sc) by cathepsin D does not reduce prion infectivity. *Biochem J*, *395*(2), 443-448. doi:10.1042/BJ20051677

- Lewis, V., Johanssen, V. A., Crouch, P. J., Klug, G. M., Hooper, N. M., & Collins, S. J. (2016). Prion protein "gamma-cleavage": characterizing a novel endoproteolytic processing event. *Cell Mol Life Sci*, *73*(3), 667-683. doi:10.1007/s00018-015-2022-z
- Li, A., Christensen, H. M., Stewart, L. R., Roth, K. A., Chiesa, R., & Harris, D. A. (2007). Neonatal lethality in transgenic mice expressing prion protein with a deletion of residues 105-125. *EMBO J*, *26*(2), 548-558. doi:10.1038/sj.emboj.7601507
- Li, R., Liu, D., Zanusso, G., Liu, T., Fayen, J. D., Huang, J. H., . . . Sy, M. S. (2001). The expression and potential function of cellular prion protein in human lymphocytes. *Cell Immunol*, *207*(1), 49-58. doi:10.1006/cimm.2000.1751
- Li, S. H., Reinke, A. A., Sanders, K. L., Emal, C. D., Whisstock, J. C., Stuckey, J. A., & Lawrence, D. A. (2013). Mechanistic characterization and crystal structure of a small molecule inactivator bound to plasminogen activator inhibitor-1. *Proc Natl Acad Sci U S A*, *110*(51), E4941-4949. doi:10.1073/pnas.1216499110
- Liang, J., & Kong, Q. (2012). alpha-Cleavage of cellular prion protein. *Prion*, *6*(5), 453-460. doi:10.4161/pri.22511
- Liberski, P. P. (2013). Kuru: a journey back in time from papua new Guinea to the neanderthals' extinction. *Pathogens*, *2*(3), 472-505. doi:10.3390/pathogens2030472
- Linsenmeier, L., Altmeppen, H. C., Wetzel, S., Mohammadi, B., Saftig, P., & Glatzel, M. (2017). Diverse functions of the prion protein - Does proteolytic processing hold the key? *Biochim Biophys Acta Mol Cell Res*, *1864*(11 Pt B), 2128-2137. doi:10.1016/j.bbamcr.2017.06.022
- Linsenmeier, L., Mohammadi, B., Wetzel, S., Puig, B., Jackson, W. S., Hartmann, A., . . . Altmeppen, H. C. (2018). Structural and mechanistic aspects influencing the ADAM10-mediated shedding of the prion protein. *Mol Neurodegener*, *13*(1), 18. doi:10.1186/s13024-018-0248-6
- Lipinski, C. A. (2004). Lead- and drug-like compounds: the rule-of-five revolution. *Drug Discov Today Technol*, *1*(4), 337-341. doi:10.1016/j.ddtec.2004.11.007
- Livak, K. J., & Schmittgen, T. D. (2001). Analysis of relative gene expression data using real-time quantitative PCR and the 2(-Delta Delta C(T)) Method. *Methods*, *25*(4), 402-408. doi:10.1006/meth.2001.1262
- Lloyd, S. E., Mead, S., & Collinge, J. (2013). Genetics of prion diseases. *Curr Opin Genet Dev*, *23*(3), 345-351. doi:10.1016/j.gde.2013.02.012
- Lopes, M. H., Hajj, G. N., Muras, A. G., Mancini, G. L., Castro, R. M., Ribeiro, K. C., . . . Martins, V. R. (2005). Interaction of cellular prion and stress-inducible protein 1 promotes neuritogenesis and neuroprotection by distinct signaling pathways. *J Neurosci*, *25*(49), 11330-11339. doi:10.1523/JNEUROSCI.2313-05.2005
- Lugaresi, E., Medori, R., Montagna, P., Baruzzi, A., Cortelli, P., Lugaresi, A., . . . Gambetti, P. (1986). Fatal familial insomnia and dysautonomia with selective degeneration of thalamic nuclei. *N Engl J Med*, *315*(16), 997-1003. doi:10.1056/NEJM198610163151605
- Lukacs, C. M., Rubin, H., & Christianson, D. W. (1998). Engineering an anion-binding cavity in antichymotrypsin modulates the "spring-loaded" serpin-protease interaction. *Biochemistry*, *37*(10), 3297-3304. doi:10.1021/bi972359e
- Luo, D., Chen, W., Tian, Y., Li, J., Xu, X., Chen, C., & Li, F. (2017). Serpin peptidase inhibitor, clade A member 3 (SERPINA3), is overexpressed in glioma and associated with poor prognosis in glioma patients. *Onco Targets Ther*, *10*, 2173-2181. doi:10.2147/OTT.S133022
- Magalhaes, A. C., Silva, J. A., Lee, K. S., Martins, V. R., Prado, V. F., Ferguson, S. S., . . . Prado, M. A. (2002). Endocytic intermediates involved with the intracellular trafficking of a fluorescent cellular prion protein. *J Biol Chem*, *277*(36), 33311-33318. doi:10.1074/jbc.M203661200
- Maheshwari, A., Fischer, M., Gambetti, P., Parker, A., Ram, A., Soto, C., . . . Hussein, H. M. (2015). Recent US Case of Variant Creutzfeldt-Jakob Disease-Global Implications. *Emerg Infect Dis*, *21*(5), 750-759. doi:10.3201/eid2105.142017

- Mallucci, G., Dickinson, A., Linehan, J., Klohn, P. C., Brandner, S., & Collinge, J. (2003). Depleting neuronal PrP in prion infection prevents disease and reverses spongiosis. *Science*, *302*(5646), 871-874. doi:10.1126/science.1090187
- Mallucci, G. R., Ratte, S., Asante, E. A., Linehan, J., Gowland, I., Jefferys, J. G., & Collinge, J. (2002). Post-natal knockout of prion protein alters hippocampal CA1 properties, but does not result in neurodegeneration. *EMBO J*, *21*(3), 202-210. doi:10.1093/emboj/21.3.202
- Mammana, A., Baiardi, S., Rossi, M., Franceschini, A., Donadio, V., Capellari, S., . . . Parchi, P. (2020). Detection of prions in skin punch biopsies of Creutzfeldt-Jakob disease patients. *Ann Clin Transl Neurol*, *7*(4), 559-564. doi:10.1002/acn3.51000
- Marijanovic, Z., Caputo, A., Campana, V., & Zurzolo, C. (2009). Identification of an intracellular site of prion conversion. *PLoS Pathog*, *5*(5), e1000426. doi:10.1371/journal.ppat.1000426
- Mattei, V., Garofalo, T., Misasi, R., Circella, A., Manganelli, V., Lucania, G., . . . Sorice, M. (2004). Prion protein is a component of the multimolecular signaling complex involved in T cell activation. *FEBS Lett*, *560*(1-3), 14-18. doi:10.1016/S0014-5793(04)00029-8
- McNally, K. L., Ward, A. E., & Priola, S. A. (2009). Cells expressing anchorless prion protein are resistant to scrapie infection. *J Virol*, *83*(9), 4469-4475. doi:10.1128/JVI.02412-08
- Medori, R., Tritschler, H. J., LeBlanc, A., Villare, F., Manetto, V., Chen, H. Y., . . . et al. (1992). Fatal familial insomnia, a prion disease with a mutation at codon 178 of the prion protein gene. *N Engl J Med*, *326*(7), 444-449. doi:10.1056/NEJM199202133260704
- Meyer, R. K., McKinley, M. P., Bowman, K. A., Braunfeld, M. B., Barry, R. A., & Prusiner, S. B. (1986). Separation and properties of cellular and scrapie prion proteins. *Proc Natl Acad Sci U S A*, *83*(8), 2310-2314. doi:10.1073/pnas.83.8.2310
- Miele, G., Seeger, H., Marino, D., Eberhard, R., Heikenwalder, M., Stoeck, K., . . . Aguzzi, A. (2008). Urinary alpha1-antichymotrypsin: a biomarker of prion infection. *PLoS One*, *3*(12), e3870. doi:10.1371/journal.pone.0003870
- Mills, J. D., Ward, M., Kim, W. S., Halliday, G. M., & Janitz, M. (2016). Strand-specific RNA-sequencing analysis of multiple system atrophy brain transcriptome. *Neuroscience*, *322*, 234-250. doi:10.1016/j.neuroscience.2016.02.042
- Mironov, A., Jr., Latawiec, D., Wille, H., Bouzamondo-Bernstein, E., Legname, G., Williamson, R. A., . . . Peters, P. J. (2003). Cytosolic prion protein in neurons. *J Neurosci*, *23*(18), 7183-7193.
- Moda, F. (2017). Protein Misfolding Cyclic Amplification of Infectious Prions. *Prog Mol Biol Transl Sci*, *150*, 361-374. doi:10.1016/bs.pmbts.2017.06.016
- Moda, F., Bolognesi, M. L., & Legname, G. (2019). Novel screening approaches for human prion diseases drug discovery. *Expert Opin Drug Discov*, *14*(10), 983-993. doi:10.1080/17460441.2019.1637851
- Moda, F., Le, T. N., Aulic, S., Bistaffa, E., Campagnani, I., Virgilio, T., . . . Legname, G. (2015). Synthetic prions with novel strain-specified properties. *PLoS Pathog*, *11*(12), e1005354. doi:10.1371/journal.ppat.1005354
- Moda, F., Vimercati, C., Campagnani, I., Ruggerone, M., Giaccone, G., Morbin, M., . . . Tagliavini, F. (2012). Brain delivery of AAV9 expressing an anti-PrP monovalent antibody delays prion disease in mice. *Prion*, *6*(4), 383-390. doi:10.4161/pri.20197
- Morales, R., Abid, K., & Soto, C. (2007). The prion strain phenomenon: molecular basis and unprecedented features. *Biochim Biophys Acta*, *1772*(6), 681-691. doi:10.1016/j.bbadis.2006.12.006
- Mouillet-Richard, S., Ermonval, M., Chebassier, C., Laplanche, J. L., Lehmann, S., Launay, J. M., & Kellermann, O. (2000). Signal transduction through prion protein. *Science*, *289*(5486), 1925-1928. doi:10.1126/science.289.5486.1925
- Na, Y. J., Jin, J. K., Kim, J. I., Choi, E. K., Carp, R. I., & Kim, Y. S. (2007). JAK-STAT signaling pathway mediates astrogliosis in brains of scrapie-infected mice. *J Neurochem*, *103*(2), 637-649. doi:10.1111/j.1471-4159.2007.04769.x

- Nabavi, S. M., Ahmed, T., Nawaz, M., Devi, K. P., Balan, D. J., Pittala, V., . . . Shirooie, S. (2019). Targeting STATs in neuroinflammation: The road less traveled! *Pharmacol Res*, *141*, 73-84. doi:10.1016/j.phrs.2018.12.004
- Nagata, K. (1996). Hsp47: a collagen-specific molecular chaperone. *Trends Biochem Sci*, *21*(1), 22-26. doi:10.1016/0968-0004(96)80881-4
- Neumann, M., Sampathu, D. M., Kwong, L. K., Truax, A. C., Micsenyi, M. C., Chou, T. T., . . . Lee, V. M. (2006). Ubiquitinated TDP-43 in frontotemporal lobar degeneration and amyotrophic lateral sclerosis. *Science*, *314*(5796), 130-133. doi:10.1126/science.1134108
- Nicolas, C. S., Amici, M., Bortolotto, Z. A., Doherty, A., Csaba, Z., Fafouri, A., . . . Peineau, S. (2013). The role of JAK-STAT signaling within the CNS. *JAKSTAT*, *2*(1), e22925. doi:10.4161/jkst.22925
- Nieznanski, K., Choi, J. K., Chen, S., Surewicz, K., & Surewicz, W. K. (2012). Soluble prion protein inhibits amyloid-beta (A β) fibrillization and toxicity. *J Biol Chem*, *287*(40), 33104-33108. doi:10.1074/jbc.C112.400614
- Nilsson, L. N., Arendash, G. W., Leighty, R. E., Costa, D. A., Low, M. A., Garcia, M. F., . . . Potter, H. (2004). Cognitive impairment in PDAPP mice depends on ApoE and ACT-catalyzed amyloid formation. *Neurobiol Aging*, *25*(9), 1153-1167. doi:10.1016/j.neurobiolaging.2003.12.011
- Nilsson, L. N., Bales, K. R., DiCarlo, G., Gordon, M. N., Morgan, D., Paul, S. M., & Potter, H. (2001). Alpha-1-antichymotrypsin promotes beta-sheet amyloid plaque deposition in a transgenic mouse model of Alzheimer's disease. *J Neurosci*, *21*(5), 1444-1451.
- O'Callaghan, J. P., Kelly, K. A., VanGilder, R. L., Sofroniew, M. V., & Miller, D. B. (2014). Early activation of STAT3 regulates reactive astrogliosis induced by diverse forms of neurotoxicity. *PLoS One*, *9*(7), e102003. doi:10.1371/journal.pone.0102003
- Palmer, M. S., Dryden, A. J., Hughes, J. T., & Collinge, J. (1991). Homozygous prion protein genotype predisposes to sporadic Creutzfeldt-Jakob disease. *Nature*, *352*(6333), 340-342. doi:10.1038/352340a0
- Parchi, P., Castellani, R., Capellari, S., Ghetti, B., Young, K., Chen, S. G., . . . Gambetti, P. (1996). Molecular basis of phenotypic variability in sporadic Creutzfeldt-Jakob disease. *Ann Neurol*, *39*(6), 767-778. doi:10.1002/ana.410390613
- Pasternack, J. M., Abraham, C. R., Van Dyke, B. J., Potter, H., & Younkin, S. G. (1989). Astrocytes in Alzheimer's disease gray matter express alpha 1-antichymotrypsin mRNA. *Am J Pathol*, *135*(5), 827-834.
- Paterson, A. W., Curtis, J. C., & Macleod, N. K. (2008). Complex I specific increase in superoxide formation and respiration rate by PrP-null mouse brain mitochondria. *J Neurochem*, *105*(1), 177-191. doi:10.1111/j.1471-4159.2007.05123.x
- Pattison, I. H., & Millson, G. C. (1961). Scrapie produced experimentally in goats with special reference to the clinical syndrome. *J Comp Pathol*, *71*, 101-109. doi:10.1016/s0368-1742(61)80013-1
- Pemberton, P. A., Stein, P. E., Pepys, M. B., Potter, J. M., & Carrell, R. W. (1988). Hormone binding globulins undergo serpin conformational change in inflammation. *Nature*, *336*(6196), 257-258. doi:10.1038/336257a0
- Polymenidou, M., Heppner, F. L., Pelliccioli, E. C., Urich, E., Miele, G., Braun, N., . . . Aguzzi, A. (2004). Humoral immune response to native eukaryotic prion protein correlates with anti-prion protection. *Proc Natl Acad Sci U S A*, *101* Suppl 2, 14670-14676. doi:10.1073/pnas.0404772101
- Porro, C., Cianciulli, A., Trotta, T., Lofrumento, D. D., & Panaro, M. A. (2019). Curcumin Regulates Anti-Inflammatory Responses by JAK/STAT/SOCS Signaling Pathway in BV-2 Microglial Cells. *Biology (Basel)*, *8*(3). doi:10.3390/biology8030051
- Prusiner, S. B. (1982). Novel proteinaceous infectious particles cause scrapie. *Science*, *216*(4542), 136-144. doi:10.1126/science.6801762

- Prusiner, S. B. (1991). Molecular biology of prion diseases. *Science*, 252(5012), 1515-1522. doi:10.1126/science.1675487
- Prusiner, S. B., Groth, D., Serban, A., Koehler, R., Foster, D., Torchia, M., . . . DeArmond, S. J. (1993). Ablation of the prion protein (PrP) gene in mice prevents scrapie and facilitates production of anti-PrP antibodies. *Proc Natl Acad Sci U S A*, 90(22), 10608-10612. doi:10.1073/pnas.90.22.10608
- Prusiner, S. B., Scott, M. R., DeArmond, S. J., & Cohen, F. E. (1998). Prion protein biology. *Cell*, 93(3), 337-348. doi:10.1016/s0092-8674(00)81163-0
- Pulford, B., Reim, N., Bell, A., Veatch, J., Forster, G., Bender, H., . . . Zabel, M. D. (2010). Liposome-siRNA-peptide complexes cross the blood-brain barrier and significantly decrease PrP on neuronal cells and PrP in infected cell cultures. *PLoS One*, 5(6), e11085. doi:10.1371/journal.pone.0011085
- Puoti, G., Bizzi, A., Forloni, G., Safar, J. G., Tagliavini, F., & Gambetti, P. (2012). Sporadic human prion diseases: molecular insights and diagnosis. *Lancet Neurol*, 11(7), 618-628. doi:10.1016/S1474-4422(12)70063-7
- Rachidi, W., Vilette, D., Guiraud, P., Arlotto, M., Riondel, J., Laude, H., . . . Favier, A. (2003). Expression of prion protein increases cellular copper binding and antioxidant enzyme activities but not copper delivery. *J Biol Chem*, 278(11), 9064-9072. doi:10.1074/jbc.M211830200
- Raeber, A. J., Race, R. E., Brandner, S., Priola, S. A., Sailer, A., Bessen, R. A., . . . Chesebro, B. (1997). Astrocyte-specific expression of hamster prion protein (PrP) renders PrP knockout mice susceptible to hamster scrapie. *EMBO J*, 16(20), 6057-6065. doi:10.1093/emboj/16.20.6057
- Rajan, P., Symes, A. J., & Fink, J. S. (1996). STAT proteins are activated by ciliary neurotrophic factor in cells of central nervous system origin. *J Neurosci Res*, 43(4), 403-411. doi:10.1002/(SICI)1097-4547(19960215)43:4<403::AID-JNR2>3.0.CO;2-J
- Ransohoff, R. M. (2016). How neuroinflammation contributes to neurodegeneration. *Science*, 353(6301), 777-783. doi:10.1126/science.aag2590
- Rawlings, J. S., Rosler, K. M., & Harrison, D. A. (2004). The JAK/STAT signaling pathway. *J Cell Sci*, 117(Pt 8), 1281-1283. doi:10.1242/jcs.00963
- Raymond, G. J., Zhao, H. T., Race, B., Raymond, L. D., Williams, K., Swayze, E. E., . . . Vallabh, S. M. (2019). Antisense oligonucleotides extend survival of prion-infected mice. *JCI Insight*, 5. doi:10.1172/jci.insight.131175
- Rieger, R., Edenhofer, F., Lasmez, C. I., & Weiss, S. (1997). The human 37-kDa laminin receptor precursor interacts with the prion protein in eukaryotic cells. *Nat Med*, 3(12), 1383-1388. doi:10.1038/nm1297-1383
- Riemer, C., Neidhold, S., Burwinkel, M., Schwarz, A., Schultz, J., Kratzschmar, J., . . . Baier, M. (2004). Gene expression profiling of scrapie-infected brain tissue. *Biochem Biophys Res Commun*, 323(2), 556-564. doi:10.1016/j.bbrc.2004.08.124
- Ritchie, D. L., & Ironside, J. W. (2017). Neuropathology of Human Prion Diseases. *Prog Mol Biol Transl Sci*, 150, 319-339. doi:10.1016/bs.pmbts.2017.06.011
- Rock, R. B., Gekker, G., Hu, S., Sheng, W. S., Cheeran, M., Lokensgard, J. R., & Peterson, P. K. (2004). Role of microglia in central nervous system infections. *Clin Microbiol Rev*, 17(4), 942-964, table of contents. doi:10.1128/CMR.17.4.942-964.2004
- Rose-John, S., Scheller, J., Elson, G., & Jones, S. A. (2006). Interleukin-6 biology is coordinated by membrane-bound and soluble receptors: role in inflammation and cancer. *J Leukoc Biol*, 80(2), 227-236. doi:10.1189/jlb.1105674
- Rosen, D. R. (1993). Mutations in Cu/Zn superoxide dismutase gene are associated with familial amyotrophic lateral sclerosis. *Nature*, 364(6435), 362. doi:10.1038/364362c0
- Saborio, G. P., Permanne, B., & Soto, C. (2001). Sensitive detection of pathological prion protein by cyclic amplification of protein misfolding. *Nature*, 411(6839), 810-813. doi:10.1038/35081095

- Safar, J., Wille, H., Itri, V., Groth, D., Serban, H., Torchia, M., . . . Prusiner, S. B. (1998). Eight prion strains have PrP(Sc) molecules with different conformations. *Nat Med*, *4*(10), 1157-1165. doi:10.1038/2654
- Sandberg, M. K., Al-Doujaily, H., Sigurdson, C. J., Glatzel, M., O'Malley, C., Powell, C., . . . Collinge, J. (2010). Chronic wasting disease prions are not transmissible to transgenic mice overexpressing human prion protein. *J Gen Virol*, *91*(Pt 10), 2651-2657. doi:10.1099/vir.0.024380-0
- Sanfilippo, C., Longo, A., Lazzara, F., Cambria, D., Distefano, G., Palumbo, M., . . . Di Rosa, M. (2017). CHI3L1 and CHI3L2 overexpression in motor cortex and spinal cord of sALS patients. *Mol Cell Neurosci*, *85*, 162-169. doi:10.1016/j.mcn.2017.10.001
- Sanrattana, W., Maas, C., & de Maat, S. (2019). SERPINS-From Trap to Treatment. *Front Med (Lausanne)*, *6*, 25. doi:10.3389/fmed.2019.00025
- Santamaria, M., Pardo-Saganta, A., Alvarez-Asiain, L., Di Scala, M., Qian, C., Prieto, J., & Avila, M. A. (2013). Nuclear alpha1-antichymotrypsin promotes chromatin condensation and inhibits proliferation of human hepatocellular carcinoma cells. *Gastroenterology*, *144*(4), 818-828 e814. doi:10.1053/j.gastro.2012.12.029
- Santuccion, A., Sytnyk, V., Leshchyns'ka, I., & Schachner, M. (2005). Prion protein recruits its neuronal receptor NCAM to lipid rafts to activate p59fyn and to enhance neurite outgrowth. *J Cell Biol*, *169*(2), 341-354. doi:10.1083/jcb.200409127
- Sarnataro, D., Pepe, A., Altamura, G., De Simone, I., Pesapane, A., Nitsch, L., . . . Zurzolo, C. (2016). The 37/67 kDa laminin receptor (LR) inhibitor, NSC47924, affects 37/67 kDa LR cell surface localization and interaction with the cellular prion protein. *Sci Rep*, *6*, 24457. doi:10.1038/srep24457
- Sastry, G. M., Adzhigirey, M., Day, T., Annabhimoju, R., & Sherman, W. (2013). Protein and ligand preparation: parameters, protocols, and influence on virtual screening enrichments. *J Comput Aided Mol Des*, *27*(3), 221-234. doi:10.1007/s10822-013-9644-8
- Savardi, A., Borgogno, M., Narducci, R., La Sala, G., Ortega, J. A., Summa, M., . . . Cancedda, L. (2020). Discovery of a Small Molecule Drug Candidate for Selective NKCC1 Inhibition in Brain Disorders. *Chem*, *6*(8), 2073-2096. doi:10.1016/j.chempr.2020.06.017
- Scheller, J., Chalaris, A., Schmidt-Arras, D., & Rose-John, S. (2011). The pro- and anti-inflammatory properties of the cytokine interleukin-6. *Biochim Biophys Acta*, *1813*(5), 878-888. doi:10.1016/j.bbamcr.2011.01.034
- Schmitt-Ulms, G., Legname, G., Baldwin, M. A., Ball, H. L., Bradon, N., Bosque, P. J., . . . Prusiner, S. B. (2001). Binding of neural cell adhesion molecules (N-CAMs) to the cellular prion protein. *J Mol Biol*, *314*(5), 1209-1225. doi:10.1006/jmbi.2000.5183
- Schoch, G., Seeger, H., Bogousslavsky, J., Tolnay, M., Janzer, R. C., Aguzzi, A., & Glatzel, M. (2006). Analysis of prion strains by PrPSc profiling in sporadic Creutzfeldt-Jakob disease. *PLoS Med*, *3*(2), e14. doi:10.1371/journal.pmed.0030014
- Scott, M., Foster, D., Mirenda, C., Serban, D., Coufal, F., Walchli, M., . . . Prusiner, S. B. (1989). Transgenic mice expressing hamster prion protein produce species-specific scrapie infectivity and amyloid plaques. *Cell*, *59*(5), 847-857. doi:10.1016/0092-8674(89)90608-9
- Sergi, D., Campbell, F. M., Grant, C., Morris, A. C., Bachmair, E. M., Koch, C., . . . Williams, L. M. (2018). SerpinA3N is a novel hypothalamic gene upregulated by a high-fat diet and leptin in mice. *Genes Nutr*, *13*, 28. doi:10.1186/s12263-018-0619-1
- Sigurdson, C. J., Bartz, J. C., & Glatzel, M. (2019). Cellular and Molecular Mechanisms of Prion Disease. *Annu Rev Pathol*, *14*, 497-516. doi:10.1146/annurev-pathmechdis-012418-013109
- Sigurdson, C. J., & Miller, M. W. (2003). Other animal prion diseases. *Br Med Bull*, *66*, 199-212. doi:10.1093/bmb/66.1.199
- Silveira, J. R., Raymond, G. J., Hughson, A. G., Race, R. E., Sim, V. L., Hayes, S. F., & Caughey, B. (2005). The most infectious prion protein particles. *Nature*, *437*(7056), 257-261. doi:10.1038/nature03989

- Silverman, G. A., Bird, P. I., Carrell, R. W., Church, F. C., Coughlin, P. B., Gettins, P. G., . . . Whisstock, J. C. (2001). The serpins are an expanding superfamily of structurally similar but functionally diverse proteins. Evolution, mechanism of inhibition, novel functions, and a revised nomenclature. *J Biol Chem*, *276*(36), 33293-33296. doi:10.1074/jbc.R100016200
- Sipione, S., Simmen, K. C., Lord, S. J., Motyka, B., Ewen, C., Shostak, I., . . . Bleackley, R. C. (2006). Identification of a novel human granzyme B inhibitor secreted by cultured sertoli cells. *J Immunol*, *177*(8), 5051-5058. doi:10.4049/jimmunol.177.8.5051
- Slapsak, U., Salzano, G., Amin, L., Abskharon, R. N., Ilc, G., Zupancic, B., . . . Legname, G. (2016). The N Terminus of the Prion Protein Mediates Functional Interactions with the Neuronal Cell Adhesion Molecule (NCAM) Fibronectin Domain. *J Biol Chem*, *291*(42), 21857-21868. doi:10.1074/jbc.M116.743435
- Song, K., Na, J. Y., Oh, M. H., Kim, S., Kim, Y. H., Park, B. Y., . . . Kwon, J. (2012). Synthetic prion Peptide 106-126 resulted in an increase matrix metalloproteinases and inflammatory cytokines from rat astrocytes and microglial cells. *Toxicol Res*, *28*(1), 5-9. doi:10.5487/TR.2012.28.1.005
- Soto, C., & Castilla, J. (2004). The controversial protein-only hypothesis of prion propagation. *Nat Med*, *10 Suppl*, S63-67. doi:10.1038/nm1069
- Soto, C., Kascsak, R. J., Saborio, G. P., Aucouturier, P., Wisniewski, T., Prelli, F., . . . Frangione, B. (2000). Reversion of prion protein conformational changes by synthetic beta-sheet breaker peptides. *Lancet*, *355*(9199), 192-197. doi:10.1016/s0140-6736(99)11419-3
- Spillantini, M. G., Schmidt, M. L., Lee, V. M., Trojanowski, J. Q., Jakes, R., & Goedert, M. (1997). Alpha-synuclein in Lewy bodies. *Nature*, *388*(6645), 839-840. doi:10.1038/42166
- Stahl, N., Borchelt, D. R., & Prusiner, S. B. (1990). Differential release of cellular and scrapie prion proteins from cellular membranes by phosphatidylinositol-specific phospholipase C. *Biochemistry*, *29*(22), 5405-5412. doi:10.1021/bi00474a028
- Stein, C. A., Subasinghe, C., Shinozuka, K., & Cohen, J. S. (1988). Physicochemical properties of phosphorothioate oligodeoxynucleotides. *Nucleic Acids Res*, *16*(8), 3209-3221. doi:10.1093/nar/16.8.3209
- Stein, P. E., & Carrell, R. W. (1995). What do dysfunctional serpins tell us about molecular mobility and disease? *Nat Struct Biol*, *2*(2), 96-113. doi:10.1038/nsb0295-96
- Steinacker, P., Hawlik, A., Lehnert, S., Jahn, O., Meier, S., Gorz, E., . . . Otto, M. (2010). Neuroprotective function of cellular prion protein in a mouse model of amyotrophic lateral sclerosis. *Am J Pathol*, *176*(3), 1409-1420. doi:10.2353/ajpath.2010.090355
- Stephan, C., Jung, K., Diamandis, E. P., Rittenhouse, H. G., Lein, M., & Loening, S. A. (2002). Prostate-specific antigen, its molecular forms, and other kallikrein markers for detection of prostate cancer. *Urology*, *59*(1), 2-8. doi:10.1016/s0090-4295(01)01449-2
- Stincardini, C., Massignan, T., Biggi, S., Elezgarai, S. R., Sangiovanni, V., Vanni, I., . . . Biasini, E. (2017). An antipsychotic drug exerts anti-prion effects by altering the localization of the cellular prion protein. *PLoS One*, *12*(8), e0182589. doi:10.1371/journal.pone.0182589
- Sunyach, C., Cisse, M. A., da Costa, C. A., Vincent, B., & Checler, F. (2007). The C-terminal products of cellular prion protein processing, C1 and C2, exert distinct influence on p53-dependent staurosporine-induced caspase-3 activation. *J Biol Chem*, *282*(3), 1956-1963. doi:10.1074/jbc.M609663200
- Sunyach, C., Jen, A., Deng, J., Fitzgerald, K. T., Frobert, Y., Grassi, J., . . . Morris, R. (2003). The mechanism of internalization of glycosylphosphatidylinositol-anchored prion protein. *EMBO J*, *22*(14), 3591-3601. doi:10.1093/emboj/cdg344
- Supattapone, S., Wille, H., Uyechi, L., Safar, J., Tremblay, P., Szoka, F. C., . . . Scott, M. R. (2001). Branched polyamines cure prion-infected neuroblastoma cells. *J Virol*, *75*(7), 3453-3461. doi:10.1128/JVI.75.7.3453-3461.2001
- Suzuki, K., Bose, P., Leong-Quong, R. Y., Fujita, D. J., & Riabowol, K. (2010). REAP: A two minute cell fractionation method. *BMC Res Notes*, *3*, 294. doi:10.1186/1756-0500-3-294

- Tagliavini, F., Prelli, F., Porro, M., Salmona, M., Bugiani, O., & Frangione, B. (1992). A soluble form of prion protein in human cerebrospinal fluid: implications for prion-related encephalopathies. *Biochem Biophys Res Commun*, *184*(3), 1398-1404. doi:10.1016/s0006-291x(05)80038-5
- Tahir, W., Abdulrahman, B., Abdelaziz, D. H., Thapa, S., Walia, R., & Schatzl, H. M. (2020). An astrocyte cell line that differentially propagates murine prions. *J Biol Chem*, *295*(33), 11572-11583. doi:10.1074/jbc.RA120.012596
- Tahiri-Alaoui, A., Gill, A. C., Disterer, P., & James, W. (2004). Methionine 129 variant of human prion protein oligomerizes more rapidly than the valine 129 variant: implications for disease susceptibility to Creutzfeldt-Jakob disease. *J Biol Chem*, *279*(30), 31390-31397. doi:10.1074/jbc.M401754200
- Tanaka, M., Chien, P., Naber, N., Cooke, R., & Weissman, J. S. (2004). Conformational variations in an infectious protein determine prion strain differences. *Nature*, *428*(6980), 323-328. doi:10.1038/nature02392
- Taubner, L. M., Bienkiewicz, E. A., Copie, V., & Caughey, B. (2010). Structure of the flexible amino-terminal domain of prion protein bound to a sulfated glycan. *J Mol Biol*, *395*(3), 475-490. doi:10.1016/j.jmb.2009.10.075
- Taylor, D. R., Parkin, E. T., Cocklin, S. L., Ault, J. R., Ashcroft, A. E., Turner, A. J., & Hooper, N. M. (2009). Role of ADAMs in the ectodomain shedding and conformational conversion of the prion protein. *J Biol Chem*, *284*(34), 22590-22600. doi:10.1074/jbc.M109.032599
- Telling, G. C., Parchi, P., DeArmond, S. J., Cortelli, P., Montagna, P., Gabizon, R., . . . Prusiner, S. B. (1996). Evidence for the conformation of the pathologic isoform of the prion protein enciphering and propagating prion diversity. *Science*, *274*(5295), 2079-2082. doi:10.1126/science.274.5295.2079
- Telling, G. C., Scott, M., Hsiao, K. K., Foster, D., Yang, S. L., Torchia, M., . . . Prusiner, S. B. (1994). Transmission of Creutzfeldt-Jakob disease from humans to transgenic mice expressing chimeric human-mouse prion protein. *Proc Natl Acad Sci U S A*, *91*(21), 9936-9940. doi:10.1073/pnas.91.21.9936
- Terada, T., Tsuboi, Y., Obi, T., Doh-ura, K., Murayama, S., Kitamoto, T., . . . Mizoguchi, K. (2010). Less protease-resistant PrP in a patient with sporadic CJD treated with intraventricular pentosan polysulphate. *Acta Neurol Scand*, *121*(2), 127-130. doi:10.1111/j.1600-0404.2009.01272.x
- Terry, C., Harniman, R. L., Sells, J., Wenborn, A., Joiner, S., Saibil, H. R., . . . Wadsworth, J. D. F. (2019). Structural features distinguishing infectious ex vivo mammalian prions from non-infectious fibrillar assemblies generated in vitro. *Sci Rep*, *9*(1), 376. doi:10.1038/s41598-018-36700-w
- Tobler, I., Gaus, S. E., Deboer, T., Achermann, P., Fischer, M., Rulicke, T., . . . Manson, J. C. (1996). Altered circadian activity rhythms and sleep in mice devoid of prion protein. *Nature*, *380*(6575), 639-642. doi:10.1038/380639a0
- Tribouillard-Tanvier, D., Striebel, J. F., Peterson, K. E., & Chesebro, B. (2009). Analysis of protein levels of 24 cytokines in scrapie agent-infected brain and glial cell cultures from mice differing in prion protein expression levels. *J Virol*, *83*(21), 11244-11253. doi:10.1128/JVI.01413-09
- Van Everbroeck, B., Dewulf, E., Pals, P., Lubke, U., Martin, J. J., & Cras, P. (2002). The role of cytokines, astrocytes, microglia and apoptosis in Creutzfeldt-Jakob disease. *Neurobiol Aging*, *23*(1), 59-64. doi:10.1016/s0197-4580(01)00236-6
- Vanni, S., Moda, F., Zattoni, M., Bistaffa, E., De Cecco, E., Rossi, M., . . . Legname, G. (2017). Differential overexpression of SERPINA3 in human prion diseases. *Sci Rep*, *7*(1), 15637. doi:10.1038/s41598-017-15778-8
- Vaure, C., & Liu, Y. (2014). A comparative review of toll-like receptor 4 expression and functionality in different animal species. *Front Immunol*, *5*, 316. doi:10.3389/fimmu.2014.00316
- Veerhuis, R., Hoozemans, J. J., Janssen, I., Boshuizen, R. S., Langeveld, J. P., & Eikelenboom, P. (2002). Adult human microglia secrete cytokines when exposed to neurotoxic prion protein peptide:

- no intermediary role for prostaglandin E2. *Brain Res*, 925(2), 195-203. doi:10.1016/s0006-8993(01)03273-5
- Victoria, G. S., Arkhipenko, A., Zhu, S., Syan, S., & Zurzolo, C. (2016). Astrocyte-to-neuron intercellular prion transfer is mediated by cell-cell contact. *Sci Rep*, 6, 20762. doi:10.1038/srep20762
- Vilette, D. (2008). Cell models of prion infection. *Vet Res*, 39(4), 10. doi:10.1051/vetres:2007049
- Vonsattel, J. P., & DiFiglia, M. (1998). Huntington disease. *J Neuropathol Exp Neurol*, 57(5), 369-384. doi:10.1097/00005072-199805000-00001
- Wagsater, D., Johansson, D., Fontaine, V., Vorkapic, E., Backlund, A., Razuvaev, A., . . . Eriksson, P. (2012). Serine protease inhibitor A3 in atherosclerosis and aneurysm disease. *Int J Mol Med*, 30(2), 288-294. doi:10.3892/ijmm.2012.994
- Wells, G. A., Scott, A. C., Johnson, C. T., Gunning, R. F., Hancock, R. D., Jeffrey, M., . . . Bradley, R. (1987). A novel progressive spongiform encephalopathy in cattle. *Vet Rec*, 121(18), 419-420. doi:10.1136/vr.121.18.419
- Wells, G. A. H., Hawkins, S. A. C., Austin, A. R., Ryder, S. J., Done, S. H., Green, R. B., . . . Kimberlin, R. H. (2003). Studies of the transmissibility of the agent of bovine spongiform encephalopathy to pigs. *J Gen Virol*, 84(Pt 4), 1021-1031. doi:10.1099/vir.0.18788-0
- Westaway, D., Goodman, P. A., Mirenda, C. A., McKinley, M. P., Carlson, G. A., & Prusiner, S. B. (1987). Distinct prion proteins in short and long scrapie incubation period mice. *Cell*, 51(4), 651-662. doi:10.1016/0092-8674(87)90134-6
- Westergard, L., Turnbaugh, J. A., & Harris, D. A. (2011). A naturally occurring C-terminal fragment of the prion protein (PrP) delays disease and acts as a dominant-negative inhibitor of PrPSc formation. *J Biol Chem*, 286(51), 44234-44242. doi:10.1074/jbc.M111.286195
- White, M. D., Farmer, M., Mirabile, I., Brandner, S., Collinge, J., & Mallucci, G. R. (2008). Single treatment with RNAi against prion protein rescues early neuronal dysfunction and prolongs survival in mice with prion disease. *Proc Natl Acad Sci U S A*, 105(29), 10238-10243. doi:10.1073/pnas.0802759105
- White, M. D., & Mallucci, G. R. (2009). Therapy for prion diseases: Insights from the use of RNA interference. *Prion*, 3(3), 121-128. doi:10.4161/pri.3.3.9289
- Whitfield, J. T., Pako, W. H., Collinge, J., & Alpers, M. P. (2017). Cultural factors that affected the spatial and temporal epidemiology of kuru. *R Soc Open Sci*, 4(1), 160789. doi:10.1098/rsos.160789
- Wieser, H. G., Schindler, K., & Zumsteg, D. (2006). EEG in Creutzfeldt-Jakob disease. *Clin Neurophysiol*, 117(5), 935-951. doi:10.1016/j.clinph.2005.12.007
- Will, R. G. (2003). Acquired prion disease: iatrogenic CJD, variant CJD, kuru. *Br Med Bull*, 66, 255-265. doi:10.1093/bmb/66.1.255
- Will, R. G., Zeidler, M., Stewart, G. E., Macleod, M. A., Ironside, J. W., Cousens, S. N., . . . Knight, R. S. (2000). Diagnosis of new variant Creutzfeldt-Jakob disease. *Ann Neurol*, 47(5), 575-582.
- Williams, E. S. (2005). Chronic wasting disease. *Vet Pathol*, 42(5), 530-549. doi:10.1354/vp.42-5-530
- Williams, E. S., & Young, S. (1980). Chronic wasting disease of captive mule deer: a spongiform encephalopathy. *J Wildl Dis*, 16(1), 89-98. doi:10.7589/0090-3558-16.1.89
- Wofford, K. L., Loane, D. J., & Cullen, D. K. (2019). Acute drivers of neuroinflammation in traumatic brain injury. *Neural Regen Res*, 14(9), 1481-1489. doi:10.4103/1673-5374.255958
- Wulf, M. A., Senatore, A., & Aguzzi, A. (2017). The biological function of the cellular prion protein: an update. *BMC Biol*, 15(1), 34. doi:10.1186/s12915-017-0375-5
- Wurster, C. D., & Ludolph, A. C. (2018). Antisense oligonucleotides in neurological disorders. *Ther Adv Neurol Disord*, 11, 1756286418776932. doi:10.1177/1756286418776932
- Xiang, W., Windl, O., Wunsch, G., Dugas, M., Kohlmann, A., Dierkes, N., . . . Kretzschmar, H. A. (2004). Identification of differentially expressed genes in scrapie-infected mouse brains by using global gene expression technology. *J Virol*, 78(20), 11051-11060. doi:10.1128/JVI.78.20.11051-11060.2004

- Yang, G. D., Yang, X. M., Lu, H., Ren, Y., Ma, M. Z., Zhu, L. Y., . . . Zhang, Z. G. (2014). SERPINA3 promotes endometrial cancer cells growth by regulating G2/M cell cycle checkpoint and apoptosis. *Int J Clin Exp Pathol*, 7(4), 1348-1358.
- Yang, X., He, G., Hao, Y., Chen, C., Li, M., Wang, Y., . . . Yu, Z. (2010). The role of the JAK2-STAT3 pathway in pro-inflammatory responses of EMF-stimulated N9 microglial cells. *J Neuroinflammation*, 7, 54. doi:10.1186/1742-2094-7-54
- You, H., Tsutsui, S., Hameed, S., Kannanayakal, T. J., Chen, L., Xia, P., . . . Zamponi, G. W. (2012). Abeta neurotoxicity depends on interactions between copper ions, prion protein, and N-methyl-D-aspartate receptors. *Proc Natl Acad Sci U S A*, 109(5), 1737-1742. doi:10.1073/pnas.1110789109
- Zamanian, J. L., Xu, L., Foo, L. C., Nouri, N., Zhou, L., Giffard, R. G., & Barres, B. A. (2012). Genomic analysis of reactive astrogliosis. *J Neurosci*, 32(18), 6391-6410. doi:10.1523/JNEUROSCI.6221-11.2012
- Zanusso, G., Ferrari, S., Cardone, F., Zampieri, P., Gelati, M., Fiorini, M., . . . Monaco, S. (2003). Detection of pathologic prion protein in the olfactory epithelium in sporadic Creutzfeldt-Jakob disease. *N Engl J Med*, 348(8), 711-719. doi:10.1056/NEJMoa022043
- Zanusso, G., Monaco, S., Pocchiari, M., & Caughey, B. (2016). Advanced tests for early and accurate diagnosis of Creutzfeldt-Jakob disease. *Nat Rev Neurol*, 12(7), 427. doi:10.1038/nrneurol.2016.92
- Zerbino, D. R., Achuthan, P., Akanni, W., Amode, M. R., Barrell, D., Bhai, J., . . . Flicek, P. (2018). Ensembl 2018. *Nucleic Acids Res*, 46(D1), D754-D761. doi:10.1093/nar/gkx1098
- Zhou, J., Cheng, Y., Tang, L., Martinka, M., & Kalia, S. (2017). Up-regulation of SERPINA3 correlates with high mortality of melanoma patients and increased migration and invasion of cancer cells. *Oncotarget*, 8(12), 18712-18725. doi:10.18632/oncotarget.9409
- Zhu, H., Liu, Q., Tang, J., Xie, Y., Xu, X., Huang, R., . . . Sun, B. (2017). Alpha1-ACT Functions as a Tumour Suppressor in Hepatocellular Carcinoma by Inhibiting the PI3K/AKT/mTOR Signalling Pathway via Activation of PTEN. *Cell Physiol Biochem*, 41(6), 2289-2306. doi:10.1159/000475648
- Zou, Z., Anisowicz, A., Hendrix, M. J., Thor, A., Neveu, M., Sheng, S., . . . Sager, R. (1994). Maspin, a serpin with tumor-suppressing activity in human mammary epithelial cells. *Science*, 263(5146), 526-529. doi:10.1126/science.8290962